

HELSINKI UNIVERSITY OF TECHNOLOGY
Department of Electrical and Communications Engineering
Laboratory of Acoustics and Audio Signal Processing

Heli Nironen

Diffuse Reflections in Room Acoustics Modelling

Master's Thesis submitted in partial fulfillment of the requirements for the degree of
Master of Science in Technology.

Espoo, October 12, 2004

Supervisor: Professor Matti Karjalainen
Instructor: D.Sc. (Tech.) Tapio Lokki

Author:	Heli Nironen	
Name of the thesis:	Diffuse Reflections in Room Acoustics Modelling	
Date:	October 12, 2004	Number of pages: 92
Department:	Electrical and Communications Engineering	
Professorship:	S-89 Acoustics and Audio Signal Processing	
Supervisor:	Prof. Matti Karjalainen	
Instructor:	D.Sc. (Tech.) Tapio Lokki	
<p>This thesis is a study of diffuse reflection modelling in room acoustics. The aim of the work is to get familiar with the most often applied physical principles and modelling methods. An objective is that the studied theory and techniques could be applied in future research work. Room acoustics modelling methods are divided in this thesis into three categories: 1. Ray-based methods, 2. Radiosity, and 3. Wave-based methods. When considering different modelling methods, emphasis is on the ray- and radiosity-based approaches. Some wave-based methods are also presented, but left out of more accurate examination. Although the approach in this work is mainly physically-based, one totally perceptually-based method is also presented. A simple implementation is carried out in order to get familiar with the studied principles and methods in practice. An early response is predicted with a model which combines the image source method and the radiosity-based approach. The implemented system is described in detail, and the modelling results are analysed. Finally, methods most applicable for estimating acoustical quality of a room, methods most suitable for auralisation purposes, and requirements of real-time dynamic systems are discussed.</p>		
<p>Keywords: diffuse reflection, scattering, room acoustics modelling, ray-based modelling methods, radiosity, auralisation</p>		

Tekijä:	Heli Nironen	
Työn nimi:	Diffuusit heijastukset huoneakustiikan mallinnuksessa	
Päivämäärä:	12.10.2004	Sivuja: 92
Osasto:	Sähkö- ja tietoliikennetekniikka	
Professori:	S-89 Akustiikka ja äänenkäsittelytekniikka	
Työn valvoja:	Professori Matti Karjalainen	
Työn ohjaaja:	TkT Tapio Lokki	
<p>Tässä diplomityössä tarkastellaan diffuusien heijastusten mallinnusta huoneakustiikassa. Työssä käydään läpi äänen etenemiseen liittyviä käsitteitä, periaatteita ja tunnetuimpia mallinnusmenetelmiä. Tavoitteena on, että opiskeltua teoriapohjaa voitaisiin hyödyntää myöhemmin aiheeseen liittyvässä tutkimuksessa. Huoneakustiikan mallinnuksessa käytetyt menetelmät jaotellaan tässä työssä kolmeen ryhmään. Ensimmäisen ryhmän menetelmissä ääniaaltojen eteneminen mallinnetaan äänisäteiden avulla. Toisen ryhmän muodostavat radiositeettimenetelmät, joissa ääntä heijastellaan diffuusisti huoneen seiniin muodostetun verkon solmujen välillä. Kolmannen ryhmän menetelmät perustuvat aaltoyhtälön ratkaisuun. Työn painopiste on kahteen ensimmäiseen ryhmään kuuluvissa menetelmissä. Vaikka mallinnusmenetelmiä tarkastellaankin enimmäkseen fysikaalisiin periaatteisiin tukeutuen, esitellään myös yksi menetelmä, joka mallintaa diffuuseja heijastuksia ihmisen havitsemiseen perustuen. Työssä myös toteutetaan yksinkertainen malli huonevasteen alkuosalle. Tässä sovelletaan kuvalähde- ja radiositeettimenetelmää. Toteutettu malli esitellään yksityiskohtaisesti ja sillä saatuja tuloksia analysoidaan. Myös työssä käsiteltyjen menetelmien soveltuvuutta erilaisiin tarkoituksiin kartoitetaan. Teoriapohjan perusteella analysoidaan, mitä menetelmistä voidaan käyttää huoneen akustisten ominaisuuksien arviointiin, mitkä menetelmistä sopivat parhaiten auralisaatioon ja minkälaisia kompromisseja vaativat dynaamiset reaaliaikasysteemit.</p>		
Avainsanat: diffuusi heijastus, äänen sironta, huoneakustiikan mallinnus, sädemenetelmät, radiositeettimenetelmä, auralisaatio		

Acknowledgements

This Master's thesis was carried out for the Uni-verse project at the Telecommunications Software and Multimedia Laboratory, Helsinki University of Technology, during the year 2004.

The work was instructed by D.Sc. (Tech.) Tapio Lokki. I would like to thank Tapio for his guidance. He has provided me with many valuable insights during the course of the work. I also thank Tapio for his comments and suggestions on the structure and content of this thesis. He has patiently given me feedback on various versions of the thesis.

I also want to thank my supervisor Prof. Matti Karjalainen for his helpful comments and supportive discussions. Prof. Lauri Savioja I would like to thank for employing me in the Uni-verse project and for providing me with an interesting topic for my thesis.

I would also like to give special thanks to Sami Kiminki, my co-worker in the Uni-verse project, for numerous helpful discussions, valuable insights, and all the practical help that he offered me during this work. Sampo Vesa and Iikka Olli, who have shared the office with me, I would like to thank for good company and for a relaxed working environment.

Furthermore, I wish to thank my friends for all the fun I have experienced with them during my studies. Sharaf Hameed I want to thank for bringing an Indian contribution to my circle of friends.

Finally, I would like to express my gratitude to my family. I want to thank my parents for their patience, encouragement, and all the support that I have got during my almost endless studies. Also, I would like to thank my dear sisters Satu and Kati for their contribution. My beloved Teemu I deeply thank for his understanding, support, and love. His positive attitude towards life has encouraged me over the past few years.

Otaniemi, October 12, 2004,

Heli Nironen

Contents

Symbols	ix
Abbreviations	x
1 Introduction	1
2 Background	4
2.1 Characteristics of Sound Waves	4
2.1.1 Velocity of Sound	4
2.1.2 Some Basic Relations	5
2.1.3 Plane Waves	6
2.1.4 Spherical Waves	7
2.1.5 Energy and Energy Density	8
2.1.6 Intensity	9
2.2 Reflection of Sound	9
2.2.1 Principal Laws of Sound Reflection	10
2.2.2 Diffraction, Scattering, and Diffuse Reflection	13
2.2.3 Diffuse Sound Field	15
2.2.4 Terminology	15
2.3 Expressing Surface Diffusion	16
2.3.1 Lambert's Law	16
2.3.2 Theoretically Calculated Scattering Functions	19

2.3.3	Measured Scattering Functions	25
2.4	Main Methods of Room Acoustics Modelling	27
2.4.1	General Issues about Room Acoustics Modelling	27
2.4.2	Ray-Based Modelling Methods	29
2.4.3	Radiosity Method	33
2.4.4	Wave-Based Methods	34
3	Modelling Diffuse Reflections	37
3.1	Methods Based on Ray Tracing	37
3.2	Combining Beam Tracing and Radiosity	40
3.3	Approach Based on the Approximate Cone Tracing	43
3.4	Utilising Schroeder Diffusers in 2D	48
3.5	Perceptually-Based Approach	51
4	Experimental Part	56
4.1	Implemented System	56
4.1.1	Modelling of Specular Reflection Response	57
4.1.2	Modelling of Diffuse Reflection Response	64
4.1.3	Combining Specular and Diffuse Reflection Responses	69
4.2	Analysis	70
4.2.1	Effect of the Scattering Coefficient	70
4.2.2	Effect of the Patch Size	72
4.2.3	Discussion about Implementation	72
5	Discussion	76
5.1	Diffuse Reflection Modelling when Predicting Acoustical Quality of a Room	76
5.2	Diffuse Reflections in Context of Auralisation	79
5.3	Real-time Dynamic Diffuse Reflection Modelling	81
6	Conclusions and Future Work	83

Symbols

a	Attenuation constant
b	Number of zeroes in an allpass filter
c	Velocity of sound
d	Diffusion coefficient
d_n	Actual depth of the n th well in a Schroeder diffusor
f	Frequency
g	Number of grid nodes on a surface
h	Number of triangular beams emitted from a grid node
i	$\sqrt{-1}$
i	Symbol of surface element
j	Symbol of surface element
k	Wave number
k_s	Specular reflection scalar
k_d	Diffuse reflection scalar
k_{diff}	Variable determining level of diffused reflection components in a response
l	Integer variable
l_{sp}, l_{pp}, l_{pl}	Coefficients related to Lambert's law in context of implemented system
$m_{j \rightarrow i}$	Form factor between surface elements j and i
\mathbf{n}	Surface normal
n	Integer variable
n_p	Total number of nonempty patches
p	Sound pressure
p_0	Static value of a pressure
p_0	Initial sound pressure
p_i	Sound pressure of an incident wave
p_r	Sound pressure of a reflected wave
p_{sc}	Sound pressure on partially diffusing surface receiver
p_{dif}	Sound pressure obtained for totally diffusely reflecting surface

p_{spec}	Sound pressure obtained for totally specularly reflecting surface
r	Distance variable
r_{sp}	Distance between a sound source and a surface patch
r_{pp}	Distance between two surface patches
r_{pl}	Distance from a surface patch to a listener
$r_{j \rightarrow i}$	Distance between surface elements j and i
\mathbf{r}, \mathbf{r}'	Location vectors of wall elements
\mathbf{r}_r	Location vector of a receiver
\mathbf{r}_0	Location vector of a source
\mathbf{r}_s	Location vector of a point on a surface
s	Scattering coefficient
s_n	Relative depth of the n th well in a Schroeder diffusor
t	Time
v	Value of particle velocity
\mathbf{v}	Particle velocity
v_i	Particle velocity of an incident wave
v_r	Particle velocity of a reflected wave
v_{rad}	Component of particle velocity, radial one
v_x	Component of particle velocity, parallel to x-axis
v_n	Component of particle velocity, normal to a wall
w	Energy density
w_d	Energy density, direct contribution from some sound source to a receiver
w_{kin}	Kinetic energy density
w_{pot}	Potential energy density
x, y, z	Location variables
x'	Location variable in a rotated coordinate system
x	Input signal in context of allpass filter
y	Output signal in context of allpass filter
x_r, y_r, z_r	Location variables of a receiver
x_0, y_0, z_0	Location variables of a source
x_s, y_s, z_s	Location variables of a point on a surface
z_d	Acoustic impedance of a cap at a closed end of a pipe
A_{es}	Area of an emitting surface
A_{rs}	Area of a receiving surface
ΔA_{es}	Area of an element in a surface which is emitting sound
A_i	Cross-sectional area of a beam
A_{vis}	Area of a surface, visible from a receiver

B	Irradiation strength
B_d	Irradiation strength, direct contribution from a sound source to a receiver
E	Energy
E_0	Initial energy at a sound source
E_l	Energy arriving to a listener
E_p	Energy arriving to a single patch
ENV	Envelope of an allpass filter
G	Green's function
\mathbf{I}	Intensity
I_0	Intensity of an incident wave
I_i	Incident sound intensity at a surface element i
I_j	Intensity, contribution from a single surface element j to a surface element i
$I_{0 \rightarrow i}$	Direct contribution from some sound source at a surface element i
dI	Intensity of energy re-radiated between surface elements
I^*	Surface intensity
I_R	Intensity at a receiver
K	Constant
L	Straight line connecting two surface elements
L'	Straight line connecting a surface element and a receiver
M	Non-negative odd prime number
N	Integer variable
P	Point inside a room
P_i	Power of a beam emanating from an image source
P_s	Power of a beam emanating from a source
Q	Volume velocity
R	Reflection factor
R_e	Energy reflection factor
RG_e	Exterior region, external to a surface
RG_s	Region in a surface
RG_i	Interior region, internal to a surface
R_s	Specular reflection
R_d	Diffuse reflection
ΔR	An area of a surface receiver
S	Area of a surface
dS, dS'	Surface area elements
ΔS	Area of surface element
T	Period of time

V	Pressure wave, travelling in positive x-direction
W	Pressure wave, travelling in negative x-direction
X	Random number
Z	Wall impedance
Z_n	Impedance at an entrance of n th pipe in context of Schroeder diffusor
α	Absorption coefficient
β	Surface admittance, outward pointing surface normal
β'	Surface admittance, inward pointing surface normal
χ	Phase angle of reflection factor
γ	Splitting coefficient
κ	Adiabatic exponent
λ_0	Design wavelength of a Schroeder diffusor
μ	Optimum decay rate of an allpass filter.
ω	Angular frequency
ψ	Coefficient of an allpass filter.
ρ	Gas density
ρ_0	Static value of a gas density
σ	Reflection coefficient
σ_j	Energy reflection coefficient at surface element j
θ_0	Angle of an incident wave
θ	Angle of a reflected wave
θ_i	Angle of sound ray which illuminates surface element i
θ_j	Angle of sound ray which irradiates from surface element j
θ_r	Angle of sound ray which irradiates from surface element to receiver
θ_{sp}	Angle of an incident wave, from source to patch
θ_{pl}	Angle of reflected wave, from patch to listener
θ_{pp}	Angle of reflected wave, from patch to another patch
ζ	Angle between L and surface normal at surface element dS
ζ'	Angle between L and surface normal at surface element dS'
ζ''	Angle between L' and surface normal at surface element dS
ζ	Specific acoustic impedance
Ω	Solid angle presented by a surface to a receiving point
$\Delta\Omega_i$	A solid angle that i th beam encloses in beam tracing
Θ	Temperature

Abbreviations

AES	Audio Engineering Society
AVE	Auditory Virtual Environment
BEM	Boundary Element Method
C	Clarity
CT	Center Time
D	Definition
DWM	Digital Waveguide Method
EDT	Early Decay Time
FDTD	Finite Difference method in Time Domain
FEA	Finite Element Analysis
FEM	Finite Element Method
IACC	Inter-Aural Cross-Correlation
IFFT	Inverse Fast Fourier Transform
IR	Impulse Response
ISM	Image Source Method
ISO	International Organization for Standardization
KHIE	Kirchhoff-Helmholtz Integral Equation
LEF	Lateral Energy Fraction
MLS	Maximum Length Sequence
RIR	Room Impulse Response
RLR	Reference Listening Room
RMS	Root Mean Square
RT	Reverberation time
S	Strength
TLM	Transmission Line Method
2D	Two dimensional geometry
3D	Three dimensional geometry

Chapter 1

Introduction

Room acoustics is concerned with sound propagation in enclosures. In most environments a sound is heard as a combination of a direct sound straight from a source/sources and indirect reflections from surfaces and other objects. If acoustics of a space is examined, both the direct sound and the reflections are keys to a sound field in the considered space.

Characteristics of the reflections depend on properties of the reflecting surfaces. The reflections can be simple like specular reflections where incoming sound is reflected out from a surface in the same angle (related to a surface normal) as it came to the surface. On the other hand, if the surface is diffusely reflecting, the reflection can be highly complicated. Enclosures with at least in parts diffusing surfaces are quite different in their acoustical behaviour from those with just specularly reflecting surfaces. Diffuse reflections result in a more uniform distribution of sound energy throughout a room [41]. Inclusion of surface diffusion in modelling of room acoustics is an important factor, if the aim is to achieve a good prediction accuracy [9].

In many virtual reality applications computational modelling of acoustical spaces is fundamental. Demands vary from real-time simulations in multimedia and computer games to non real-time situations with high accuracy needs. Prediction of room acoustical conditions in music performance spaces is an example of the latter. Possibility to listen to results has always been essential [79].

Inaccurate modelling of diffuse reflections remains a particular weakness of room acoustics auralisation. Various mathematical models for diffuse reflections have not yet been fully exploited and optimised for rooms. Today, room impulse responses are often simulated using approximate, ray-based models and energy-based diffusion methods. Even with these approaches the lack of reliable input data (scattering functions, scattering coefficients, etc.) is, however, a real problem.

This Master's thesis examines modelling of diffuse reflections in room acoustics. The

purpose is to familiarise oneself with physical principles and basic methods applied to room acoustics modelling. The objective is to find out how diffuse reflections have been treated in computational modelling and simulation of acoustic spaces until now. Some applied methods are considered in detail. The emphasis is on ray-based methods and radiosity. Also some wave-based methods are presented, mainly in context of predicting scattering from a single diffusely reflecting surface. However, these wave-based methods are left out for more accurate analysis in this work. In addition, two methods which could be used in situations where real-time processing is required, are presented. A simple implementation which applies the studied techniques is carried out in order to in practice familiarise oneself with physically-based room acoustics and diffuse reflection modelling. The implementation is presented in detail and the modelling results are analysed. Finally, based on the studied techniques and the implemented system, modelling techniques most suitable for different situations are discussed. The methods which could be applied to predict an acoustical quality of a real room are covered. Applicability of the methods for auralisation purposes is also considered. The question how diffuse reflections could be treated efficiently in dynamic real-time auralisation is studied as well.

This thesis serves as an initial investigation in the field of diffuse reflection modelling. The purpose is, that the theory and techniques studied here could be applied in a future research work.

Structure of the Thesis

The thesis is divided into six separate chapters. Contents of the chapters are the following:

Chapter 1: Introduction. The scope, the objectives, and the structure of the thesis is presented here.

Chapter 2: Background. This chapter covers the theoretical basis needed to understand physically-based diffuse reflection modelling. First, characteristics of sound waves are discussed. After that the concept of sound reflection is studied in detail in order to understand what is diffuse reflection. Next, ways of expressing the diffusing effect of a surface are considered. Finally, main methods applied to room acoustics modelling are presented.

Chapter 3: Modelling Diffuse Reflections. Some proposed methods for predicting diffuse reflections are considered in detail in this chapter. The first three subsections present methods which apply ray tracing, beam/cone tracing, and radiosity. All these methods can be categorised to physically-based approaches. In addition, two methods, meant to be

used in reverberation engines, are presented. The first of these is physical in a sense that it utilises physical models of the components of Schroeder diffusers. The other method applies a completely perceptually-based approach.

Chapter 4: Implemented system. In order to familiarise oneself with physically-based room acoustics modelling methods and especially with problems related to modelling diffuse reflections a simple implementation is carried out. The early part of a response in a shoe-box shaped room is modelled. Used methods and algorithms, resulting responses, and analysis of modelled responses are presented in this chapter.

Chapter 5: Discussion. On the grounds of the studied principles and techniques, different diffuse reflection modelling methods are discussed here. First, the methods most suitable for predicting the response of a real space are discussed. Then problems of aforementioned methods in context of auralisation are considered. Also, the methods which could be used in dynamic real-time simulation of diffuse reflections are discussed.

Chapter 6: Conclusions and Future Work. Characteristics of diffuse reflections and properties of different diffuse reflection modelling methods are summarised in this chapter. In addition, suggestions are made for future investigations.

Chapter 2

Background

In order to understand how diffuse reflections have been and in the future could be modelled with physically-based methods, some background knowledge is needed. This chapter covers fundamental principles and main methods used in physically-based room acoustics, and especially in diffuse reflection modelling. Basic physical principles like characteristics of sound waves, reflections, and particularly diffuse reflections are discussed. Furthermore, some ways of expressing the diffusing effect of a surface are introduced. Finally, the main modelling methods used in a field of room acoustics prediction are examined.

2.1 Characteristics of Sound Waves

An important property of sound waves is their ability to transport energy and information from one place to another. This happens through a medium which itself is not transported. When a wave propagates, a change in pressure and in density is passed along from point to point. As the wave has passed, the medium reverts to its undisturbed state [67].

In principle, any complex sound field can be considered as a superposition of numerous elementary sound waves. In the following subsections quantities and concepts related to the propagation of sound waves are considered. The presentation follows the way Kuttruff has introduced these characteristics of the sound waves [41], if not otherwise mentioned. However, the same principles have also been discussed more thoroughly by Pierce [61], for example.

2.1.1 Velocity of Sound

If sound propagation is free of losses, the medium where a sound wave propagates is unbounded in all directions, and the medium itself is homogeneous and at rest, a velocity of sound is constant with reference to space and time. For the air, the velocity of sound is

defined as

$$c = (331.4 + 0.6\Theta) \text{ m/s}, \quad (2.1)$$

where Θ is the temperature in centigrade.

2.1.2 Some Basic Relations

A sound wave can be completely described by indicating instantaneous displacements of particles of a medium. However, often, instead of the displacement itself, a velocity of particle displacement (a *particle velocity*) is considered as a basic acoustical quantity.

Vibrations in the sound wave do not take place at all points with a same phase. At some points in a sound field particles vibrate in the opposite phase. Therefore, in certain regions the particles are pushed together and in other regions pulled apart. Under an influence of the sound wave variations occur in *gas density* and *pressure*. These are functions of *time* and *position*. Difference between an instantaneous pressure and a static pressure is called a *sound pressure*.

Because changes of the gas pressure caused by the sound wave occur generally so rapidly that heat can not be exchanged between adjacent volume elements, the sound wave causes adiabatic variations of *temperature*. As a consequence, the temperature can also be considered as a quantity characterising the sound wave.

A number of basic laws connect various acoustical quantities. By utilising these laws it is possible to set up a general differential equation governing sound propagation:

At first conservation of momentum has to be defined. It can be expressed by the following relation:

$$\text{grad } p = -\rho_0 \frac{\partial \mathbf{v}}{\partial t}, \quad (2.2)$$

where p is the sound pressure, ρ_0 is a static value of the gas density, \mathbf{v} is the particle velocity, and t is the time.

Conservation of mass leads to the following expression:

$$\rho_0 \text{ div } \mathbf{v} = -\frac{\partial \rho}{\partial t}, \quad (2.3)$$

where ρ is the total gas density including its variable part, $\rho = \rho_0 + \delta\rho$. Changes of p and ρ are assumed to be small when compared to the static values p_0 and ρ_0 . On the contrary, the particle velocity \mathbf{v} is assumed to be much smaller than the sound velocity.

If it is assumed that a gas is ideal, the following relations hold between the sound pressure, the gas density variations, and the temperature changes $\delta\Theta$:

$$\frac{p}{p_0} = \kappa \frac{\delta\rho}{\rho_0} = \frac{\kappa}{\kappa - 1} \frac{\delta\Theta}{\Theta + 273}. \quad (2.4)$$

In the previous expression κ is an adiabatic exponent. By eliminating the particle velocity \mathbf{v} and the variable part $\delta\rho$ of the gas density from Eqs. (2.2) and (2.4) the following differential equation is achieved:

$$c^2 \Delta p = \frac{\partial^2 p}{\partial t^2}, \quad (2.5)$$

where

$$c^2 = \kappa \frac{p_0}{\rho_0}. \quad (2.6)$$

This differential equation is referred to as a *wave equation*. It governs propagation of sound waves in any lossless fluid and is therefore of central importance for almost all acoustical phenomena.

2.1.3 Plane Waves

If it is assumed that acoustical quantities depend only on time and on one single direction which may be chosen as x-direction of a cartesian coordinate system, Eq. (2.5) can be expressed as:

$$c^2 \frac{\partial^2 p}{\partial x^2} = \frac{\partial^2 p}{\partial t^2}. \quad (2.7)$$

This differential equation has the following general solution:

$$p(x, t) = V(ct - x) + W(ct + x). \quad (2.8)$$

In the previous expression the first term on the right, V , presents a pressure wave travelling in positive x-direction with velocity c . The second term, W , describes a sound pressure wave which propagates in negative x-direction. Each term of this equation represents a progressive *plane wave*, where the sound pressure p is constant in any plane perpendicular to the x-axis. These planes of constant sound pressures are called *wavefronts*. Any line perpendicular to the wavefront is a *wave normal*.

The particle velocity, as Eq. (2.2) states, has only one non-vanishing component. This is parallel to a gradient of the sound pressure. As a consequence, in fluids, sound waves are longitudinal waves. By applying the Eq. (2.2) to Eq. (2.8) the following expression is obtained for the particle velocity:

$$v = v_x = \frac{1}{\rho_0 c} [V(ct - x) - W(ct + x)]. \quad (2.9)$$

The ratio of sound pressure and particle velocity in the plane wave which propagates in positive direction ($W = 0$) is frequency independent as can be seen from Eqs. (2.8) and (2.9):

$$\frac{p}{v} = \rho_0 c. \quad (2.10)$$

This ratio is called a *characteristic impedance* of the medium. When the wave is travelling in negative x-direction also this ratio is negative.

Harmonic waves are of particular importance when characteristics of sound waves are considered. In harmonic waves, time and space dependence of acoustical quantities follows a sine or a cosine function. If W is set to zero and V specified as the cosine function, the following expression is obtained for a plane, harmonic wave:

$$p(x, t) = \hat{p} \cos[k(ct - x)] = \hat{p} \cos(\omega t - kx), \quad (2.11)$$

where $\hat{p} = |p(x, t)|$ is the absolute value of the sound pressure at place x at time t , $k (= \omega/c)$ is a propagation constant or a *wave number* and $\omega (= kc = 2\pi f)$ is an *angular frequency*. Complex notation of the previous expression (Eq. 2.11) reads as follows:

$$p(x, t) = \text{Re} \{ \hat{p} \exp[i(\omega t - kx)] \}, \quad (2.12)$$

or, when Re is omitted:

$$p(x, t) = \hat{p} \exp[i(\omega t - kx)]. \quad (2.13)$$

Until now it has been assumed that the wave medium is free of losses. However, if this is not the case, the pressure amplitude does not remain constant in the course of wave propagation. Decreasing of the amplitude occurs according to an exponential law and Eq. (2.13) has to be modified in the following way:

$$p(x, t) = \hat{p} \exp(-ax/2) \exp[i(\omega t - kx)], \quad (2.14)$$

where a is an attenuation constant.

Finally, it can be concluded that a plane wave is an idealised wave type. It does not exist in the real world, not at least in its pure form.

2.1.4 Spherical Waves

In *spherical waves* surfaces of constant pressure (wavefronts) are concentric spheres. A vanishingly small source, a *point source*, which introduces or withdraws fluid, has to be imagined in the common centre of these concentric spheres. For this kind of geometry, polar coordinates with distance r from the centre as a relevant space coordinate are appropriate.

The differential equation, Eq. (2.5), which has now been transformed into polar coordinate system, can be expressed as follows:

$$\frac{\partial^2 p}{\partial r^2} + \frac{2}{r} \frac{\partial p}{\partial r} = \frac{1}{c^2} \frac{\partial^2 p}{\partial t^2}. \quad (2.15)$$

A simple solution for the previous equation is

$$p(r, t) = \frac{\rho_0}{4\pi r} Q' \left(t - \frac{r}{c} \right). \quad (2.16)$$

This solution represents a spherical wave produced by a point source at r , with a *volume velocity* Q . Volume velocity tells the rate at which fluid is expelled by the source. Q' means partial differentiation with respect to time. The argument $t - r/c$ indicates that any disturbance created by the sound source is propagated outward with velocity c and its strength is decreasing as $1/r$.

In case of the spherical wave, the only non-vanishing component of the particle velocity is the radial one. By applying the Eq. (2.2) into Eq. (2.16) this component can be expressed as

$$v_{rad} = \frac{1}{4\pi r^2} \left[Q \left(t - \frac{r}{c} \right) + \frac{r}{c} Q' \left(t - \frac{r}{c} \right) \right]. \quad (2.17)$$

When the volume velocity of the source varies according to $Q(t) = \hat{Q} \exp(i\omega t)$, where \hat{Q} is the absolute value of the volume velocity, Eq. (2.16) yields a harmonic spherical wave in complex notation:

$$p(r, t) = \frac{i\omega \rho_0}{4\pi r} \hat{Q} \exp[i(\omega t - kr)]. \quad (2.18)$$

Again, the particle velocity, obtained from Eq. (2.17), is

$$v_{rad} = \frac{p}{\rho_0 c} \left(1 + \frac{1}{ikr} \right). \quad (2.19)$$

The previous formula indicates that the ratio of the sound pressure and the particle velocity in the spherical sound wave depends on the distance r and on the frequency $\omega = kc$. In addition, it is complex. This means that between both quantities there is a phase difference. However, for distances which are large compared to the wavelength, the ratio p/v tends asymptotically to the characteristic impedance of the medium. For this reason, when distance from the centre is large compared to all wavelengths involved, a limited region of the spherical wave may be considered as a good approximation of the plane wave.

2.1.5 Energy and Energy Density

When a sound source generates a sound wave, it delivers some *energy* to a fluid which is then carried away by a sound wave. When this sound wave is considered as a function of time it can be understood as a sound signal. *Energy* of a time-limited sound signal is expressed in the following way [42]:

$$E = \int_T p^2(t) dt, \quad (2.20)$$

where T is an observation period of the sound signal, p is the pressure of the sound signal, and t is the time.

Energy contained in a unit volume of a wave is characterised by a quantity called *energy density*. When considering energy density it is important to distinguish between potential

and kinetic energy densities. These can be expressed as follows:

$$w_{pot} = \frac{p^2}{2\rho_0 c^2}, \quad w_{kin} = \frac{\rho_0 |\mathbf{v}|^2}{2}. \quad (2.21)$$

The total energy density w is now:

$$w = w_{pot} + w_{kin}. \quad (2.22)$$

It should be noted that energetic quantities do not simply add, if two waves are superimposed on each other.

2.1.6 Intensity

Another important quantity is *sound intensity*. It is a measure of energy transported in a sound wave. This quantity can be understood by imagining a window of 1m^2 perpendicular to the direction of sound propagation. The intensity, which can be seen also as a power of a sound signal, is an amount of energy per second which passes this window. In general, the intensity is a vector parallel to a vector \mathbf{v} of the particle velocity. The intensity is given by:

$$\mathbf{I} = p\mathbf{v}, \quad (2.23)$$

where p is the pressure and \mathbf{v} is the particle velocity of the sound. As a consequence of energy conservation:

$$\frac{\partial w}{\partial t} + \text{div}\mathbf{I} = 0. \quad (2.24)$$

Because intensity is also an energetic quantity, either intensities do not simply add if two waves are superimposed on each other.

2.2 Reflection of Sound

In order to understand what is diffuse reflection and how it could be modelled in room acoustics, principal laws of sound reflection have to be known. The simplest kind of reflection from a wall is a specular reflection. In the specular reflection illumination and irradiation angles (in relation to the surface normal) of a sound wave are the same. The theory related to the specular reflection in context of a plane wave is explained first in this section. After that, more complicated reflections caused by diffraction, scattering, and diffuse reflections are considered. Also, the concept of diffuse field is introduced. Finally, section ends with a discussion about terminology used in context of diffuse reflection. Kuttruff's book [41] has again been used as the reference if not otherwise mentioned. Another source of information, where these issues have been considered is [23], for example.

2.2.1 Principal Laws of Sound Reflection

In reality, all sound waves originating from a sound source are spherical waves or superpositions of spherical waves. A reflection of the spherical wave from a non-rigid wall is highly complicated. However, when the sound source is not too close to a reflecting wall or to a scattering obstacle, the situation can be often simplified by neglecting the curvature of a wavefront. This is done also here. An incident, undisturbed wave is assumed to be a plane wave.

The situation where the plane wave strikes a surface or a uniform plane of infinite extent is considered first. In such a situation, in general, part of irradiating sound energy reflects from the plane in the form of reflected wave originating from the plane. The amplitude and the phase of the reflected wave differs from those of an incident wave. The incident and the reflected waves interfere with each other and form together (at least partially) a standing wave.

Reflection Factor

Changes in the amplitude and the phase can be expressed by a complex *reflection factor*:

$$R = |R| \exp(i\chi). \quad (2.25)$$

R is a property of the wall. Its absolute value $|R|$ and phase angle χ depend on the frequency and direction of the incident wave.

Absorption Coefficient

The intensity of a plane wave is proportional to the square of pressure amplitude. For this reason, the intensity of the reflected wave is smaller by a factor $|R|^2$ than that of the incident wave. Fraction $1 - |R|^2$ of an incident energy is therefore lost during reflection. Quantity

$$\alpha = 1 - |R|^2 \quad (2.26)$$

describes this loss. It is called an *absorption coefficient* of the wall.

Wall Impedance

By the reflection factor the acoustical properties of a wall surface are completely described for all angles of incidence and for all frequencies. Another quantity that is even more closely related to physical behaviour and to construction of the wall is based on the particle velocity normal to the wall and to the sound pressure at the surface. This quantity is called

the *wall impedance*. It is defined by

$$Z = \left(\frac{p}{v_n} \right)_{surface}, \quad (2.27)$$

where p denotes the sound pressure at the surface and v_n the velocity component normal to the wall. The wall impedance, like the reflection factor, is generally complex and function of the angle of sound incidence. The impedance usually changes as frequency changes.

The wall impedance Z is often divided by the characteristic impedance of the air:

$$\zeta = \frac{Z}{\rho_0 c}. \quad (2.28)$$

In the previous expression ρ_0 is the static value of the gas density and c is the velocity of sound. The resulting quantity ζ is called a *specific acoustic impedance*.

Sound Reflection at Normal Incidence

Next, let's assume that a wall is normal to the direction in which the incident wave is travelling, as illustrated in figure 2.1. The direction of the incident wave is chosen as the x -axis of a cartesian coordinate system and the wall intersects the x -axis at $x = 0$. The wave is coming from the negative x -direction. Its sound pressure $p_i(x, t)$ and particle velocity $v_i(x, t)$ are:

$$p_i(x, t) = \hat{p}_0 \exp[i(\omega t - kx)], \quad (2.29)$$

$$v_i(x, t) = \frac{\hat{p}_0}{\rho_0 c} \exp[i(\omega t - kx)], \quad (2.30)$$

where \hat{p}_0 is the absolute value of the initial sound pressure of the incident wave, ω is the angular frequency of the wave, k is the wave number, t is the time, x is the place in the x -axis, ρ_0 is the static value of the gas density, and c is the velocity of sound.

As mentioned before, the reflected wave has a smaller amplitude and its phase has changed. Both changes are described by the reflection factor R . In addition, when defining an expression for the reflected wave, the sign before the wave number k has to be reversed because the direction of travel has reversed. Furthermore, also the sign of the particle velocity must be changed, because $\partial p / \partial x$ has opposite signs for waves travelling in positive and negative direction. The sound pressure $p_r(x, t)$ and the particle velocity $v_r(x, t)$ of the reflected wave can now be expressed in the following way:

$$p_r(x, t) = R \hat{p}_0 \exp[i(\omega t + kx)], \quad (2.31)$$

$$v_r(x, t) = -R \frac{\hat{p}_0}{\rho_0 c} \exp[i(\omega t + kx)]. \quad (2.32)$$

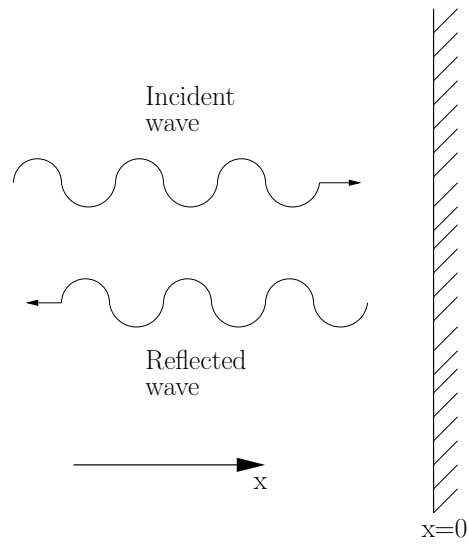


Figure 2.1: Sound reflection, normal incidence [41].

Sound Reflection at Oblique Incidence

A more general case of sound waves whose angles of incidence may be any value, θ_0 , is considered next. Let's assume that a wall normal as well as a wave normal of the incident wave lie in the $x - y$ plane of a cartesian coordinate system, as depicted in figure 2.2.

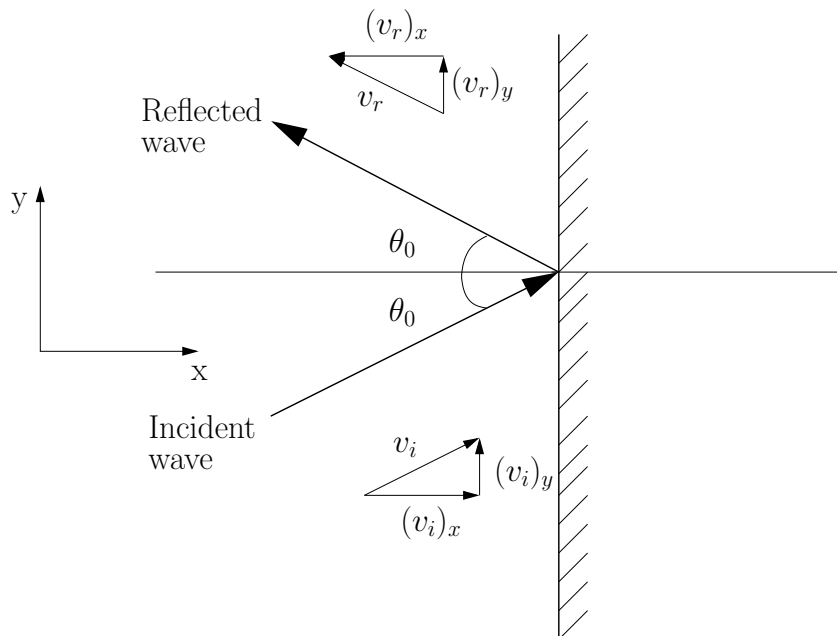


Figure 2.2: Sound reflection, oblique incidence [41].

In this kind of situation, in Eq. (2.29) x is now replaced by x' . The latter belongs to a coordinate system, for which axes are rotated by the angle θ_0 with respect to the $x - y$ system. The result is a plane wave propagating in the positive x' -direction. Now, according to the coordinate transformation formula, x and x' are related by

$$x' = x \cos \theta_0 + y \sin \theta_0, \quad (2.33)$$

and when this is inserted to Eq. (2.29)¹:

$$p_i = \hat{p}_0 \exp[-ik(x \cos \theta_0 + y \sin \theta_0)]. \quad (2.34)$$

A velocity component normal to the wall (x -component) is required for computation of the wall impedance (See Eq. 2.27). This is obtained from the following expression:

$$v_x = -\frac{1}{i\omega\rho_0} \frac{\partial p}{\partial x}. \quad (2.35)$$

When this is applied to Eq. (2.34)

$$(v_i)_x = \frac{\hat{p}_0}{\rho_0 c} \cos \theta_0 \exp[-ik(x \cos \theta_0 + y \sin \theta_0)]. \quad (2.36)$$

Also in the case of oblique incidence, the sign on x must be reversed when the wave is reflected. Furthermore, the pressure and the velocity are multiplied by reflection factors R and $-R$, respectively:

$$p_r = R\hat{p}_0 \exp[-ik(-x \cos \theta_0 + y \sin \theta_0)], \quad (2.37)$$

$$(v_r)_x = -\frac{R\hat{p}_0}{\rho_0 c} \cos \theta_0 \exp[-ik(-x \cos \theta_0 + y \sin \theta_0)]. \quad (2.38)$$

Again, the direction of propagation includes the angle θ_0 with the wall normal.

2.2.2 Diffraction, Scattering, and Diffuse Reflection

Simple laws of sound reflection hold only for walls with an infinite extent. In reality, any free edge of reflecting wall or panel will scatter some sound energy in all directions. The same happens when a sound wave hits any other obstacle of limited extent. Scattered wave spreads more or less in all directions. The phenomenon is called *diffraction*. It is common in room acoustics and sometimes referred also as *sound scattering*. In some connections, diffuse reflection is seen as a consequence of diffraction. For this reason, diffraction is considered here before diffuse reflection itself is discussed.

¹Term $\exp(i\omega t)$, which is common to all pressures and particle velocities, is omitted from this and the following expressions.

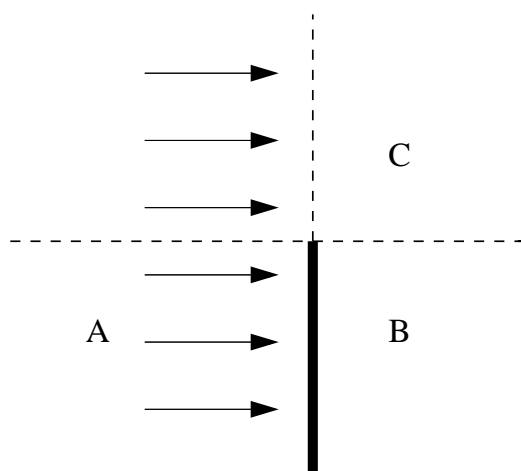


Figure 2.3: Illustration related to diffraction of a plane wave from a rigid half-plane [41].

Diffraction can be introduced in the following way: Let's imagine a rigid plane with one straight edge as depicted in figure 2.3. When this rigid plane is exposed to a plane wave at normal incidence, it can be expected that the plane reflects some sound into region A. At the same time another region, region B, which can be called the *shadow zone*, remains completely free of sound. If the wavelength of an incident sound wave were vanishingly small, the aforementioned situation would be true. In reality, however, a diffraction wave, originating from the edge of the plane modifies this picture. Behind the plane there is still some sound intruding into the shadow zone. Furthermore, in the region C, the plane wave is disturbed by interferences with the diffraction wave. In summary, the boundary between the shadow zone (B) and the illuminated region (C) is not sharp but blurred by the diffraction wave. A similar effect occurs at the upper boundary of region A.

A wall is not often completely plane. It contains regular or irregular coffers, bumps, and other projections. If these are very small compared to the wavelength of the incident sound wave, they do not disturb the specular reflection of the wall. In the opposite case, if irregularities are large compared to the wavelength, each of their faces may be treated as a plane or a curved wall section. Incident sound can then be reflected specularly. There is an intermediate range of wavelengths, however, in which each projection adds a scattered wave to the specular reflection of the whole wall. A large fraction of reflected sound energy will therefore scatter in all directions if the wall has an irregular surface structure, as illustrated in figure 2.4. The term *diffusely reflecting wall* is often used in this context. Diffuse or partially *diffuse reflections* occur also at walls which are smooth and have non-uniform impedance, not only at walls with a geometrically structured surface.

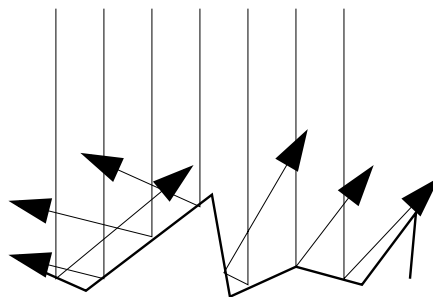


Figure 2.4: Diffusely reflecting wall with an irregular surface structure.

2.2.3 Diffuse Sound Field

A typical sound field in a closed room is composed of many single plane waves. Each of them has its own particular amplitude, phase, and direction. To find the effect of a wall on such a complicated sound field, the reflection of each sound wave should be considered separately. When this has been done, sound pressures of all waves can be added.

Another possibility is to turn on to some simplifications. With the following assumptions, general statements on the effect of the wall on the sound field are allowed: First of all, if the phases of the waves incident on the wall are randomly distributed, it is possible to neglect all phase relations and interference effects caused by them. In this kind of situation, it is sufficient to add or to average energies of the waves which are proportional to the squares of the pressures of the elementary waves. Secondly, if it is assumed that intensities of an incident sound are uniformly distributed over all possible directions, each solid angle element carries the same energy per second to the wall. In such a situation it is possible to speak about *random sound incidence*. The sound field associated with a situation defined above is referred to as a *diffuse sound field* [41], [40], [53].

2.2.4 Terminology

On the grounds of the previous subsections it can now be confirmed, that in room acoustics the term *diffusion* denotes two conceptually different things. On one hand diffusion is a property of a sound field. It describes an isotropy of directional uniformity of sound propagation. Secondly, diffusion is an ability of a surface to scatter incident sound into non-specular directions. Although sound field diffusion may be a consequence of diffusely reflecting boundaries, both items must be well distinguished.

The term scattering is somewhere used in connection with diffraction and elsewhere in connection with diffuse reflection. Among others Dalenbäck et al. [18] have considered different concepts used in context of diffuse reflection. They have defined and grouped

applied terms in the following way:

Diffraction. In a microscopic wave-theoretical view diffraction is one of the causes of diffuse reflection. In applied acoustics diffraction most often means edge diffraction from reflectors and similar objects.

Scattering. Often used in general linear acoustics for the result of diffraction. In applied acoustics this term is used for reflection from a surface with roughness in a more general way.

Diffuse reflection. The most appropriate term to describe the process of reflection from a diffusor or from a diffusive surface.

In this thesis the terms diffuse reflection and scattering are used when reflection from the diffusive surface is considered.

2.3 Expressing Surface Diffusion

Within physically-based computerised prediction, every implementation of diffuse reflection needs to utilise some scattering function. Unfortunately there are not plenty of reliable laboratory measurements about diffusing properties of surfaces which could be used as guidelines in modelling. Usually, only available data are from manufacturers of dedicated diffusers. Therefore, diffusing effects of other surfaces have to be estimated. Often the only possible estimate is to assign diffusion factors in relation to roughness-to-wavelength ratios [18], and to model the scattering function for diffused part of the sound with the Lambert's law.

Although the Lambert's law has been widely used also, for example, in computer graphics, there is no physical background to support it. The Lambert's law is based on empirical observations and describes a perfectly rough or diffuse surface [57]. For these reasons, an alternative, and a more accurate approach would be to use theoretically calculated scattering functions. Of course, measured scattering functions can be utilised if reliable ones are available. In the following subsections, the above mentioned different ways of expressing the diffusion of a surface are discussed.

2.3.1 Lambert's Law

According to the Lambert's law, when directional distribution of reflected or scattered energy does not depend in any way on the direction of an incident sound, the reflection from a surface is totally diffuse. However, as mentioned, in acoustics and particularly in room

acoustics, only partially diffuse reflections occur. Even so, especially when many successive ray reflections from different walls or portions of walls are considered, the assumption of totally diffuse reflections comes often closer to the actual reflecting properties of real walls than that of specular reflections. In particular, with reverberation processes and in reverberant enclosures this is the case [41].

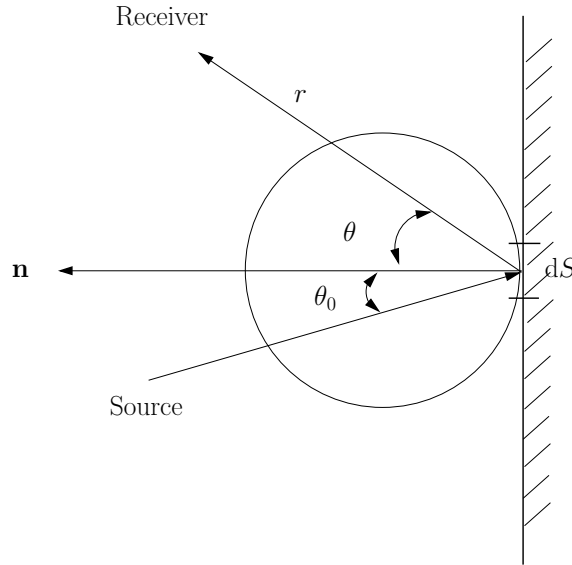


Figure 2.5: Ideally diffuse sound reflection from acoustically rough surface [41].

In order to understand the basic principles of the Lambert's law, the concept of sound ray needs to be known. The ray-concept is explained more thoroughly later in subsection 2.4.2 in context of ray-based room acoustics modelling methods. Here it is enough to know that a sound ray is a small portion of a spherical wave. It originates from a certain point and has a well defined direction of propagation.

When applying the Lambert's law, totally diffuse reflections from a wall take place in the following way [41]. The situation is illustrated in figure 2.5.

If an area element dS is illuminated by a bundle of parallel or nearly parallel rays which make an angle θ_0 to a wall normal and have an intensity I_0 , an intensity $I(r, \theta)$ of the sound which is scattered in a direction characterised by an angle θ , measured at a distance r from dS , can be given by

$$I(r, \theta) = I_0 dS \frac{\cos \theta \cos \theta_0}{\pi r^2} = B dS \frac{\cos \theta}{\pi r^2}, \quad (2.39)$$

where B is so-called *irradiation strength*. The variable B expresses the amount of energy incident on a unit area of the wall per second. Eq. 2.39 is valid if there is no absorption. In other cases, $I(r, \theta)$ has to be multiplied by an appropriate factor $1 - \alpha(\theta)$.

When applying Eq. (2.39), each surface element has to be considered as a secondary sound source. The distance r , which determines intensity reduction due to propagation, has to be measured from the reflecting area element dS . With a specular reflection, this is not a case. In the specular reflection the total length of the path between an initial sound source and a receiver determines the intensity decrease of a sound ray. The observation whether this path is bent or straight is not needed.

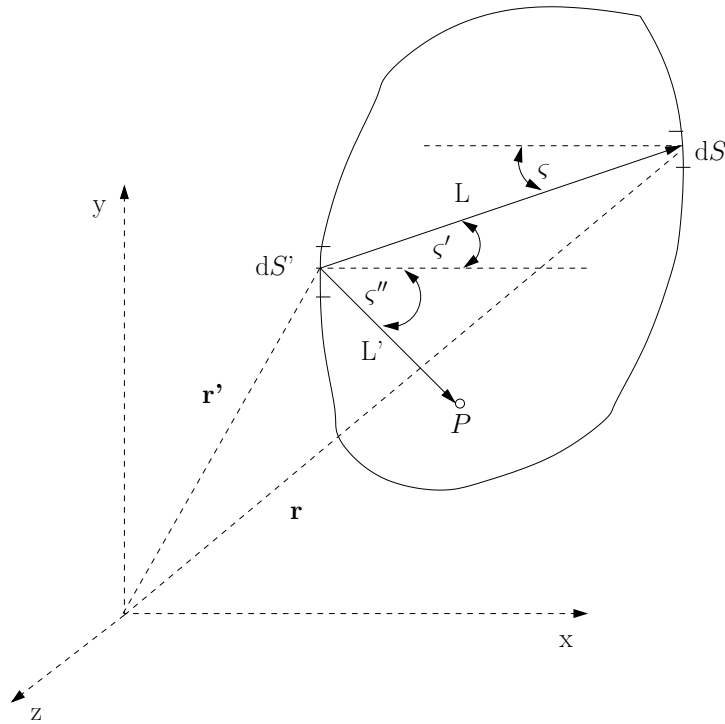


Figure 2.6: Illustration related to the definition of Eq. (2.42) [41].

Next, a situation in an enclosure where the whole boundary is assumed to reflect impinging sound in a completely diffuse manner according to the Lambert's law is considered [41]:

The sound field within a room can be described in a closed form by an integral equation. In order to derive this integral equation, two wall elements dS and dS' are considered. The situation is illustrated in figure 2.6. The room is assumed to be of arbitrary shape. Locations of the wall elements are characterised by vectors \mathbf{r} and \mathbf{r}' . Straight line connecting them has a length L . Angles between this line and wall normals of dS and dS' are denoted in the following by ζ and ζ' . When the element dS' is irradiated by energy $B(\mathbf{r}')dS'$ per second, fraction σ of it is re-radiated from the dS' into a space. σ , the *reflection coefficient*, is

defined as

$$\sigma = 1 - \alpha. \quad (2.40)$$

The absorption coefficient α and hence the reflection coefficient σ are supposed to be independent of angles ζ and ζ' .

According to the Lambert's law, intensity dI of the energy re-radiated by the dS' and received at dS is

$$dI = B(\mathbf{r}')\sigma(\mathbf{r}')\frac{\cos\zeta'}{\pi L^2}dS', \quad (2.41)$$

where $B(\mathbf{r}')$ is the irradiation strength as a function of location \mathbf{r}' and $\sigma(\mathbf{r}')$ is the reflection coefficient as a function of location \mathbf{r}' . ζ' and L have been explained before and also in figure 2.6.

Multiplication of Eq. (2.41) by $\cos\zeta$ and integration over all wall elements dS' gives the total energy per second and unit area received at \mathbf{r} from the whole boundary. The following relation is achieved by adding a direct contribution B_d from a sound source:

$$B(\mathbf{r}, t) = \frac{1}{\pi} \int \int_S \sigma(\mathbf{r}')B\left(\mathbf{r}', t - \frac{L}{c}\right) \frac{\cos\zeta\cos\zeta'}{L^2}dS' + B_d(\mathbf{r}, t). \quad (2.42)$$

The previous expression takes into account the finite travelling time of the sound energy from the transmitting wall element dS' to the receiving one dS by replacing time argument t with $t - L/c$, where c is a velocity of sound.

Eq. (2.42) is an inhomogeneous, fairly general integral equation for the irradiation strength B of the wall. It contains both a steady state case and that of a decaying sound field. After solving this equation, energy density $w(\mathbf{r}, t)$ as a function of location \mathbf{r} and time t at any point P inside a room can be obtained from

$$w(\mathbf{r}, t) = \frac{1}{\pi c} \int \int_S \sigma(\mathbf{r}')B\left(\mathbf{r}', t - \frac{L'}{c}\right) \frac{\cos\zeta''}{L'^2}dS' + w_d(\mathbf{r}, t), \quad (2.43)$$

where L' is a distance from the surface element dS' to a receiver P , ζ'' is the angle of sound which irradiates from the surface element dS' to the receiver, and $w_d(\mathbf{r}, t)$ is the direct contribution from some sound source to the energy density at the receiver point P .

Closed form solutions for the integral equation are available only for simple room shapes. For this reason, in general, the integral equation Eq. (2.42) must be solved numerically. One example of numerical solution methods has been presented in [40].

2.3.2 Theoretically Calculated Scattering Functions

Another choice for the application of the Lambert's law is to utilise theoretically calculated scattering functions. Calculations can be included in the prediction and solved for the actual case. However, usually this means a much more complicated computation scheme [18].

For example Cox and D'Antonio [14] have gathered together methods for defining theoretically calculated scattering functions from isolated surfaces. These are discussed next. The emphasis is on frequency domain models, but also some time domain methods are considered. The presentation of Cox and D'Antonio [14] has been used as a reference, if not otherwise mentioned.

Boundary Element Methods

The most accurate model for predicting scattering from a diffusing surface is the Boundary Element Method (BEM). It is based on the Kirchhoff-Helmholtz integral equation (KHIE). The Kirchhoff-Helmholtz integral equation formulates the pressure at a point as a combination of the pressure direct from sources and surface integral of the pressure and its derivative over reflecting surfaces. The pressure $p(\mathbf{r}_r)$ at position \mathbf{r}_r is given by the following single frequency form of the integral equation :

$$\left. \begin{array}{l} \mathbf{r}_r \in RG_e \quad p(\mathbf{r}_r) \\ \mathbf{r}_r \in RG_s \quad \frac{1}{2}p(\mathbf{r}_r) \\ \mathbf{r}_r \in RG_i \quad 0 \end{array} \right\} = p_i(\mathbf{r}_r, \mathbf{r}_0) + \int_S p(\mathbf{r}_s) \frac{\partial G(\mathbf{r}_r, \mathbf{r}_s)}{\partial n(\mathbf{r}_s)} - G(\mathbf{r}_r, \mathbf{r}_s) \frac{\partial p(\mathbf{r}_s)}{\partial n(\mathbf{r}_s)} dS, \quad (2.44)$$

where $\mathbf{r}_r = \{x_r, y_r, z_r\}$ is a vector which describes the location of the receiver, $\mathbf{r}_0 = \{x_0, y_0, z_0\}$ is a vector describing the location of the source, $\mathbf{r}_s = \{x_s, y_s, z_s\}$ is a vector for a point on the surface, $p(\mathbf{r}_s)$ is the pressure at \mathbf{r}_s , $p_i(\mathbf{r}_r, \mathbf{r}_0)$ is the direct pressure radiated from the source at \mathbf{r}_0 to the receiver at \mathbf{r}_r , G is the Green's function, n is the normal to the surface pointing out from the surface, RG_e is the external region, RG_s is the surface and RG_i is the interior of the surface.

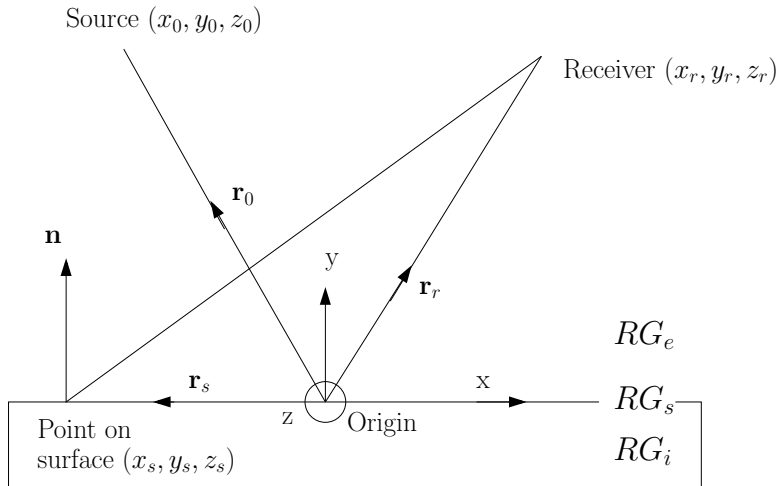


Figure 2.7: Geometry related to BEM prediction models [14].

The geometry related to the previous integral equation is illustrated in figure 2.7. The first term on the right-hand side of Eq. (2.44) represents the direct pressure. The second term, where the integral is carried out over the surface, gives contribution of the reflected energy to the pressure at \mathbf{r}_r . As mentioned, the form of Eq. (2.44) is a single frequency form. This means that the system is in steady state condition so that a time variation $\exp(i\omega t)$ can be neglected. The Green's function G gives, how the pressure and its derivative propagate from one point in a space to another point.

The integral equation, Eq. (2.44), includes three possible cases:

1. $\mathbf{r}_r \in RG_e$, the point \mathbf{r}_r is external to the scattering surface
2. $\mathbf{r}_r \in RG_s$, \mathbf{r}_r is on the surface
3. $\mathbf{r}_r \in RG_i$, \mathbf{r}_r is internal to the scattering surface.

The integral part of Eq. (2.44) has two terms. One involves the surface pressure $p(\mathbf{r}_s)$ and the other the surface pressure derivative $\partial p(\mathbf{r}_s)/\partial n(\mathbf{r}_s)$. For a locally reacting surface² the derivative of the surface pressure is related to the surface pressure by the surface admittance, which can be expressed in terms of equation in the following way:

$$ikp(\mathbf{r}_s)\beta'(\mathbf{r}_s) = \frac{\partial p(\mathbf{r}_s)}{\partial n(\mathbf{r}_s)}, \quad (2.45)$$

where the surface admittance is denoted by β' . In BEM modelling, quantities are defined in terms of an outward pointing normal. Surface admittances, however, are normally defined with an inward pointing normal. This difference is signified here by a prime: $\beta' = -\beta$, where β is the more usual surface admittance. The definition of an outward pointing normal also affects to the interrelations between the admittance and the surface reflection factor. It is relevant when implementing the Kirchhoff solution.

There exist various solutions for the BEM. The general solution requires application of Eq. (2.44) twice. First, the surface pressures $p(\mathbf{r}_s)$ on scattering surfaces need to be found. After that a numerical integral is carried out over the surface pressures to determine the pressures at desired external points. When determining the surface pressures, it is important to notice that they depend not only on the incident sound field, but also on each other. To model mutual interactions across the surface, the surface is usually discretised into a number of surface/boundary elements. It is assumed that the pressure across these elements is constant. In order to prevent errors in representing continuous pressure variation by a set of discrete values the elements must be chosen to have sufficiently small dimensions. For very simple surfaces this is usually achieved by making the elements smaller than a

²An assumption of a local reaction means that the surface admittance is independent of the incident and the reflected pressure wave.

quarter of wavelength in size. When the surface has been discretised, a set of simultaneous equations can be set up with one equation for each boundary element. These equations will be for the surface pressures with \mathbf{r}_r being taken from positions on the surface in the middle of each element.

In addition to the general solution there exist also several solutions derived for specific situations. For example, a solution for thin panels has been presented by Terai [84]. Periodic formulations have been derived as well [44].

Kirchhoff Approximation

In order to reduce solution time of the BEM, faster methods for solving the simultaneous equations which determine the surface pressures have been derived. For example in optics, the Kirchhoff approximation has been used to determine the propagation of light through an aperture. The Kirchhoff approximation yields the wave function and its derivative across an aperture as unaltered from an incident wave. Both the wave function and its derivative are assumed to be zero on a surround defining the aperture. When this kind of approach is adopted to acoustics it yields reasonably accurate results for far field scattering. However, there are cases where the method is imprecise. Therefore, it should be applied with care.

The Kirchhoff approximation can be introduced by considering a large planar surface with constant surface impedance across the whole surface. The pressure on the surface $p(\mathbf{r}_s)$ can be given according to the definition of the pressure reflection factor with the following expression:

$$p(\mathbf{r}_s) = [1 + R(\mathbf{r}_s)]p_i(\mathbf{r}_s, \mathbf{r}_0), \quad (2.46)$$

where R is the pressure reflection factor of the surface. This equation is sometimes referred to as a *Kirchhoff boundary condition*. In case that a surface is totally non-absorbing, the surface pressure is simply twice the incident sound pressure. On the contrary, on a completely absorbing surface the surface pressure is just the incident sound pressure. When solving the surface pressures with the Kirchhoff approximation Eq. (2.46) is substituted into Eq. (2.44) and the resulting expression is then solved with a straightforward numerical integration over the front face.

Application of the Kirchhoff approximation requires some further assumptions in addition to those explained until now. First of all, it is necessary to suppose that the diffusing surface is thin, since the pressure from sides of the surface is neglected. Furthermore, the surface needs to be assumed large compared to the wavelength. The pressure on the rear of a panel can then proposed to be zero. When applying the Kirchhoff approximation problems thus arise when the surface has a significant thickness or is small compared to the wavelength. This is a case also if the surface has a rapidly changing surface impedance.

Furthermore, oblique sources and receivers cause troubles.

Methods Applying Further Simplifications

If the Kirchhoff boundary conditions are assumed, numerical integration can be further simplified by applying the *Fresnell diffraction*. The Fresnell diffraction is designed to work with non-absorbing panels. When applying the Fresnell diffraction, approximations lead to a solution which includes integration that does not have an analytical solution. In the past this was overcome by using the *Fresnell integrals*. These integrals are numerical solutions which are readily available in tables. These days computer power has increased to such an extent that the Kirchhoff approximation might be used and so there is only a little point in using the Fresnel integrals. However, if the speed is at a premium some neat and simple shortcuts for solving the Fresnell integrals exist. These have been proposed by Rindel [64].

One more simplified method is called the *Fraunhofer* or the *Fourier solution method*. This is valid only in the far field. The Fraunhofer solution is most useful when analysing surfaces which do not have unity reflection coefficient. A simplified form of the Fraunhofer solution is called also the Fourier theory, since integration in this form is essentially a Fourier transform.

Finite Element Analysis

The Finite Element Analysis (FEA) [82] uses volumetric meshes instead of surface meshes. It is much slower than the boundary element modelling when dealing with exterior domain acoustics problems, such as scattering from diffusing surface. The FEA is advantageous in fluid and structural motion.

Edge Diffraction Models

Edge diffraction models produce scattering from wedges and simple shapes. The total field of a plane rigid surface can be seen as a sum of a direct sound, specular reflections, and edge diffraction components [77]. As a consequence, it is possible to solve the scattering problem by integrating over edges present in a diffusely reflecting surface. If high orders edge diffraction needs to be considered, the method becomes rather slow. However, advantageous is that an edge diffraction model leads directly to a sampled impulse response. Thus, it is particularly useful when broadband time domain scattering is needed to be computed. It is also feasible if the results are to be integrated into geometric room acoustics models.

Wave Decomposition and Mode-Matching Approaches

If the spatial distribution of a diffusing surface is known, a wave field decomposition of an acoustic wave can be carried out. When this type of theory is applied, it is normal to assume that the structure of the diffusing surface is periodic. When this assumption has been made, it is possible to decompose a scattered wave into different diffraction lobes by using the Fourier decomposition. Then, simultaneous equations into diffraction lobe scattered amplitudes can be set up and solved.

Mode-matching approaches [75] are particularly powerful when predicting effects of large arrays of periodic structures. The size of the problem to be solved gets much smaller than with a BEM model. Wave decomposition and mode-matching approaches offer an alternative approach to the boundary element models. The BEMs are, however, more useful since they can be applied to arbitrary surfaces.

Random Roughness

For large-scale surfaces with small roughness it may be advantageous to use a statistical approach. In this, the surface is only determined by some shape statistics [11]. When applying a random roughness model, there needs to be a sufficiently wide sample of surface roughness. Otherwise shape statistics do not properly represent the surface.

Among others Cox and D'Antonio [12] and Embrechts et al. [22] have used statistical approaches to model scattering. Cox and D'Antonio have investigated random rough surfaces with respect to design of fractal diffusers. Embrechts et al. have been interested in scattering coefficients from surfaces. Both of these approaches assume the Kirchhoff boundary conditions. When applying the random roughness models, it is essential that surface gradients are not too steep. Otherwise second and higher order reflections become important and the statistical approach breaks down.

Boss Models

Examples of hybrid models are boss models [11], which use a deterministic solution for scattering from a single element. The distribution of the elements is modelled in a statistical manner. The best known approach has been developed by Twersky [86]. With the proposed method it is possible to model high order scattering across all frequencies, both in 2D and 3D. Up to date versions of the theory enable scattering from different sized bosses. Problems of the model relate to situations where complex surfaces are represented by a series of regular-sized bosses.

2.3.3 Measured Scattering Functions

As mentioned in the beginning of this section, a lack of reliable measured data about diffusing properties of different materials has been a real problem in the field of diffuse reflection modelling. Surface scattering elements have been used accidentally or by design in rooms for centuries, but only in recent decades concerted efforts have been made into developing methods for measuring scattering from these surfaces and into characterising scattering on the grounds of measurements [14].

In this section some measuring methods are discussed. Also characterisation of diffuse reflections with the aid of two different measures: a *diffusion coefficient* and a *scattering coefficient* is considered.

Measurement of Scattered Polar Responses

Systems used for measuring reflections from surfaces have been based on techniques which use a source to irradiate a test surface, and measurement microphones at radial positions in front of the surface to record pressure impulse responses. Microphone positions usually map out a semicircle or a hemisphere. After measuring the pressure impulse responses, time gating is used to separate the reflections from the incident sound.

Impulse responses can be measured in various ways. The most common method uses a Maximum Length Sequence (MLS) signal. Swept sine waves, time delay spectroscopy or pulses are also possible choices. However, MLS signals are currently the most efficient to be used if time variance and non-linearity are not an issue [14].

With the aid of the described measurement system a polar response of a surface can be generated. A polar response characterises reflecting properties of the surface. It tells designers how a surface reflects sound. Polar responses contain a large amount of data since a different polar response is required for each frequency band and for each angle of incidence [14]. It would be useful, if the scattering could be characterised with single coefficients instead of the huge amount of polar data. For this purpose two coefficients, the diffusion and the scattering coefficient, have been developed.

Despite an obvious need to quantify surface diffusion in both computer modelling and diffuser design, no standard definition of the diffusion or the scattering coefficient, and no standard method for measuring or predicting such coefficients existed before year 2001. However, through co-ordinated efforts of two working groups under International Organisation for Standardisation (ISO) and Audio Engineering Society (AES), basis for scattering has now been established [1], [2]. As a result, the already mentioned two different measures, the diffusion coefficient and the scattering coefficient, have been introduced with somewhat different applications [65], [13].

Diffusion Coefficient

The diffusion coefficient (d) aims on condensation of polar data. AES has derived a method for measuring the diffusion coefficient of a surface as a function of the angle of incidence [2], [65]. This method has become the first ever international standard³ on characterisation of surface scattering/diffusion [13].

The diffusion coefficient measures the quality of reflections produced by a surface by measuring similarity between a scattered polar response and a uniform distribution [14]. The diffusion coefficient can thus be used to characterise the uniformity of scattering from the surface [65]. The measure is intended mainly for evaluation of quality of sound diffusers and in situations where it is important to achieve scattered first-order reflections, e.g. in sound studios [14].

Considerations that led to the proposed diffusion coefficient have been described in [30]. The diffusion coefficient is derived from the autocorrelation function of the polar response measured on a semicircle or a hemisphere. The coefficient can take values between 0 and 1. $d = 1$ means that the polar response is completely uniform [65].

Limitations of the diffusion coefficient relate to the fact that the measurement method does not distinguish between surface scattering and edge scattering. Both of these are included in the measurement results. For this reason it is important that a test sample is large enough so that surface effects rather than edge effects are prominent in the scattering when the method is applied [65].

Scattering Coefficient

The scattering coefficient (s) is a measure of the amount of sound scattered away from a particular direction or distribution [14]. In year 2004, ISO has standardised a measurement method for a random incidence scattering coefficient.

In this method the scattering coefficient is measured in a reverberation chamber [1], [65]. The method is based on an idea proposed by Vorländer and Mommertz [90]. It utilises a variance of a sound field when a test surface is moved [13]. When applying the method, the scattering coefficient is defined as one minus the ratio between the specularly reflected acoustic energy and the total reflected acoustic energy. When measured in an approximate diffuse sound field, the scattering coefficient is called the random-incidence scattering coefficient. Values of this coefficient can vary between 0 and 1. The scattering coefficient, measured with the previously described method, is meant to be used to characterise the degree of scattering due to roughness or irregularity of the surface. Scattering due to diffraction from the edges is not included in the coefficient [65].

³Published in 2001

The scattering coefficient has the greatest similarity with coefficients required as inputs to geometric room acoustics models [14]. According to Rindel [65] the scattering coefficient gives the quantity of scattered reflections, which may be sufficient to be used in room acoustics computer models.

Contrasting Diffusion and Scattering Coefficients

The scattering coefficient s and the diffusion coefficient d don't have a direct relationship. A high value of d implies that s is also high whereas a high value of s can be combined with any value of d [65]. It would be useful to be able to translate between these coefficients. For example Mommertz [55] has forwarded a method where correlation between pressures scattered from a test sample and a plane surface are utilised. The proposed method allows the scattering coefficient s to be obtained from polar responses.

2.4 Main Methods of Room Acoustics Modelling

In the previous section, some methods for predicting scattering from diffusely reflecting surfaces were presented. Now methods which are commonly used for predicting a response of an entire room are discussed. Whether presented methods are suitable for modelling scattering/diffuse reflections is not considered in detail here. Suitability of different methods for this purpose is discussed in chapters 3 and 5.

2.4.1 General Issues about Room Acoustics Modelling

A general approach to room acoustics modelling is based on the impulse response (IR) of a space. Several different methods have been developed for prediction of the room impulse response (RIR). These methods can be divided into three categories, as depicted in figure 2.8: 1. Methods based on the concept of a sound ray, 2. Radiosity method, and 3. Methods that rest on a general solution of the wave equation. Different methods are suitable for different problems.

Room acoustics modelling can be done for various purposes. For example, when designing new spaces, like concert halls, room acoustics modelling helps to find out acoustical characteristics of a space. From the modelled room impulse response parameters, such as reverberation time (RT), early decay time (EDT), clarity (C), definition (D), center time (CT), strength (S), lateral energy fraction (LEF), and inter-aural cross-correlation (IACC), can be defined. These parameters characterise acoustics of the modelled space [60].

Sometimes it is desirable that modelled room acoustics can also be listened to. When an audible result is sought for, RIR modelling can be seen as a part of an auralisation process,

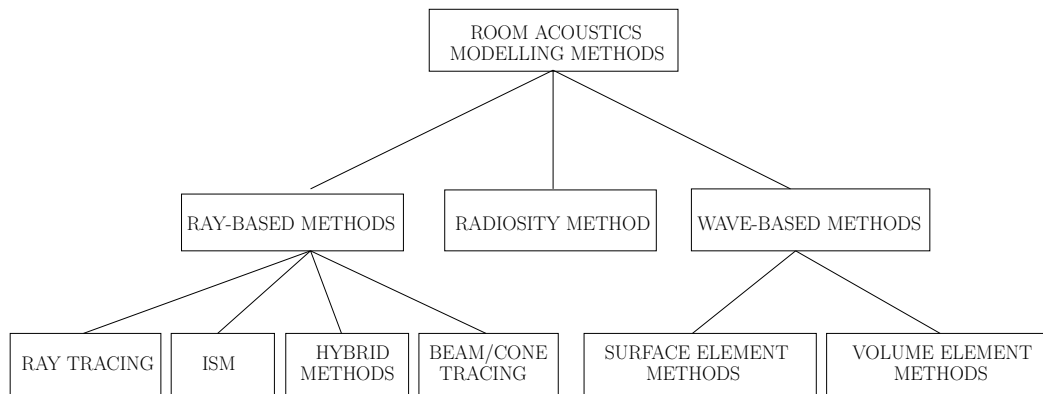


Figure 2.8: Room acoustics modelling methods.

as illustrated figure 2.9. The term auralisation is normally used in analogy with visualisation to describe rendering of audible sound fields [34]. By convolving modelled RIR with anechoically recorded audio, an audible result is achieved. Modelling of a sound source and a receiver can be combined to the RIR computation stage. There exist several different reproduction techniques. These include binaural reproduction through headphones [29], binaural cross-talk canceled reproduction over loudspeakers [54], [26] and multichannel loudspeaker reproduction [62], [50]. For dynamic auralisation, the RIR must be updated in real time. This implies recomputation of the RIR, and interpolation of it in the convolution process [79].

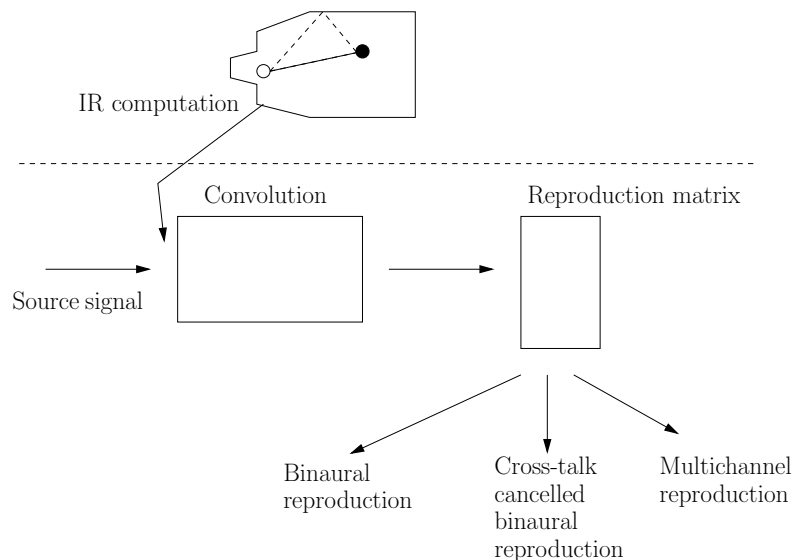


Figure 2.9: Auralisation system [79].

Choosing suitable modelling methods for predicting a RIR is not simple. Various things should be taken into account. First of all, the goal of modelling must be well defined. Is the purpose to model acoustics of a space highly accurately or is it enough that the acoustics is simulated more approximately? Also, available computational resources and memory capacities need to be found out. Furthermore, properties of an acoustical space which is going to be modelled should be taken into account. Acoustical spaces include single room and multi room spaces with simple and complex geometries and boundary conditions. Furthermore, if modelling is done for auralisation purposes it is important to notice that for a naturally sounding sound, a wide bandwidth is required. Luckily the frequency resolution of human hearing decreases for higher frequencies. Computational methods should exploit this characteristic. Furthermore, modelling methods should take an advantage of the fact that early and late parts of an IR can be modelled separately with different methods. The late part of the response is usually much more complex, computation-wise, but less important perceptually. Perceptual weight is greatest for the direct sound and for the first early reflections. In practice, it is difficult to apply a single method to all cases and to the entire frequency region. This is true especially when there are high demands on fast processing [79].

2.4.2 Ray-Based Modelling Methods

Ray-based modelling methods are built on the concept of a sound ray. The sound ray means a small portion of a spherical wave with a vanishing aperture which originates from a certain point. This sound ray has a well-defined direction of propagation and it is subject to the same laws of propagation as a light ray, despite the fact that it has a different propagation velocity. Total energy conveyed by the ray remains constant, provided that the medium itself does not cause any energy losses. However, the intensity within a diverging bundle of rays falls as $1/r^2$, as in every spherical wave, where r denotes the distance from its origin [41].

Ray-based modelling methods are grounded on geometrical room acoustics. For example, Dalenbäck [16] has defined the geometrical room acoustics in the following way:

The geometrical room acoustics exploits the concept of wavefront⁴. Common to all methods based on the geometrical room acoustics is the assumption that an amplitude across the wavefront varies only slightly. Also, the curvature of the wavefront is supposed to be substantially larger than the wavelength. Use of the rays is justified by the Fermat's principle, which states that in the case of homogeneous, isotropic media, sound travels by the shortest path which is possible [61], [16]. Furthermore, the geometrical room acoustics

⁴The concept of wavefront has been explained in subsection 2.1.3.

rests on the Huygens principle. According to this, a new wavefront can be constructed by placing elementary sources along the previous wavefront [16].

According to Dalenbäck, there exists also a variant of the geometrical room acoustics. In this, a more practically oriented approach, the Huygens principle is not used [16]. As a consequence, when applying this approach, the phase of a sound signal is not allowed to be taken into account. Furthermore, all surfaces must be large in comparison to the wavelengths of interest [15]. The surfaces must be smooth and have low absorption factors in order to render sound rays distinctly [6]. In addition, locally reacting surfaces need to be assumed. This is supposed because the sound ray must be affected only by surface absorption at the point of impact. Furthermore, the phase of a surface reflection factor should be neglected. In basic solutions, point sources are used. Sound sources must be placed far from the reflecting surfaces. This last constraint follows from requirements of the wavefront curvature [61], [16]. The sound signals need to be assumed to be wideband signals. Wave-related phenomena, such as interference, are not accounted for [15]. Because power summation of elementary ray contributions is used, incoherent impulses must be assumed [41].

Well-known ray-based, and thus also geometrical room acoustics -based, modelling methods are image-source method (ISM), ray tracing, hybrid methods and cone-/beam-tracing method. These are considered next in separate subsections.

Image Source Method

The image source method (ISM) is one of the most common ray-based modelling methods. Allen et al. [4] have shown that the image source solution gives an exactly correct solution for a rectangular room with rigid walls. According to Svensson et al. [79], image source presentation can fulfill the boundary conditions exactly, if two semi-infinite planes are connected so that the interior corner that is constructed has an angle of 180, 90, 60, 45, 36, ... degrees, and if the walls are either rigid or ideally soft. However, in reality, image sources complemented by edge sources give a correct solution for a non-rectangular room with flat rigid walls [78].

The concept of image sources has been applied to various field problems in electromagnetic and acoustic wave propagation. It has been extended to arbitrary geometries with plane walls, and a number of papers, [28], [4], [8], [46], [35], [76], among others, have applied this to room acoustics. The concept is based on the principle that a source can be represented by a source and so-called image sources that radiate in a free space. In other words, the source is reflected against all surfaces in a room in order to find reflection paths from the sound source to a listener. The principle is illustrated in figure 2.10.

After finding the image sources, a visibility check and obstruction tests must be per-

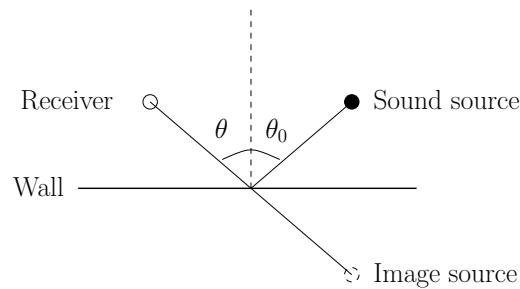


Figure 2.10: Creating an image source.

formed [79]. In the visibility check it is examined that each image source can be seen through a reflecting plane as depicted in figure 2.11. A reflection point must thus be inside a finite plane. The obstruction test is done by forming an actual reflection path and by checking that it does not intersect any surface in the room. Also this is illustrated in figure 2.11. Noteworthy is, that image sources are not dependent on the listener's position and only the visibility of each image source may change when the listener moves [69]. Boundary conditions of the walls are fulfilled at positions in a free space that represent the walls. The amplitudes of the image sources are adjusted at these points accordingly [79].

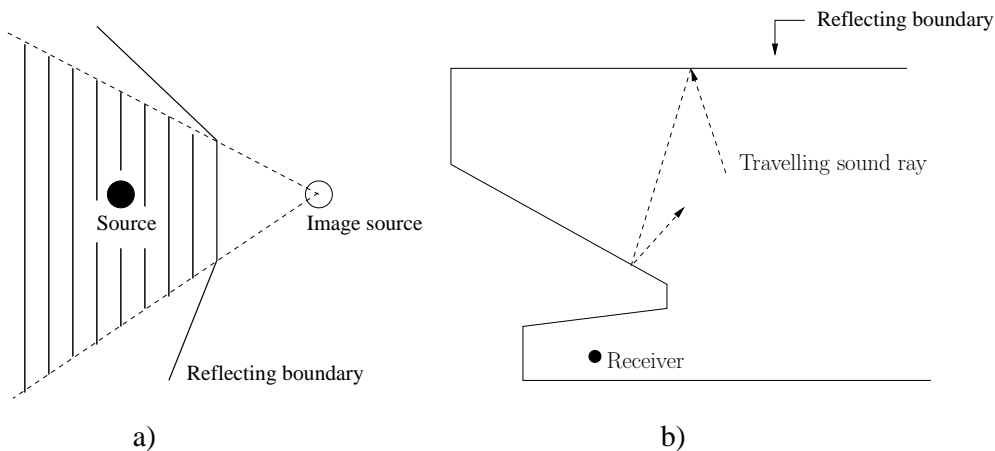


Figure 2.11: a) Region where the listener must be for the image source to be visible [8]. b) Balcony obstructing the sound [8].

All possible sound reflection paths should be discovered in order to model an ideal IR. An advantage of the ISM is that it really finds all the paths. However, computational requirements are such that only a set of early reflections can be found in practice. Maximum achievable order of reflections depends on a room geometry and on available computation capacity [69].

When applied to dynamic situations, use of the ISM causes the modelled sound field to be discontinuous. One reflection will suddenly disappear or emerge every time the receiver passes a zone boundary. This is one of the signs that the ISM is an approximation, even if it is asymptotically correct for high frequencies [79]. Another big drawback of the image source concept is that it can not handle diffuse reflections/surface scattering [69].

Ray Tracing

Another well-known ray-based algorithm for simulating high-frequency behaviour of an acoustic space is the ray tracing (See [36], [37], [20], [38], [88], [47], for example). It applies Monte Carlo simulation to sample reflection paths and gives thus a statistical result. By the ray tracing also higher order reflections can be searched for. However, there is no guarantee that all paths will be found [69].

There are several variations of the algorithm. In the basic solution sound rays emitted by a sound source are reflected at surfaces according to certain rules. The listener keeps track of which rays have penetrated it as audible reflections. A specular reflection is the most common reflection rule [69]. More advanced methods which include some diffusion to the algorithm have also been developed, and are discussed in detail in section 3.1.

In the ray tracing the listeners are typically modelled as volumetric objects, like spheres or cubes, but the listener may also be planar. The listener can be of any shape in theory as long as there are enough rays to penetrate the listener to achieve statistically valid results. The sphere is in most cases the best choice. It provides an omnidirectional sensitivity pattern and is also easy to implement [69].

Hybrid Methods

The hybrid methods combine the ISM and the ray tracing. The method presented by Vorländer et al. [89] is an example of these kind of approaches. The hybrid methods are based on an arrangement where the first reflections are computed with the image sources whereas the late reflections are handled by the ray tracing. Such an approach guarantees that the accuracy of the ISM is exploited for the early part of a response whereas at the same time exponential growth of the number of image sources is avoided [69].

Beam/Cone Tracing

The beam tracing has evolved from the ray tracing. As in the ray tracing, a number of rays are emitted from the source. Adjacent rays are treated as constructing a beam, a cut-out of a wavefront. Each ray is checked for plane-hits and a hit with one of the finite reflection planes causes a specular reflection of the ray. New children rays are generated when two

adjacent rays hit different walls. The incident beam is thus split-up into two re-radiated beams. Whenever a receiver is inside one of the beams, a hit is registered. Such a hit represents a valid image source [79].

Early versions of the beam tracing were approximate. They used just single rays, as in the ray tracing, with attached circular (cone tracing) or triangular (beam tracing) cross-sections that were growing along the propagation [74], [25]. When the beams hit an edge, no split-up was performed. Split-up has been later explored in [19] and [85], for example.

The beam/cone tracing algorithm is more efficient for finding allowed image sources than the classical ISM. However, even larger computational gains can be achieved by subdividing a volume into sub-domains, as have been done in [5] and [69], for example.

2.4.3 Radiosity Method

The radiosity method has been used for a long time in studies of heat and light radiation, and also in computer graphics. Application of this method and developments to room acoustics have been described in the following papers: [40], [45], [24], for example. The radiosity method belongs to the methods which are based on the geometrical room acoustics. However, at some points, the radiosity differs from conventional ray-based methods and can be, for this reason, classified to its own category and considered in its own subsection here. The method is based on the assumption of Lambertian diffuse surfaces. Svensson and Kristianssen [79] have introduced the radiosity in the following way:

The radiosity method is very closely related to the ray tracing. However, instead of launching a large number of rays and letting them sample boundary surfaces, the radiosity method divides boundaries into smaller elements. After this subdivision the rays are sent between these predefined surface elements. Contribution strengths, which are called *form factors*, are computed for each element-to-element combination. Intensities, incident on each element can be described by an integral equation as a sum of the contributions from all other elements and from the original source.

The integral equation for a discretised model⁵ can be expressed in connection of the radiosity method as

$$I_i(t) = I_{0 \rightarrow i}(t) + \sum_{j: j \neq i} m_{j \rightarrow i} \sigma_j I_j \left(t - \frac{r_{j \rightarrow i}}{c} \right) \Delta S_j, \quad (2.47)$$

where $I_i(t)$ is the incident sound intensity at element i at time t , $I_{0 \rightarrow i}(t)$ is the contribution straight from a source at that time at element i , $m_{j \rightarrow i}$ is the form factor between elements j and i , which can be expressed for completely diffusely reflecting walls according to the

⁵Compare to Eqs. (2.42) and (2.43.) presented already in subsection 2.3.1.

Lambert's law:

$$m_{j \rightarrow i} = \frac{\cos \theta_i \cos \theta_j}{\pi r_{j \rightarrow i}^2}, \quad (2.48)$$

σ_j is the reflection coefficient, $I_j(t - \frac{r_{j \rightarrow i}}{c})$ is the contribution from a single surface element j , t is the time, c is the velocity of sound, $r_{j \rightarrow i}$ is the distance between sending (j) and receiving (i) element, ΔS_j is the area of j th surface element, θ_j is the angle of a sound ray which irradiates from the surface element j and θ_i is the angle of the sound ray which illuminates the surface element i .

When applying the radiosity method, surface elements need not to be smaller than a wavelength. They merely need to be small enough so that the form factor doesn't vary too much across the elements. The basic formulations such as the Lambert's diffusion indicated by Eq. (2.48) assume that reradiation angle is independent of the incidence angle [79]. In order to include specular reflections as well as diffuse reflections, more complicated relationships are possible and also necessary [87]. Furthermore, in the radiosity, intensity at a surface is assumed to be the same as in an incident ray. This is the Kirchhoff diffraction approximation⁶. In reality this is true only for an element which is part of a large surface. As a consequence of edge diffraction, surroundings of each element modify sound field at the surface. More complicated form factors could, in principle, take such an effect into account. The form factors would then be frequency dependent [79].

2.4.4 Wave-Based Methods

Wave-based methods are grounded on the general solution of the wave equation. Analytic solutions for the wave equation are available only for very few simple cases. Therefore, usually, numerical methods must be applied. Numerical solution methods either divide the boundary which surrounds a space into surface elements or divide the space into volume elements. Since computational efforts increase rapidly with increasing bandwidth, these methods are primarily used only for the low-frequency range [79].

Computational perspective is not the only one which supports the use of the general solution of the wave equation only for the low-frequency range. As mentioned already in the beginning of this section, the frequency resolution of human hearing decreases at high frequencies. As a consequence, detailed interference patterns can not be anymore perceived at that frequency range. The general solution offers a detailed sound field. As a result of the aforementioned characteristics of human hearing, such a detailed solution would, however, be useless at high frequencies. This is true at least as long as the sound field contains several interfering components. For this reason, the general solution for the low-frequency range

⁶See subsection 2.3.2.

combined with other approximate methods for mid-to-high frequency range makes sense [79]. Such an approach has been applied in [81] and [7], for example.

Surface Element Methods

Some surface element methods were considered already in subsection 2.3.2 in context of predicting scattering from a single diffusely reflecting wall. Here the surface element methods are discussed from the room impulse response prediction point of view.

In all surface element methods a surface is subdivided into elements. These elements typically need to be smaller than approximately $1/8$ of a wavelength. An advantage of the surface element methods is that open space needs no special considerations [79]. Conventionally surface element formulations for room acoustics modelling have been determined in the frequency domain, but there exist also some time domain solutions. These have been presented by Tanaka et al. [83] and Svensson et al. [80], for example.

In terms of contributions from sound pressure and normal particle velocity on boundary surface of a modelled space the KHIE gives the sound field in an interior or exterior space. This is exploited by the BEM, the most common of the surface element methods. In room acoustics modelling the BEM can be understood as a method which gives a numerical solution of the KHIE [79].

There is some similarity between the surface element methods and the radiosity method. Important point to notice is, however, that in the radiosity the computed quantity is intensity, averaged over elements that are large compared to a wavelength. On the contrary, in the surface element methods, surface elements must be smaller than the wavelength. Quantities that are computed are sound pressure and particle velocity [79].

Volume Element Methods

A number of numerical methods which subdivide an air volume into volume elements have been developed for solving the wave equation. In subsection 2.3.2 the application of these kind of approaches for predicting scattering from a single diffusely reflecting wall was already shortly discussed. It was mentioned that these methods are much slower than for example BEM and that they are most suitable for modelling fluid and structural motion. Anyway, the volume element methods are quite popular in the field of room acoustics modelling.

Also, when applying the volume element methods, it is important that the elements are small enough. 6-10 or even more elements per wavelength are needed. Arbitrary partial differential equations can be handled by several of the methods. This means that including medium losses, non-linearities, and other phenomena is straightforward [79].

Modelling of open spaces is a specific problem for the volume element methods. Late research has put much effort into developing absorbing boundary conditions so that an open-ended air volume could be truncated and modelled with such boundary conditions [79]. Examples of the volume element methods are Finite Element Method (FEM) [91], Finite Difference Method in Time Domain (FDTD) [10], Digital Waveguide Method (DWM) [73], and Transmission Line Method (TLM) [33]. A good overview of volume element methods can be found from [70], for example.

Chapter 3

Modelling Diffuse Reflections

Diffuse reflections have been modelled in several ways in room acoustics. In reality a diffuse reflection from a wall is highly complicated and for this reason methods applied until now have been forced to make more or less crude simplifications in the prediction.

When the intention is to predict a wideband response, wave-based prediction methods can not normally be utilised due to computational limitations, not at least for the whole band. Therefore, physically-based prediction of a RIR, and so also prediction of the diffused part of the response, is often forced to apply ray-based or radiosity methods. In addition, in cases where accuracy of the modelling result is not highly critical, perceptually-based approaches can be utilised.

In this chapter, some modelling methods applied to diffuse reflections are described in detail. The first three sections present physically-based approaches which are meant to be used in the prediction of acoustical characteristics of a real space. Presented models apply ray-based methods and radiosity. Section 3.4 presents a method which utilises Schroeder diffusers to build up an audio scene. In section 3.5 a perceptually-based approach, originally meant to be used for modelling a virtual reference listening room, is introduced.

3.1 Methods Based on Ray Tracing

Introduction of sound diffusion into the ray tracing in the room acoustics modelling is not a new thing. Among the first suggestions has been a method presented by Kuttruff [39]. In this method each ray hitting a diffusing surface is reflected in a random direction given by a generation of two random angles. Reflections are done in such a way that the whole process creates a Lambert's cosine distribution of the reflected intensity [21].

The method proposed by Kuttruff [39] can be applied also to partially diffusing walls. The partially diffusing walls reflect a given fraction of reflected energy diffusely and the

remainder specularly. However, in this connection a third random number, which is comprised between 0 and 1, is needed to control the amount of energy reflected diffusely. If this number is smaller than the scattering coefficient, reflection of a ray is diffuse. In the other case it is specular [21].

Several authors [39], [31], [43], [27] have applied the randomised ray tracing model. Common to all these approaches is that they are relatively easy to implement. Elaborate corrections which are needed, for example, in approaches based on the approximate cone or beam tracing [17], [74] are avoided. Furthermore, models based on the randomised ray tracing are able to handle all orders of mixed (specular and diffuse) reflections. The main disadvantage of these methods is the great number of rays required for computation of detailed responses [17]. Typically 100000 rays are needed. Furthermore, the ray tracing process has to be repeated for each frequency band [43], [17], [89]. This is required since scattering of rays depends on the value of the scattering coefficient, which itself depends on the frequency.

Broadband Diffusion Model for Ray Tracing Algorithms

Among others Embrechts [21] has considered the problem of frequency dependence of sound diffusion. He has described an implementation of randomised ray tracing model which computes all frequency components simultaneously. With the proposed method, repetition of the algorithm for each different value of the scattering coefficient is thus avoided. Embrechts' proposal is introduced next.

Embrechts applied his method on an algorithm suggested earlier in [20]. The proposed method is not, however, restricted to this specific algorithm. It can be used in any process based on the same general principles of randomised ray tracing. The general framework of the randomised ray tracing algorithm need not to be changed. Embrechts' algorithm does not require any particular assumption on a decay time. Also, it handles any combination of specular and diffuse reflections.

The method is based on a particular coefficient called a *splitting coefficient*, γ , which controls sequences of consecutive diffuse and specular reflections. This coefficient is defined for each surface. The value of this coefficient is chosen independently of the scattering coefficient. The value does not depend on the frequency. The actual modelling process with the proposed method can start after definition of the splitting coefficient. For each ray hitting a diffusing surface a random number X is generated. If $X \leq \gamma$, the reflection is diffuse. In reversed situation the reflection is specular.

Next, the following expression is exploited. In case of a partially diffusing surface, the expectation value of averaged squared RMS pressure $\langle \hat{p}_{sc}^2 \rangle$ on a surface receiver ΔR can be

expressed as follows for a single frequency band:

$$\langle \hat{p}_{sc}^2 \rangle = s p_{dif}^2(\Delta R) + (1 - s) p_{spec}^2(\Delta R), \quad (3.1)$$

where s is the scattering coefficient, p_{dif} is the sound pressure obtained for totally diffusing surfaces, and p_{spec} is the sound pressure obtained for totally specularly reflective surfaces.

Now, in the proposed broadband method, the scattering coefficient s in Eq. (3.1) is replaced by the splitting coefficient γ in all frequency bands. Ray tracing procedure is executed for all frequency bands simultaneously and during this procedure the energy of a sound ray is corrected at all frequencies f by a factor $s(f)/\gamma$ if the reflection is diffuse, and by a factor $(1 - s(f))/(1 - \gamma)$ if it is specular.

According to Embrechts, the proposed energy compensation is valid in theory. However, he noticed that in reality it is not totally trouble-free. When applying the method, statistical errors of computed results increase for the same number of sound rays compared to the traditional ray tracing methods which compute frequency bands separately. In order to compensate this, a greater number of rays are needed. This in turn requires a greater computing time and the benefit of a single pass is then lost.

In order to preserve the efficiency of the algorithm, an appropriate control of the splitting coefficient is necessary. After analysing how different choices of the splitting coefficient influence on the ray tracing process, Embrechts proposes a compromise where the splitting coefficient is set to an average value of the scattering coefficients of all frequencies. Another suggestion is to use a formal expression for computing an optimal value for the splitting coefficient. When applying formal expressions a new value should be computed at each reflection of the sound ray.

Embrechts proposes also further improvements to the algorithm. According to him, a still more efficient algorithm could take an advantage of differences observed in reverberation times as a function of frequency. Because very long rays are useful only in octave bands where the reverberation time is long, the adaptation process of the splitting coefficient could take this into account. In addition, differences in statistical errors among frequency bands could be exploited. Naturally, it does not make sense to spend more computing efforts for a particular frequency band where required accuracy is obtained with less rays than in other frequency bands. Modification of the splitting coefficient could be used to progressively concentrate efforts in the frequency bands which require more rays. A drawback of the aforementioned procedure is, however, that now statistical errors need to be evaluated periodically in all bands.

3.2 Combining Beam Tracing and Radiosity

An example of approaches based on the beam tracing is Lewers suggestion which utilises advantages of the image source method, the ray tracing, and the radiosity [48]. This method combines two different methods, the beam tracing and the radiosity. Basic ideas behind the beam tracing and the radiosity method have already been introduced in section 2.4. Here the way how Lewers applied these methods is discussed.

As mentioned already in section 2.4, the beam tracing finds image sources very quickly. However, it alone is not adequate for modelling spaces with diffusely reflecting boundaries, because it can not produce a diffuse sound field. In situations where surfaces are diffusely reflecting, decays obtained with the beam tracing are unrealistic. Lewers solved this problem by combining two methods. In his approach specular reflections are formed with the beam tracing approach while diffused part is predicted with the radiosity.

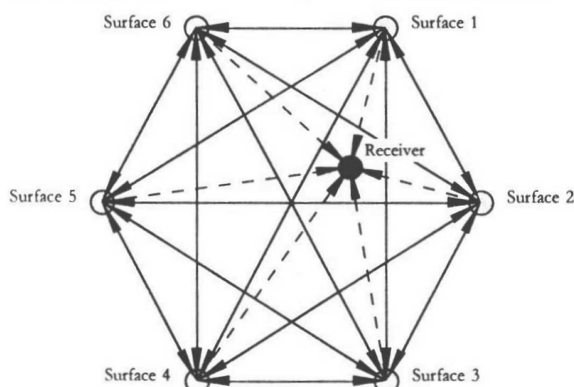


Figure 3.1: In Lewers' model for diffuse reflections surfaces and receivers are presented with nodes in a network [48].

At the time Lewers introduced his diffusion model, a suggestion for the use of this kind of approach in acoustic models had already come from Moore [56]¹. Therefore, the idea of using the radiosity model in room acoustics prediction wasn't new. However, the novelty of Lewers' method was the idea to combine the beam tracing and the radiosity methods.

Because the interest here and in this thesis is on ways of modelling the diffused part of a response, characteristics of Lewers' version of triangular beam tracing algorithm are not considered further here. Interested readers can turn to [48]. Instead, the diffusion model is presented in detail.

¹According to Lewers [48]

Proposed Diffusion Model

In the Lewers' radiosity-based method surfaces are replaced with nodes and sound paths with lines forming a network as depicted in figure 3.1. The energy which moves between the nodes depends on form factors between pairs of surfaces. Before Lewers' diffusion model can be applied, the scattering coefficient, s , needs to be defined for each surface within a room. Specularly reflected energy is now reduced not only by $(1 - \alpha)$ by absorption but also by $(1 - s)$ by diffusion. The energy removed from the model by diffusion is stored in *plane impulse responses*. A plane impulse response is an array associated with each surface where every time bin stores the energy that has arrived within its time period.

In the beam tracing beams emanate from a source with a power P_s . These beams are reflected across a surface with an absorption coefficient α , forming an image with a power

$$P_i = P_s(1 - \alpha). \quad (3.2)$$

At a distance r from the image, receivers receive the intensity I :

$$I = \frac{P_i}{4\pi r^2}. \quad (3.3)$$

A plane impulse response stores now the energy E :

$$E = \frac{sA_i P_i}{4\pi r^2}, \quad (3.4)$$

where A_i is a cross-sectional area of the beam and r is the length of a beam axis as it hits the surface. The diffuse model disseminates total energy received by the surface in a period of a time bin through the network. A surface intensity I^* can be now expressed as

$$I^* = \frac{E}{A_i}. \quad (3.5)$$

The diffuse model is applied after the specularly reflecting process has ended. At this point diffuse energy resides in the plane impulse responses. When the energy is driven through the network, processing starts with the first time bin for the first surface. It continues with the first time bin for the second surface and then for the remaining surfaces. After this, the algorithm moves on with the second time bin for the first surface and so on. The amount of energy which moves from one surface to another depends on the plane form factors between the surfaces. The energy acquired by receivers depends on the distance and on listener's angle of incidence to the surface.

The plane form factor $m_{j \rightarrow i}$ tells the fraction of energy which is diffusely emitted from a surface j and reached at a surface i . According to Lewers, Moore [56] has defined the plane form factor in the following way²:

$$m_{j \rightarrow i} = \frac{1}{A_{es}} \int_{A_{es}} \int_{A_{rs}} \frac{\cos \theta_j \cos \theta_i}{\pi r_{j \rightarrow i}^2} dA_{es} dA_{rs}. \quad (3.6)$$

²Compare to equation (2.48) in subsection 2.4.3.

In the previous expression A_{es} is the area of the emitting surface, A_{rs} is the area of the receiving surface, $r_{j \rightarrow i}$ is the length of a line joining two elemental areas, and θ_j and θ_i are angles formed by this line and respective normals. Since for most pairs of the planes there is no analytic solution to the previous equation, Lewers used the following discrete approximation:

$$m_{j \rightarrow i} = \frac{\Delta\Omega_i \Delta A_{es}}{A_{es} \pi} \sum_g \sum_h \cos \theta_{j(g,h)}. \quad (3.7)$$

The variables of the previous expression are defined during the following process:

Each surface i is examined in turn. Over each surface a rectangular grid is generated, forming areas ΔA_{es} . g is the number of grid nodes on the surface. From each grid node a hemisphere of h triangular beams is emitted. Each beam encloses a solid angle $\Delta\Omega_i$. Usual ray tracing process is used to find a surface j each beam hits. The length of a central ray and a sum of $\cos \theta_{j(g,h)}$ terms is recorded.

As mentioned already, the radiosity technique has been used traditionally in computer models for the behaviour of light. In this connection the time aspect of an arrival of energy has not been concerned. On the contrary, room acoustical analysis depends on the time of arrival of the energy. A line which joins two surfaces varies in length. This length depends on a point at which the line meets each surface. Hence, the sound energy varies in length of time it takes to travel from one surface to another. This variation depends on the path. When computing the plane form factors a range of distances from one surface to another is obtained. According to Lewers this can be expressed in a frequency distribution table which can be simplified again into a polynomial function in the following way:

An array records the number of times a line of a particular length occurs between each pair of surfaces. Next, an array of 100 numbers is computed such that each integer distance is represented with a frequency that it occurred during the computation. Every time an energy moves from surface to surface, a random number X between 1 and 100 is generated in order to find the distance between surfaces. The distance will be the X th term of this array. By compressing the array of 100 integers for each surface pair into a four-term polynomial, the amount of computer memory the process requires can be reduced. According to Lewers this can be done by applying the method of least squares.

As Lewers' diffusion algorithm proceeds, energy is absorbed by surfaces in usual way as it moves around the network. It is important to notice that each receiver must be irradiated for every time bin and for every surface. As mentioned, this method creates a model for diffuse reflections. So, it represents a completely diffuse field. Energy density per unit solid angle in such a field is uniform in all directions [15]:

$$\frac{\partial I}{\partial \theta_r} = \frac{wc}{4\pi}. \quad (3.8)$$

In the previous expression I is the intensity, θ_r is the angle between a surface normal and a line joining a receiver to the surface, w is the energy density, and c is the velocity of sound. According to Lewers, if a surface intensity I^* of an emitting surface with area S is wc and a solid angle presented by this surface to a receiving point at a distance r is

$$\Omega = \frac{S \cos \theta_r}{r^2}, \quad (3.9)$$

and θ_r is an angle between the surface normal and the line joining the receiver to the surface, then the intensity at the receiver is

$$I_R = \frac{I^* A_{vis} \cos \theta_r}{4\pi r^2}, \quad (3.10)$$

where A_{vis} is the area of the surface visible from the receiver.

The angle that is made by a line which presents the path along which the sound energy travels when leaving a diffusing surface and the length of a path from the surface to a receiver is needed by Eq. (3.9). In Lewers' solution both of these variables are subjected to the same treatment which was used in context of establishing distribution of lengths between the surfaces. At each receiving position a spherical source of triangular beams is placed. For finding the surfaces the beams hit, usual beam tracing process is executed. The lengths and the angles are converted with the aid of the frequency distribution technique to polynomials in a way explained before. Each time bin is examined and a random number determines for each receiver the value of $\cos \theta_r$ and r .

At the time Lewers proposed his method, finding the form factors and the lengths was a time-consuming process. For this reason preprocessing was required. However, when preprocessing was applied, the proposed diffuse model run according to Lewers very quickly. One reason for this is that with the proposed method it is not necessary to search for reflecting planes. Furthermore, in this model no decision is required when to finish the specular model and when to start the diffuse model. As time progresses after the sound leaves a source, the proportion of energy in the specular model decreases. At the same time that in the diffuse model increases. According to Lewers the need for an arbitrary reverberant tail can thus be replaced by this technique when computing an impulse response.

3.3 Approach Based on the Approximate Cone Tracing

An example of models based on the approximate cone tracing is Dalenbäck's suggestion which treats specular and diffuse reflections in an unified way [17]. The proposed method handles diffuse reflections by a split up of cones incident on diffusing surfaces. The term *approximate* is used since instead of an actual cone face only a centre ray is traced.

In the proposed model the approximate cone tracing is implemented as the ray tracing with a spherical receiver. A radius of the receiver is continuously increased to match the density of primary rays on a sphere described by the rays if they were allowed to extend unrestrictedly. With this kind of approach the spatial accuracy can be made very high for the early part of a response whilst accuracy for a late part can be gradually decreased.

According to Dalenbäck, the terms cone and ray tracing can be used almost interchangeably in context of approximate cone tracing. These methods differ only in the way how rays are detected and weighted at the receiver. Specular cone tracing presents several computational difficulties. However, because the interest here is on modelling diffuse reflections, problems of specular cone tracing are not considered further. On contrary, treatment of diffuse reflections is discussed.

General Principles

In order to model diffuse reflections, each diffusing surface is divided into square-shaped patches that act as receivers for an incident energy and later serve as secondary sources. According to Dalenbäck, all cones originating from an active source that encounter a particular patch, can be represented by a single secondary source if a time delay and a level of each contribution is preserved. As a consequence, in the proposed algorithm, each ray that strikes a diffusing surface creates a new source that spawns a set of secondary rays. Each of these rays continues as any other ray but from a new origin. This process continues until a response is saturated.

Dalenbäck's algorithm is multipass. This means that each pass creates specular-only responses while energy to be diffusely reflected is recorded at patches where reflections occur. In the first pass only the primary source is active. In the second pass, the patches act as secondary sources giving one specular-only response from each patch. In the second pass the fraction to be diffusely reflected is again recorded at the patches to be used for subsequent pass. This same process is then repeated. In the second and higher passes specular-only responses originate from the secondary sources and therefore consist of diffuse reflections, or, more precisely, reflections that have encountered a diffusing surface at least once.

Ray Split-up

The general idea of the algorithm is illustrated in Fig. 3.2. Ray split-up can be explained accurately as follows:

First, some symbols have to be introduced. An arbitrary number of sequential specular reflections is denoted by R_s^l ($l \geq 0$). R_d denotes reflection from a diffusing surface. For all surfaces two octave band dependent factors are assigned: the absorption coefficient α , and

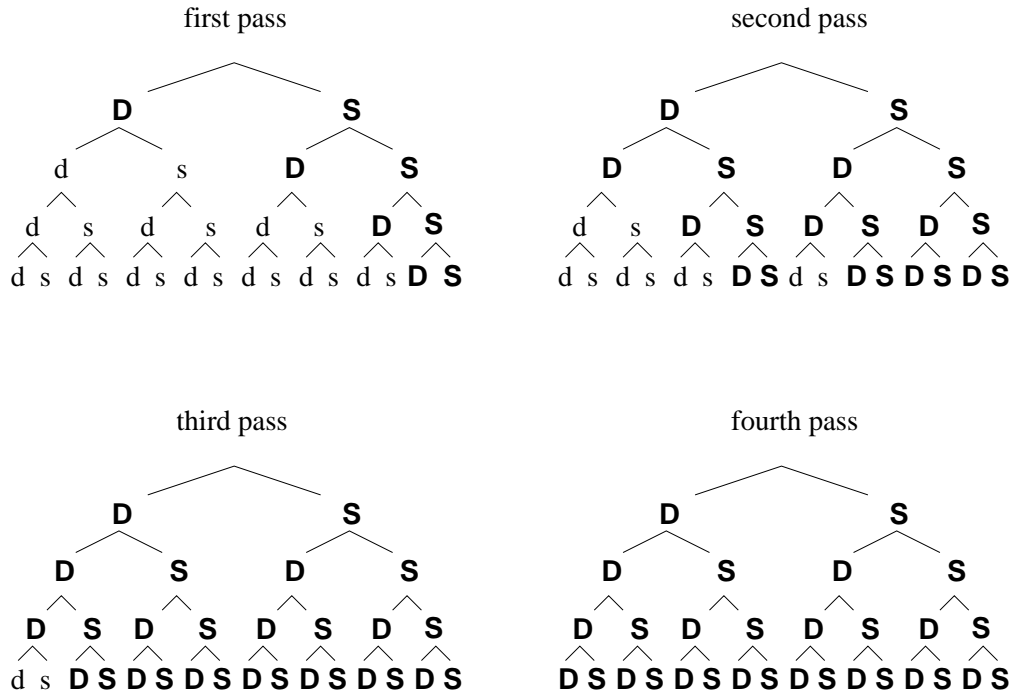


Figure 3.2: Ray split-up in the proposed algorithm [17]. *s* and *d* : Specular and diffuse reflection combinations to be included, *S*: Specular reflections treated during current or previous passes, *D*: Diffuse reflections recorded to the primary lists during the current or the previous passes.

the scattering coefficient *s*. The ray split-up itself proceeds in the following way:

At first the square-shaped surface patches are placed on all surfaces where $s \neq 0$. When a primary ray encounters a patch, the patch records the arrival time and an octave band spectrum of the diffused part in a list of reflections associated with the patch, referred to as a *primary list*. When all primary rays have been traced, most surface patches have recorded a list of reflections, representing $R_s^l - R_d$ reflections.

Next, by using the method described above for the specular reflections, all patches are run through in turn. The centre of each patch functions as a small secondary source sending out n secondary rays. Power carried out by each ray is weighted according to the diffuse reflection model assigned to the surface. When the ray encounters a receiver, not just one reflection, but the whole list of reflections associated with the patch acts now as a diffuse source and is so added to the response. Similarly, each time a secondary ray encounters a diffusing surface patch, the whole primary list is adjusted by $s(1 - \alpha)$ and recorded in a second list associated with this patch, referred to as a *secondary list*.

When the second pass, covering all patches, is complete, secondary reflection lists that

correspond to $R_s^l - R_d - R_s^l - R_d$ reflections, are associated with the patches. Old primary lists are now discarded and the secondary lists serve as new primary lists. It is possible that l is zero, so that $R_d - R_s^l - R_d$, $R_s^l - R_d - R_d$, and $R_d - R_d$ combinations are registered during the second pass. All reflection combinations, which have been introduced in figure 3.3, can thus be modelled with this method. Next, the same process is repeated with the following pass. This creates a new set of secondary lists for $R_s^l - R_d - R_s^l - R_d - R_s^l - R_d$ combinations. The processing may continue until details considered necessary are achieved. In each pass the rays carrying the specular portion of the reflected power are traced to the full length of the response.

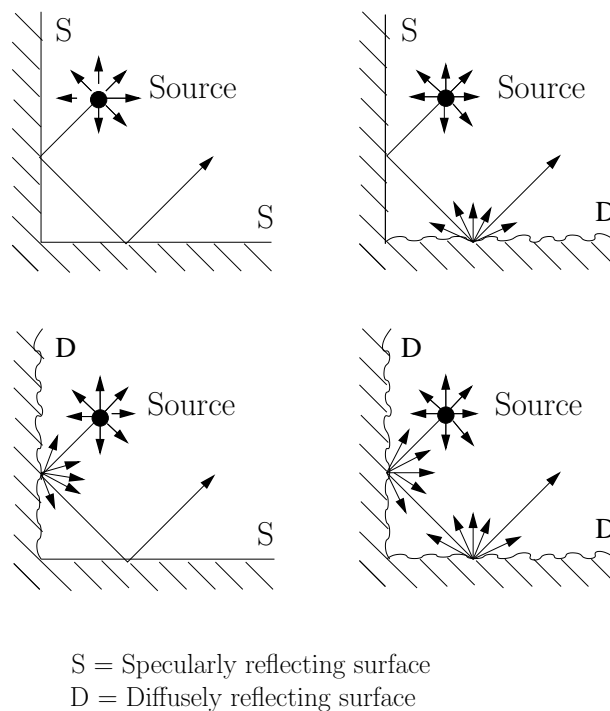


Figure 3.3: Four possible reflection combinations [17].

Ray direction randomisation is applied for diffuse reflections in the final pass. Energy recorded at the patches would otherwise be lost. During this pass no secondary lists need to be recorded and processing is therefore faster. According to Dalenbäck, for most applications, including auralisation, one diffuse pass seems to be adequate since even with this simplification the reflection density is very high. Prediction time is then also short enough for the processing to be done on a personal computer.

Important Characteristics of the Algorithm

In the proposed algorithm the manner in which the secondary rays are sent out from a patch is not affected by the angle the incident ray is recorded (the Lambert's law). As long as the arrival time and the power carried by each recorded incident ray are preserved, a single secondary source can function for the whole list of impulses associated with a patch. Time consuming geometrical computations are thus greatly reduced. The algorithm is most efficient if the applied diffusion model follows the Lambert's law. It is, however, possible to use also an incidence angle dependent diffusion models, if angles of incidence along with strengths are stored in lists. For each surface, or for a part of each surface, a different diffusion model can be assigned.

Furthermore, according to Dalenbäck, the algorithm is computationally more efficient than a direct implementation of a ray split-up algorithm. Each new pass requires only a time proportional to $n_p n$, where n_p is the total number of nonempty patches.

The proposed implementation is designed especially to meet specific requirements of auralisation. Split-up of cones creates an incomputable number of weak diffuse reflections resulting in a very smooth late decay.

Further Improvements

Dalenbäck has also suggested some further refinements to his algorithm. First of all, in order to maintain high accuracy for early diffuse reflections without excessively increasing the computation time, a nominal number of secondary rays could be computed to give the same cone face area at truncation time as the primary rays. This would lead to a situation where early excited patches create secondary sources that use a high number of rays. The algorithm could be economised further by decreasing the number of secondary rays from nominal number in proportion to the importance of the secondary source. The number of rays could be multiplied by a factor proportional to $s(1 - \alpha)$. This would give the lowest reduction in accuracy for hard surfaces with strong diffusion. Furthermore, also the patch density could be made dependent on the same factor. High density would be given for hard surfaces with strong diffusion. The algorithm could thus be made adaptive to properties of each specific environment.

Further improvements of the algorithm could also include the possibility to determine a time dependent criterion so that a ray could be safely neglected when its energy has dropped below a certain level. For this purpose the expected number of reflections from a specific primary or secondary source should be specified. However, in this connection it is important to notice that even if the energy of a certain ray no longer can contribute significantly to the response, it has to be traced to its full length and registered at all receiver positions.

Otherwise extrapolation does not work properly.

3.4 Utilising Schroeder Diffusers in 2D

One more example of modelling methods which combine two different approaches is Martin et al.'s [52] suggestion which is designed for simulation of diffused early reflections. The proposed method uses a combination of phenomenological models of reflection with physical models of components of Schroeder diffusers. The implemented algorithm incorporates both specular and diffused components with a relationship controlled by the end user. The modelling in the proposed method is restricted to 2D geometry.

The system described by Martin et al. [52] was a prototype module that was planned as an addition to the sceneBuilder software/hardware package which has been developed at the Multichannel Audio Research Laboratory (MARLab) at McGill University [63], [51]. The system was designed to model a recording environment and can be understood as a kind of reverberation engine.

In the proposed system specular and diffused components of reflections are modelled independently and combined afterwards in a mixing process. Methods for computing directivities of source and receiver are also suggested, but not discussed here. Specular reflection components are designed with ISM.

As mentioned, the proposed method utilises physical models of components of Schroeder diffusers for diffused part of a response. In order to understand the method, the concept of Schroeder diffusers needs to be familiar. Martin et al. [52] have explained it in the following way. Schroeder diffusers have been considered in detail also in [41], for example.

Schroeder Diffusers

In 1979 Schroeder introduced a new system labeled a *quadratic residue diffuser* [72], a system which has been afterwards called also the Schroeder diffuser. Since its invention this device has been widely accepted as one of the de facto standards for easily creating diffusive surfaces with predictable characteristics.

The idea behind the Schroeder diffusor is to build a flat reflective surface with a varying computed local acoustic impedance. This can be accomplished by using series of wells of various specific depths. These wells are arranged in a periodic sequence based on residues of a quadratic function as

$$s_n = n^2, \text{ mod}(M). \quad (3.11)$$

In the previous expression s_n is a sequence of relative depths of the wells, n is a number in the sequence of non-negative consecutive integers $\{0,1,2,3, \dots\}$ denoting the well number,

and M is a non-negative odd prime number. Thin dividers separate these wells ensuring that each is a discrete quarter wavelength resonator. A relationship between the relative value s_n and the design wavelength λ_0 of the diffusor determines an actual depth d_n of each of the wells:

$$d_n = \frac{\lambda_0}{2M}. \quad (3.12)$$

The width of the wells determines the highest frequency affected by the structure. The width should be constant and less than one quarter of the design wavelength.

The sequence of the wells results in an apparently flat reflecting surface with a varying periodic impedance corresponding to the impedance at the mouth of each well. This kind of surface has an interesting property that, for a frequency band typically within one half octave on either side of the design frequency, reflections will be scattered to propagate along predictable angles with very small differences in relative amplitude. According to Martin et al., each of the wells in a quadratic residue diffusor can be simplified to a quarter wavelength resonator consisting of a circular pipe which is open on one end and terminated by a known impedance at the other end.

When considering the situation from outside of the pipe, impedance Z_n at the entrance of the pipe, which is closed on the opposite end from the point of view, can be expressed as:

$$Z_n = \frac{\rho_0 c z_d + i \frac{\rho_0 c}{s_n} \tan(kd_n)}{s_n \frac{\rho_0 c}{s_n} + i z_d \tan(kd_n)}, \quad (3.13)$$

where ρ_0 is the volume density of the air, c is the velocity of sound in the air, z_d is the acoustic impedance of a cap at the closed end of the pipe, s_n and d_n have been explained already, and k is the wave number.

Modelling Diffuse Part of a Response

After explanation of the basic ideas behind the concept of the Schroeder diffusor, the suggested modelling method for diffused part of the early response is now presented:

Martin et al. have exploited in their method the same abilities of diffused components which have been utilised also by several other methods described before in this chapter. One of these is that, in the case of diffused components, each reflection point along a surface can be considered to be a new and independent sound source. Each of these points is thus a modified copy of the original sound source. Sound levels on these points depend on the sound level of the sound source and its distance³ from the reflection points. As a consequence, the gain of each individual discrete component in the diffused reflection is a product of the gain applied to the sound source to determine its level at a point of reflection

³And orientation, source directivity functions take care of this

and the gain applied to radiation from the point of reflection to determine its level at the receiver.

Because the received diffuse reflection component is the result of superimposition of the spatially distributed individual reflections off a surface, these are computed individually in the system. Particular characteristics of the reflection off a reflection point are determined by its local acoustic impedance. The local impedance is dependent upon the width and the depth of an individual well in the diffuser. The impedance can be computed using equation (3.13).

In order to determine the impulse response of a mouth of an individual well, its impedance function must be converted from the frequency domain to the time domain using the *Inverse Fast Fourier Transform*, IFFT. Herein, it is important to notice that if the ordinary recording were convolved through the achieved time domain representation of an impedance function, the resulting output would be a simulation of the reflected velocity wave. In order to avoid this, Martin suggests that the output of the system should be converted back to a representation of the pressure wave by convolving the velocity signal with a first-order difference equation, which approximates a derivation filter:

$$y[n] = \frac{x[n+1] - x[n]}{T}. \quad (3.14)$$

In the previous expression n is an integer variable pointing out the sampling instant, and T is the sampling period of the system.

Mixing Specular and Diffused Components

Martin et al. have also described how to mix the specular and diffused components. In the implemented system a summed power of the specular and diffused parts is kept constant while at the same time the system gives to a listener the possibility to adjust the amount of diffusivity. It is thus required that $k_s^2 + k_d^2 = 1$. The proposed implementation is based on the standard constant power panning curve [66], which is applied by the following equations:

$$k_s = \cos(k_{diff} \frac{\pi}{2}), \quad (3.15)$$

$$k_d = \sin(k_{diff} \frac{\pi}{2}), \quad (3.16)$$

where k_{diff} is the level of the diffused component which can be adjusted by the listener. The value of k_{diff} ranges linearly from 0 to 1. k_s , a specular reflection scalar, and k_d , a diffuse reflection scalar, are coefficients applied to the source signal when the levels of single specular and diffused reflections are computed at the receiver position.

3.5 Perceptually-Based Approach

Pellegrini's [59] suggestion for modelling diffuse reflections is one example of perceptually-based approaches. The proposed method was originally used for modelling a virtual Reference Listening Room (RLR). RLR is a room with high-quality listening conditions intended for recordings and for critical assessment of the quality of transmission equipment, for instance. In order to overcome deficiencies of real RLRs, Pellegrini suggests simulation of the RLR by using an Auditory Virtual Environment (AVE). Virtual RLRs could be used in recording studios in broadcasting, television, film, mastering, and recording, for example.

Simulation of a RLR is targeting on the same perception rather than on the same physical properties of an environment. Therefore, plausible reproduction is sufficient in this connection. As a result, the proposed simulation algorithm is more efficient and less memory consuming than an authentic reproduction algorithm, which uses a physical model.

In the implemented system the specular part of a response is modelled with the ISM. The method used for diffuse reflections is described below. In order to understand choices made in the method, an introductory experiment, introduced by Pellegrini, is described before the method itself is presented.

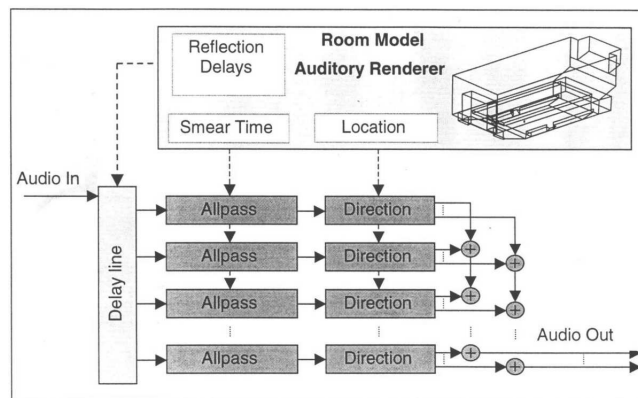


Figure 3.4: Block diagram for discrete reflection patterns with smooth energy decay. Specular reflections + smearing allpass filters [59].

Introductory Experiment

The block diagram of a system implemented in this experiment is shown in figure 3.4. In the experiment single reflections were widened using the Schroeder's allpass filter structure [71]. The allpass filter structure was used to average sound energy between specular reflections by smearing out the signal over a time period between adjacent reflections. As a result the modelled impulse response's energy distribution was smoother in time.

When diffuse reflections were modelled with this method, Pellegrini observed that filtering introduced unpleasant colouration of the source signal. He suggested several reasons for the colouration. First of all, according to him, colouration can be understood by looking at the short time spectrum of a given allpass filter. A spectrum of Schroeder's allpass filter is flat only when a long term filter spectrum is considered. Furthermore, colouration arise when the allpass filter is longer than the integration time of the auditory system. Problematic is also that, as a consequence of temporal degradation of single reflection signals, most of the localisation cues are heavily degraded. Spectral cues, which would normally be used by the auditory system, not only for localisation but also for decolouration of perceived sound, fail to work because of the ambiguous temporal and spectral cues.

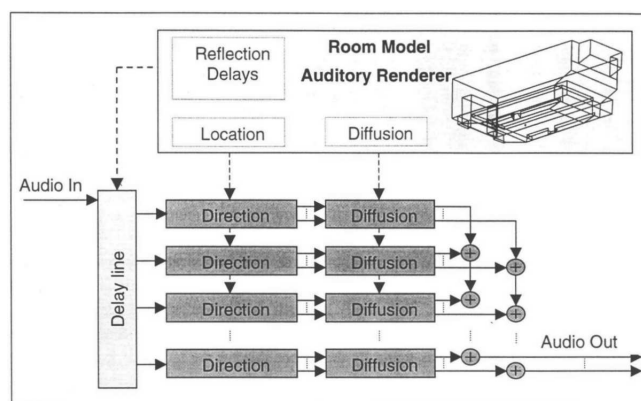


Figure 3.5: Block diagram for discrete reflection patterns with smooth energy decay. Specular reflections + Pellegrini's diffusion filters [59].

Proposed Method

In order to avoid some of the problems described above, Pellegrini suggested a new filter structure to fill gaps between the specular reflections. The proposed filter consists of two different filter parts. It is inserted after directional filtering, as shown in figure 3.5. Figure 3.6 shows ideal impulse responses of this filter for the left and the right ear.

The proposed filter transfers a specular reflection slightly attenuated to the output. The impulse response of the filter consists of a peak that is followed by an uncorrelated noise-like part. The peak assures clearly marked specular localisation cues. According to Pellegrini, localisation cues are preserved because they are correlated for each output. On the contrary, in order to simulate diffuse field, the following noise-like part for all output channels should be decorrelated.

Pellegrini insists that the proposed kind of filter structure is equivalent in terms of per-

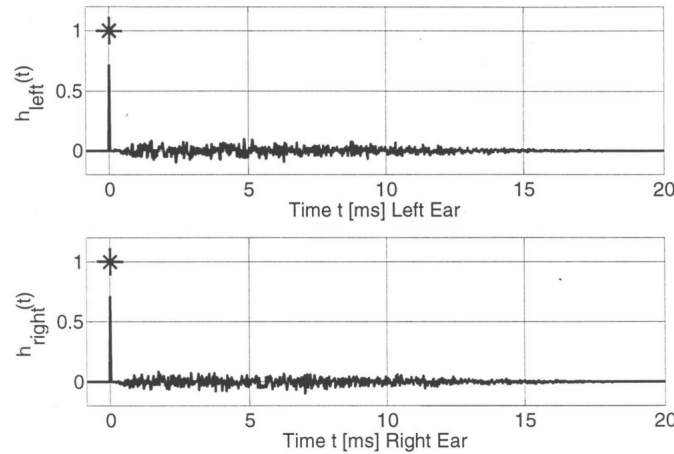


Figure 3.6: Suggested diffusion filters to smear energy over time [59].

ception to an early diffuse sound field which is accompanied by strong discrete reflections. The noise-like part smears out and equalises energy distribution. If the impulse response is considered from room rendering point of view, resulting signal can be viewed as a combination of a discrete reflection and a very high number of diffuse reflections coming from similar direction as the discrete specular reflection. The spectral behaviour of the noise-like part can be chosen to be flat. On the other hand, it can be adapted to the short time spectrum of the desired measured room impulse response depending on the delay time of the specular reflection.

As mentioned, the diffusion filter needs to produce uncorrelated signals for each output channel. The diffusion filter needs therefore to be inserted after directional filters in the implemented system. For binaural reproduction, for example, this means that diffusion filters need to be implemented twice. Compared to the simple allpass model, shown in figure 3.4, this results in a massive increase of processing costs. The aforementioned is true at least as long as the diffusion filters are to be adjusted in length and level individually. According to Pellegrini, for the case of constructed ideal impulse response, it has been found that a non-individual diffusion filter where noise's time and level ratio compared to a direct peak is fixed [58] is sufficient to get rid off the perceptual artifacts described above. However, the peak-to-noise-level may need to be readjusted for different sound materials. The system, which uses only one diffusion filter per output channel after the summing stage is processing-cost efficient even when compared to the simple allpass structure shown in figure 3.4.

Suggested Filter Implementation

Pellegrini has also suggested an implementation for the proposed diffusion filter [59]. The new structure makes use of complementary delayed allpass filters that cancel each other after some time. In the proposed approach, for each Schroeder's allpass, a complementary delayed allpass is generated that zeroes all non-zero filter values after a specified delay as depicted in figure 3.7. The proposed filter is still close to an allpass filter with a reduced length of an impulse response. It keeps the decay rate of the longer allpass filter. The optimum decay rate is depending on the number of zeroes and on the level of the initial negative value in the impulse response of the Schroeder's allpass. It is important to notice that the absolute value of the initial negative peak should be exactly the same as the exponential envelope at that time. Pellegrini has expressed a difference equation for the allpass $y[n]$, and corresponding formulas which show dependencies in the following way:

$$y[n] = -\psi x[n] + x[n-b] + \psi y[n-b], \quad n = 0, 1, 2, \dots, \quad (3.17)$$

where b = number of zeroes, $\psi = e^{b\mu}$, $0 < \psi < 1$, and

$$\mu = \frac{\ln\left(\sqrt{\frac{1}{2}}\right)}{b+1}, \quad \mu = \text{Optimum decay rate.} \quad (3.18)$$

If ψ is chosen as stated above, the initial peak has an appropriate level corresponding to the exponential decay. For smaller values the initial peak approaches zero while the decay rate will flatten. The envelope of the above filter can be given by:

$$ENV = \frac{1 - \psi^2}{\psi} e^{\mu n}. \quad (3.19)$$

According to Pellegrini an implementation using eight improved Schroeder's filters in a cascaded structure leads to a very dense reverberation without colouration that is very similar to the desired function for diffusion. The desired functions for the left and the right ear are depicted in figure 3.6 whereas the implemented functions are illustrated in figure 3.8. An uncorrelated noise-like output is assured by using slightly different delays for the filters for each ear.

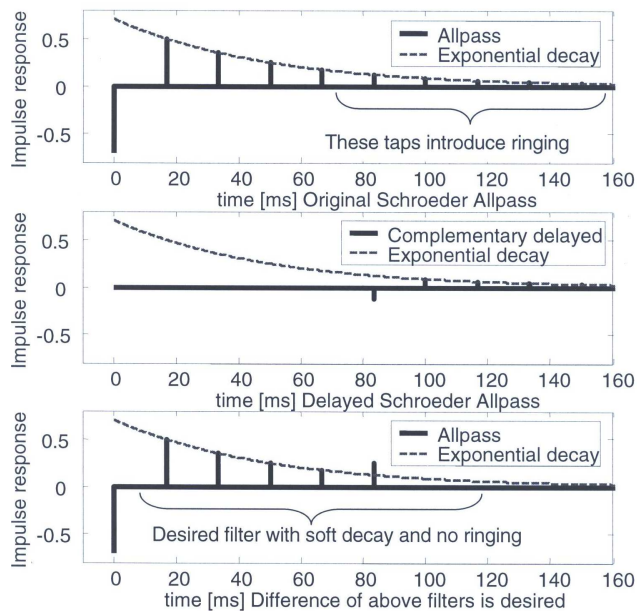


Figure 3.7: Suggested improved Schroeder allpass using two complementary allpass filters [59].

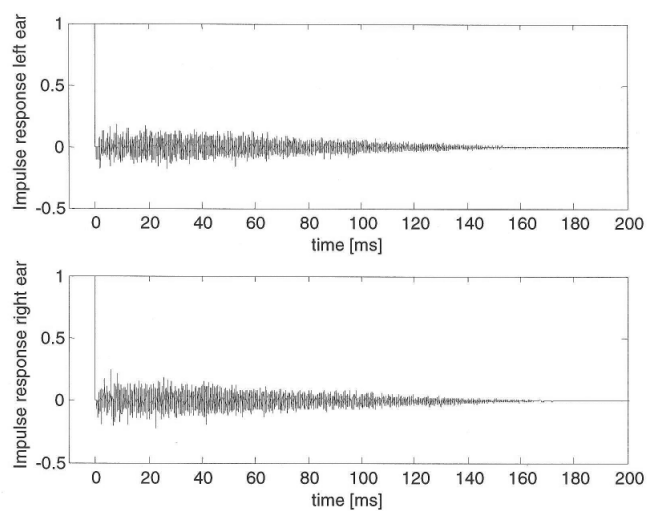


Figure 3.8: Implemented diffusion filters which smear energy over time [59].

Chapter 4

Experimental Part

Until now physical principles and different methods used in literature in diffuse reflection modelling have been considered. Based on this background a simple implementation was carried out in this study. The purpose was to familiarise oneself with problems of physically-based room acoustics and especially diffuse reflection modelling.

Modelling was done by combining the ISM and the radiosity-based approach. It restricted only to an early part of a response. The ISM was chosen, because in a simple geometry, up to reflection orders 2-3, it finds specular reflections fast. In addition, it is reliable, since it really finds all specular reflections. For these reasons it is commonly used for modelling an early part of a response, which is perceptually more important than the late part. However, when using only the ISM in the modelling, diffuse reflections of the early response are lost. In order to avoid this, a radiosity-based approach, somehow similar as suggested by Lewers [48] or Dalenbäck [17], was chosen for diffused part of the response. The implemented system is described in detail in this chapter. In addition, the modelling results are analysed.

4.1 Implemented System

Modelling was carried out in Matlab. The modelled space was chosen to be simple. Shoe-box shaped room was used, although it does not correspond to any real space. In this kind of geometry, if walls are assumed rigid, the image source solution gives an exactly correct solution [4]. Diffraction modelling with edge sources is thus not needed [79]. Because the diffuse reflection response was here modelled separately, the walls could be assumed to be rigid when the specular part of the response was modelled. The diffraction modelling could therefore be left out. Another advantage of the shoe-box shaped room geometry is that it is easy to implement.

As mentioned, in the realised implementation the specular reflections were modelled with the ISM, whereas the diffuse reflections were treated with the radiosity-based approach. After separate modelling of specular¹ and diffuse reflection responses, these were combined to a single response as depicted in figure 4.1. Reflections were modelled only up to the second order specular and diffuse reflections. Because the propagation medium inside the room was supposed to be air, which is not totally lossless, its effect was taken into account by air absorption filtering the direct sound and the reflections. Furthermore, because part of the sound is usually lost in each reflection as a consequence of material absorption, all reflections were material filtered. Modelling was carried out with sound energies. In order to make it possible to listen to the modelled room acoustics, the response was converted after modelling to a pressure response by taking the square root of the modelled energy response.

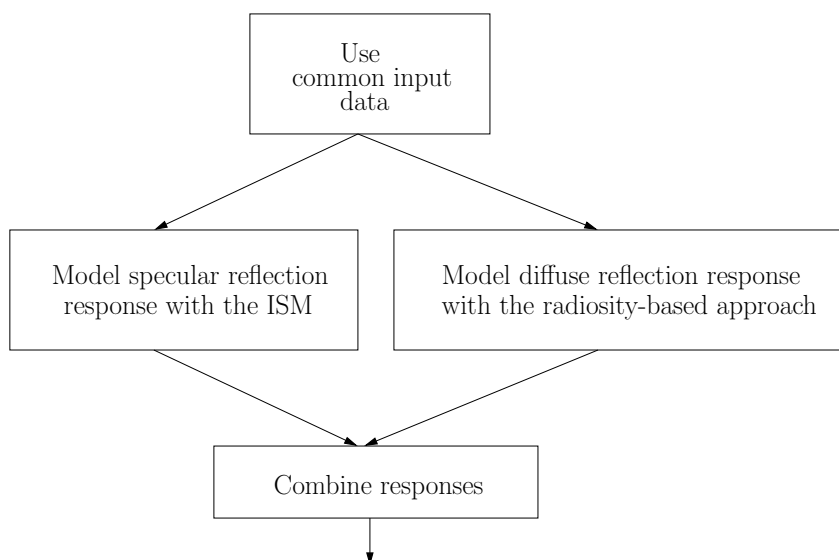


Figure 4.1: In the implemented system specular and diffuse reflections were modelled separately with different methods.

4.1.1 Modelling of Specular Reflection Response

Modelling of the specular reflection response proceeded in the way illustrated in figure 4.2. In addition to specular reflection response, the response of the direct sound was predicted during the execution of the algorithm. It was included to the modelling result.

The applied coordinate system is depicted for 2D case in figure 4.3. The actual modelling was done in 3D, but to make visualisation in figure 4.3 more illustrative, it is presented in

¹Direct sound was included in the specular reflection response.

2D. For the 3D case, the origin as well as the x- and y-axis were chosen as in the 2D-case. The positive z-axis was chosen to point up to the direction of the ceiling whereas the negative direction pointed down to the floor. Separate parts of the algorithm are considered next.

Input Data

Some initial information was needed before the actual response computation was possible. The following data was used in the modelling:

- Dimensions of the room: 24 m, 30 m, 18 m (x, y, z)
- Location of the sound source: 8.5 m, 6.3 m, 1.0 m
- Location of the listener: 11.7 m, 22.5 m, 1.7 m
- Sampling rate: 48000 Hz
- Scattering coefficient: 0.0 - 1.0
- Length of the response to be modelled: 15000 samples
- Air absorption filtering coefficients
- Material absorption filtering coefficients

Finding Locations of Image Sources

First in the actual modelling algorithm, locations of image sources were searched for. The first order image sources were found by reflecting the sound source against each surface of the room. In a shoe-box shaped room six first order image sources were found. In figure 4.3 four of these (2D case) are illustrated.

Image sources that corresponded to the second order specular reflections were searched for by reflecting each first order image source against all other surfaces, except the surface which had been used as the reflecting surface when the first order image source in question had been modelled. In the shoe-box shaped room 30 second order reflections were found. However, 6 of these were overlapping, and as a consequence, the number of second order reflections was 24. In figure 4.3 the image sources corresponding to the second order specular reflections, when modelled in the 2D, are illustrated.

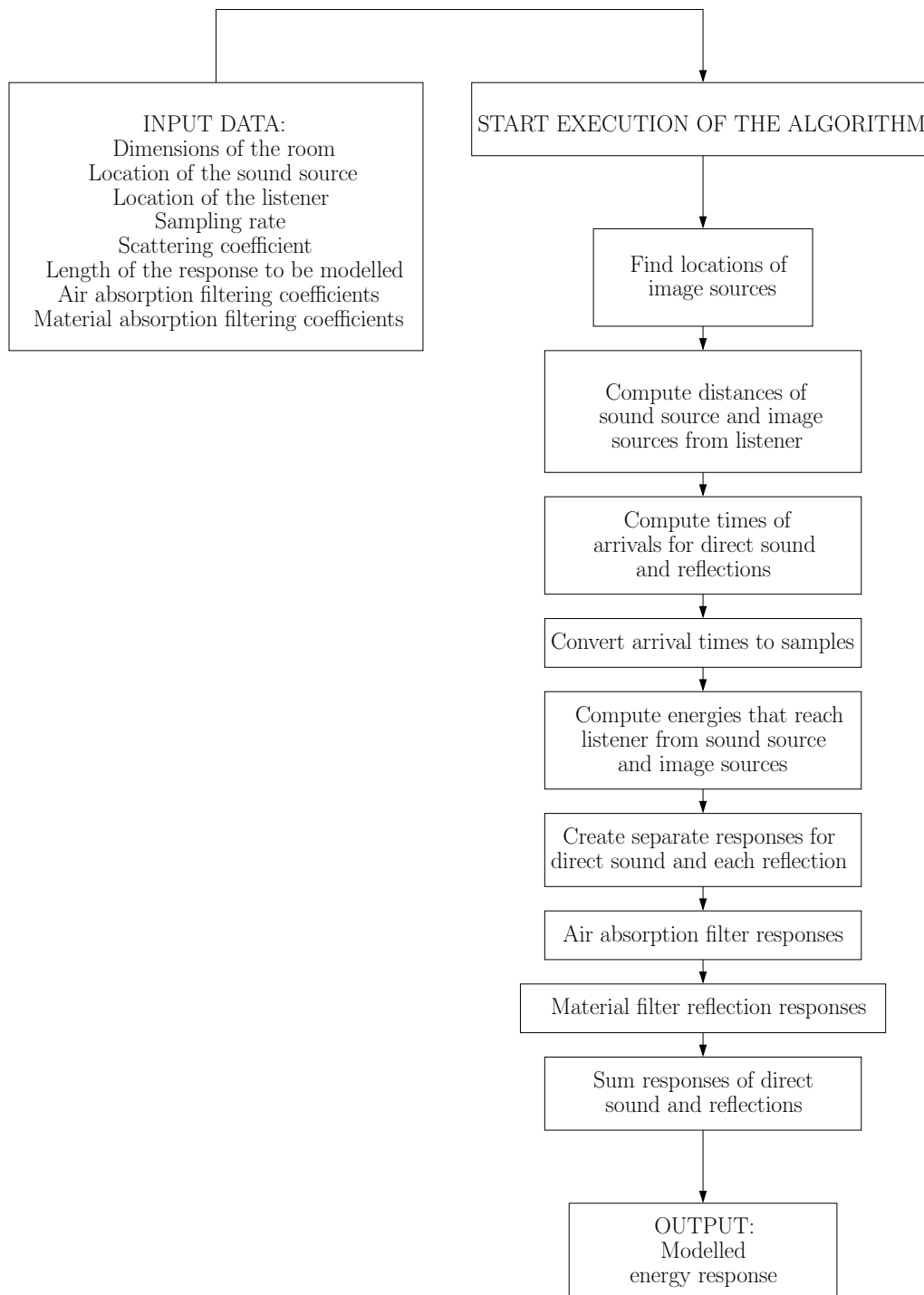


Figure 4.2: A flow chart of the algorithm which models the response for the direct sound and specular reflections.

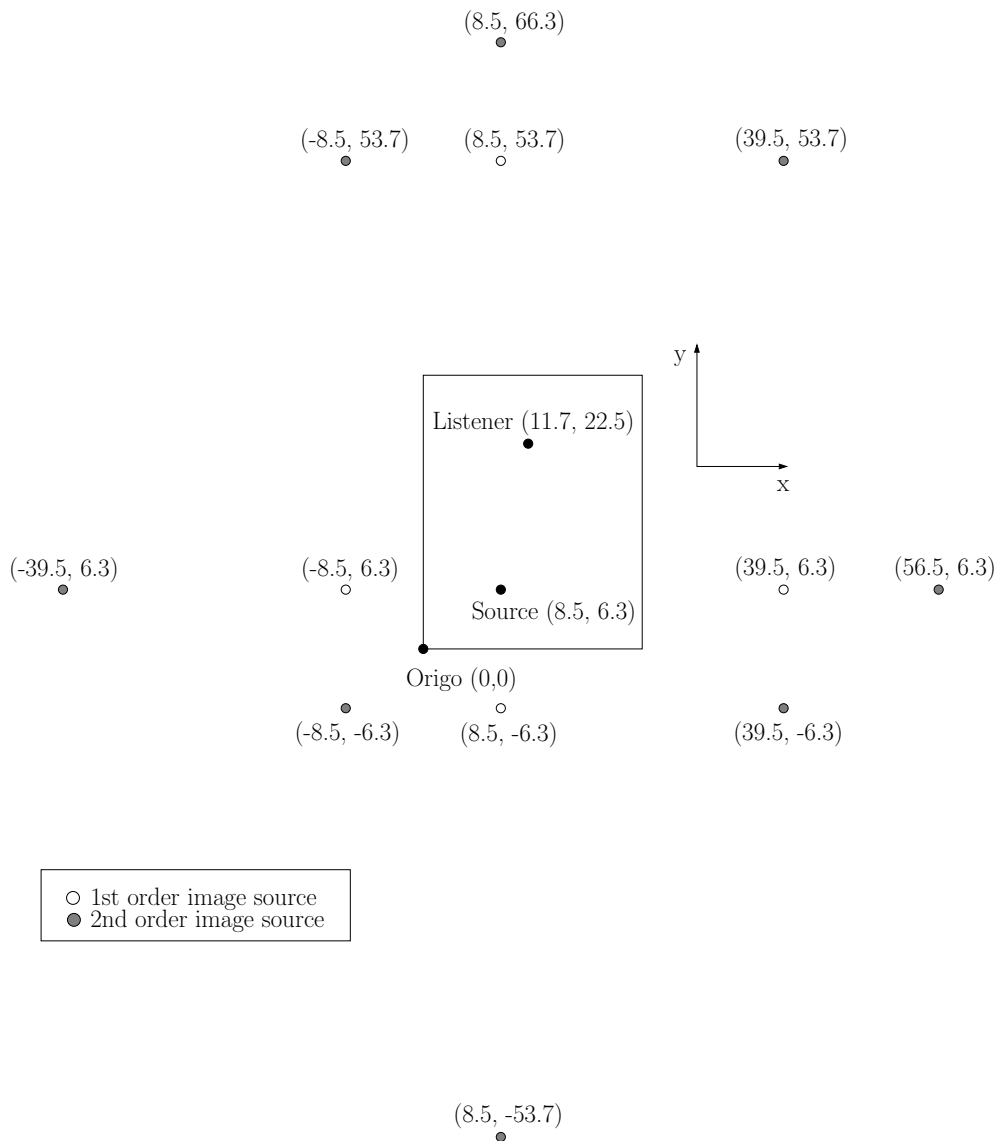


Figure 4.3: The first and the second order image sources in 2D.

Distance Delay and Attenuation

After finding locations of the image sources, arrival times of the direct sound and the specular reflections, and energies that they carry on to the listener position, could be defined. In order to do this, distances between the image sources and the listener were defined. Also, the distance between the original sound source and the listener was computed. By utilising the distance information and the fact that the velocity of sound in air is approximately 340

m/s, the arrival times of the direct sound and the specular reflections were computed² and then converted to samples. Energies at the listener at these sample instants were defined by applying frequency independent distance attenuation law which states that sound energy attenuates in relation to $1/4\pi r^2$, where r is the distance which the sound has travelled from a point source. With the aid of information about the distance delay and attenuation, it was now possible to create separate energy responses for the direct sound and each specular reflection.

Air Absorption Filtering

Energy responses of the direct sound and the specular reflections were next filtered with air absorption filters. Distance, temperature, and humidity have all an impact on air absorption. There exist standardised equations for the computation of air absorption [3]. These have been utilised in [69], for example. The same principles as used in [69] were applied here when the target responses of air absorption filters were computed. Magnitude responses of the designed air absorption filters, IIRs of order 6 with 10 meter step spacing, are shown in figure 4.4. In the implementation a 1 meter step spacing was applied.

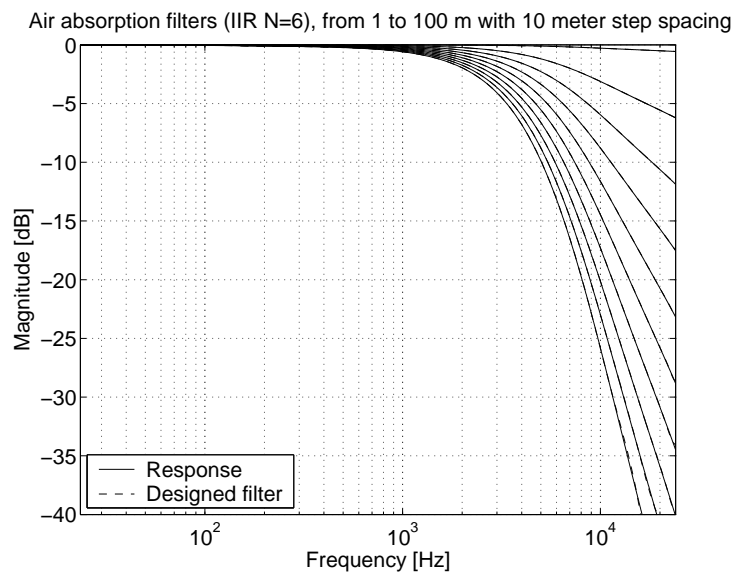


Figure 4.4: Magnitude responses of air absorption filters corresponding to distances from 1m to 100m with 10 meter step spacing.

²arrival time = distance / speed of sound

Material Absorption Filtering

Material absorption was performed with reflection filters in the way proposed in [69]. Generally, when material filtering the reflection responses, each surface of a room must have a reflection filter which corresponds to the absorption characteristics of its material. In the implemented system, walls of the modelled room were chosen to be from the same material. As a consequence their reflection filters were the same. Only the floor and the ceiling had different reflection filters. In the case of second order reflections, the reflection responses were filtered twice. The first filtering corresponded to the characteristics of the first reflecting surface and the second naturally to the second reflecting surface. Only angle independent absorption characteristics were applied.

Chosen materials and corresponding absorption coefficients, which were used as data in reflection filter design, are shown in tables 4.1 and 4.2 in octave bands. Ideas behind the algorithm used for realising absorption coefficient data with a digital filter has been presented in [32]. Here the algorithm was applied in the following way: Absorption data was first transformed into (energy) reflectance data by relation $R_e = |R|^2 = 1 - \alpha(\omega)$. The square of $|R|^2$ was not taken because modelling was performed with the energies, not with the pressures. Next, the resulting amplitudes were transformed into the frequency domain. Filter fitting was performed in a warped frequency domain. Magnitude responses of the modelled material filters are shown in figure 4.5.

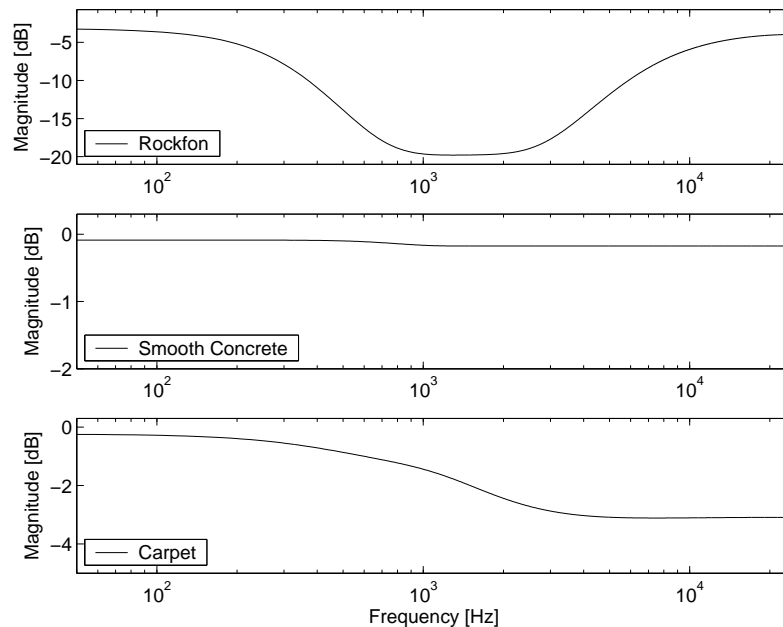


Figure 4.5: Magnitude responses of used reflection filters.

Table 4.1: Material absorption filtering coefficients, octave bands 1-5.

Surface	ID	Material name	63 Hz	125 Hz	250 Hz	500 Hz	1 kHz
Ceiling	1	Rockfon	0.150	0.300	0.700	0.850	0.900
Walls	2	Smooth Concrete	0.010	0.010	0.010	0.010	0.020
Floor	3	Carpet	0.020	0.020	0.050	0.100	0.150

Table 4.2: Material absorption filtering coefficients, octave bands 6-9.

Surface	ID	Material name	2 kHz	4 kHz	8 kHz	16 kHz
Ceiling	1	Rockfon	0.900	0.850	0.600	0.350
Walls	2	Smooth Concrete	0.020	0.020	0.020	0.020
Floor	3	Carpet	0.250	0.300	0.300	0.300

Output of the Algorithm

Finally, the response of the direct sound and responses of the specular reflections were combined to a single energy response. One example of modelled energy response is illustrated in figure 4.6.

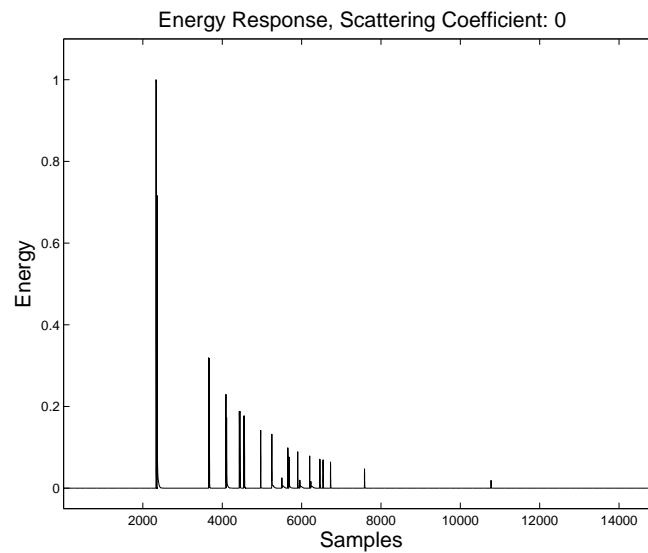


Figure 4.6: Modelled energy response for the direct sound and the first and the second order specular reflections.

4.1.2 Modelling of Diffuse Reflection Response

Diffuse reflections were modelled with the radiosity-based approach. In the modelling, each surface of the modelled space was divided into square shaped surface patches as depicted in figure 4.7. Sound energy originating from the sound source was carried between the patches until it reached the listener. The Lambert's law was applied in the reflections. Air and material absorption filtering was performed.

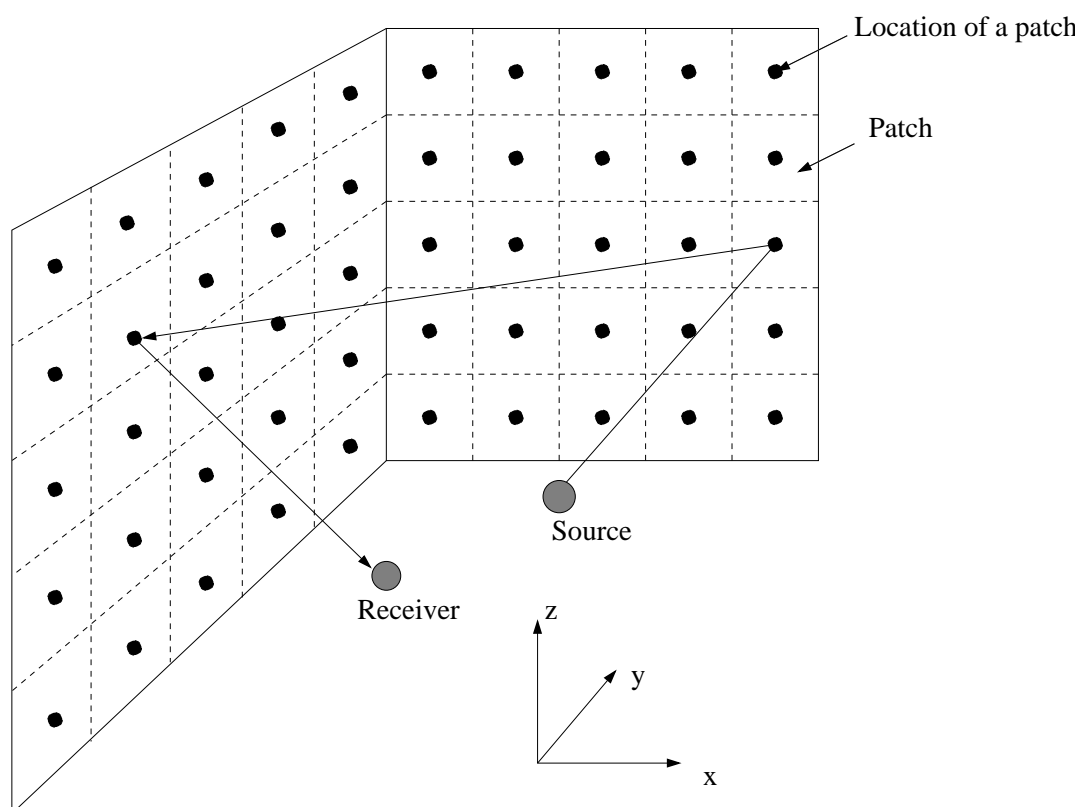


Figure 4.7: Surfaces were divided into square shaped surface patches.

In the implemented system the first and the second order diffuse reflections were modelled separately and then combined together, as depicted in figure 4.8. In figure 4.9 a flow chart of the algorithm in a general case of the Nth order diffuse reflections is illustrated. Separate parts of the algorithm are considered in detail in the following subsections.

Preparatory Computations

Before actual modelling of the diffused part of a response was possible some preparatory computations were needed. Modelling of both reflection orders required as input data some common variables whose values were defined beforehand.

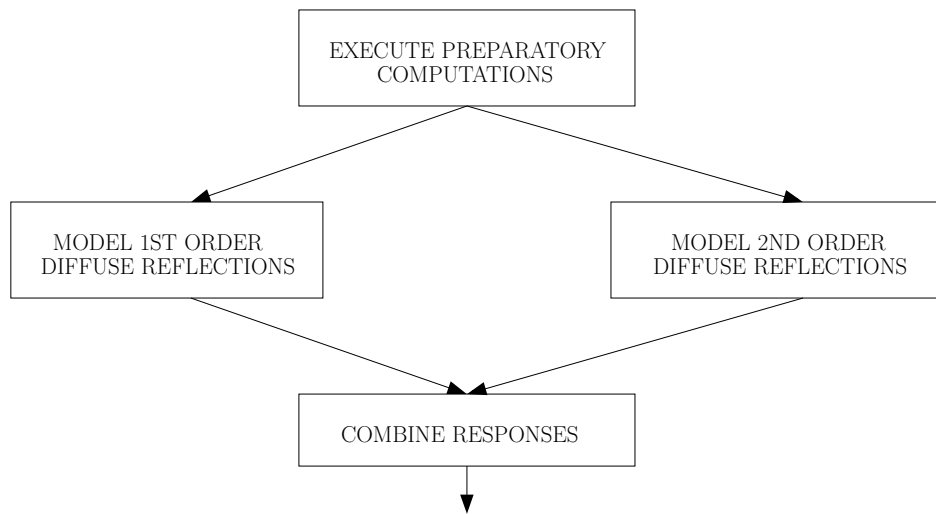


Figure 4.8: Flow chart of the algorithm computing diffused part of a response.

First, locations of the surface patches and distance information needed in actual modelling were computed. Distances defined here were: 1. distances from the sound source to the surface patches, 2. distances between the patches, and 3. distances from the patches to the listener. In order to find out distances, a point from each patch had to be chosen as the location point of the patch. The centre of each patch was selected and locations of these centre points were defined with three coordinates x, y, z in the current geometry. Next, the distance information needed could be computed and saved to matrices, in order to be used when total lengths of reflection paths were computed during the modelling.

The Lambert's law was applied in reflections³. At each reflection, sound energy illuminating a surface patch was multiplied with $\Delta S \cos \theta$, where ΔS was the area of the surface patch, and θ was the angle of a sound ray which irradiated from the surface element to a receiver. The receiver could be a listener or another surface patch. Also, exceptionally, when the first diffuse reflection was considered, the initial energy originating from a point source was multiplied with $\cos \theta_0$, where θ_0 was the angle of the sound ray which illuminated the surface element from the sound source.

Coefficients computed here with the Lambert's law were term $l_{sp} = \cos \theta_{sp}$, where θ_{sp} was the angle of a sound ray which illuminated a single surface element from the sound source, term $l_{pp} = \cos \theta_{pp}$, where θ_{pp} was the angle of a sound ray which irradiated from a single surface element to another surface element, and term $l_{pl} = \cos \theta_{pl}$, where θ_{pl} was the angle of a sound ray which irradiated from a single surface element to the listener. Angles are illustrated in figure 4.10. Coefficients l_{sp} , l_{pp} , and l_{pl} were computed for each surface

³The Lambert's law has been considered already in subsection 2.3.1.

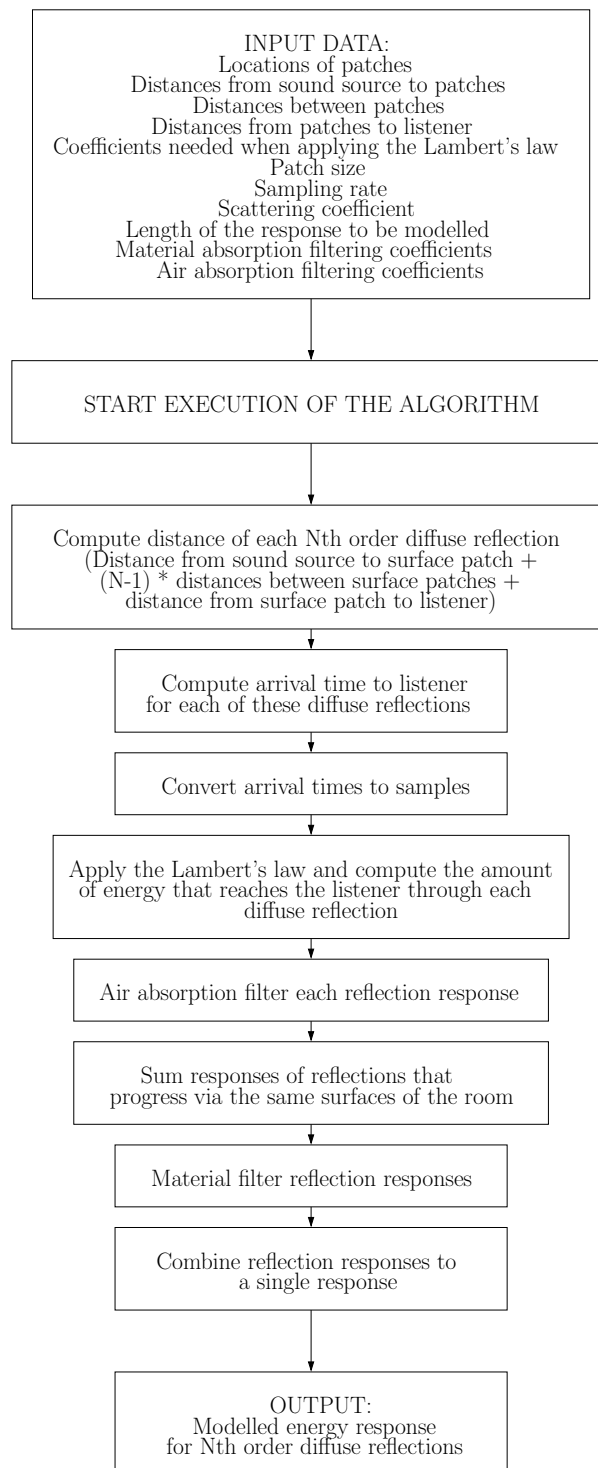


Figure 4.9: Algorithm for computing the energy response for Nth order diffuse reflections.

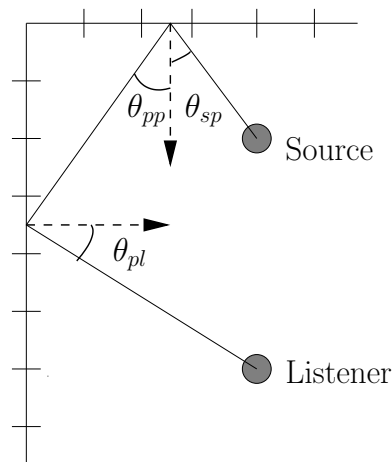


Figure 4.10: Illustration related to the angles needed when computing the coefficients with the Lambert's law.

element in the modelled room. Results were again saved to matrices in order to be used later in the modelling.

Actual Modelling of the Nth Order Diffuse Reflection Response

The following input data was used for Nth order diffuse reflection modelling:

- Locations of surface patches. The size of a patch prescribed the locations. These were defined during preparatory computations.
- Distance information and coefficients for the Lambert's law. Also these were defined during preparatory computations.
- Patch size: 1.5 m - 6.0 m. This was the length of a side of a square patch.
- Sampling rate: 48000 Hz
- Scattering coefficient: 0.0 - 1.0
- Length of the response to be modelled: 15000 samples
- Air absorption filtering coefficients
- Material absorption filtering coefficients

The modelling algorithm started by computing the lengths of the Nth order diffuse reflection paths with the aid of distance information defined during preparatory computations.

Arrival times of the reflections to the listener were defined in samples in the same way as was done for the specular reflections. Energies that arrived at the listener at the computed sample instants were defined with the following expression in the case of the first order diffuse reflections:

$$E_l = s \frac{E_0}{4\pi r_{sp}^2} \Delta S \frac{l_{sp} l_{pl}}{\pi r_{pl}^2}, \quad (4.1)$$

where s is the scattering coefficient, E_0 is the initial energy at a source point, r_{sp} is the distance between the sound source and the surface patch, ΔS is the area of the surface patch, l_{sp} and l_{pl} are coefficients needed when applying the Lambert's law, which were defined during preparatory computations, and r_{pl} is the distance from the surface patch to the listener.

On contrary, the energies of the second order reflections were computed with the following expression:

$$E_l = s E_p \Delta S \frac{l_{pl}}{\pi r_{pl}^2}, \quad (4.2)$$

where

$$E_p = s \frac{E_0}{4\pi r_{sp}^2} \Delta S \frac{l_{sp} l_{pp}}{\pi r_{pp}^2}. \quad (4.3)$$

In this expression all other variables are what has been explained in the connection of equation (4.1), but l_{pp} is a coefficient needed when applying Lambert's law between patches and r_{pp} is the distance between patches where the first and the second reflections occur.

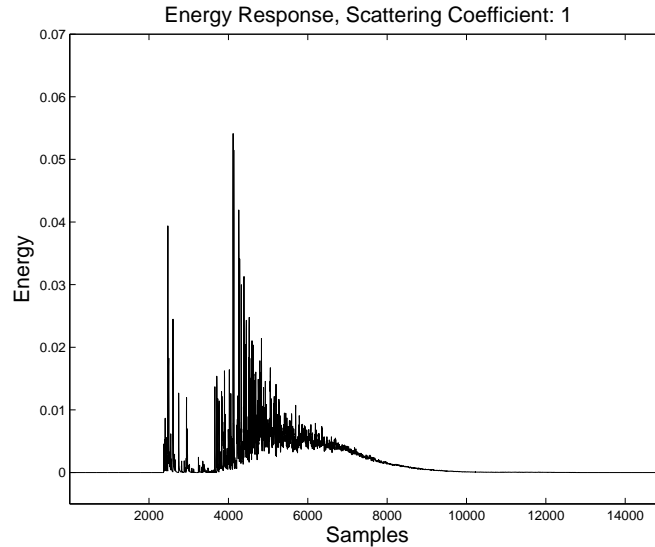


Figure 4.11: Modelled energy response for diffuse reflections (without direct sound), patch size 9 m^2 .

Next, by utilising the arrival times and the energies, responses for all reflections were created. Air absorption filtering was performed in the same way as this was done with the specular reflections. After air absorption filtering, responses of diffuse reflections which travelled through the same surfaces were combined. Now, it was possible to material absorption filter these responses with corresponding material filters. Naturally, also here the same filters were applied as with the specular reflections. After material absorption filtering all reflection responses were added together to a single energy response.

Combining First and Second Order Diffuse Reflection Responses

Finally, the modelled first and second order diffuse reflection responses were combined to a single energy response. One example of the modelling results is depicted in figure 4.11.

4.1.3 Combining Specular and Diffuse Reflection Responses

After modelling separate energy responses for specular⁴ and diffuse reflections, these were now added up. Yet, the achieved energy response was converted to a pressure impulse response by taking the square root from the modelled response. This was done in order to enable convolution with an anechoic recording which is a sound pressure signal. After convolution, the modelled room acoustics could be listened to. An example of a modelled early pressure impulse response is shown in figure 4.12.

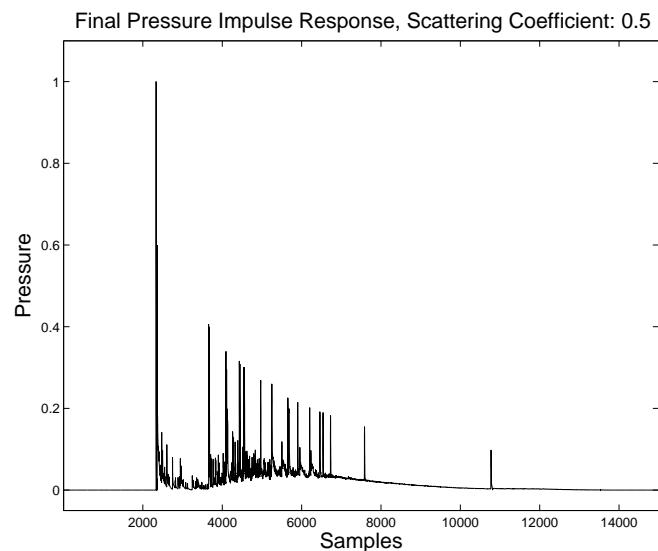


Figure 4.12: Modelled early pressure impulse response, patch size 9 m².

⁴The direct sound was included in the specular response.

4.2 Analysis

To find out the effect of the scattering coefficient, as well as the effect of the patch size, several impulse responses were computed and analysed.

4.2.1 Effect of the Scattering Coefficient

The value of the scattering coefficient was changed from 0.0 (= only specular reflections) to 1.0 (= totally diffuse reflections) with 0.1 step spacing. Resulting pressure impulse responses are depicted in figures 4.13 and 4.14. These responses were also convolved with anechoic recordings (a theme played with a guitar and a rhythm played with a snare drum), and resulting sound samples were listened to in informal listening tests. Clear differences were perceived between cases where modelled responses were totally specular and totally diffuse. The differences were more prominently heard in the snare drum sound samples. However, when the diffusion was increased step by step, differences between adjacent sound samples were hardly noticed.

Listening only to the beginning of a response is not natural. A noticeable echo was heard in the end of those responses where the specular reflections were prominent. As can be seen from figures 4.13 and 4.14, the last specular second order reflection arrives considerably later than others. This reflection is the source of the above mentioned echo. If a formal listening test would be organised with sound samples convolved with the modelled responses, the last specular reflection should be neglected from the responses.

In figure 4.15 frequency responses (between 500 - 24000 Hz)⁵ of the whole modelled early response are illustrated in cases where reflections are totally specular and totally diffuse. It can be seen that the frequency response in the case of totally diffuse reflections is much smoother than with totally specular reflections. In the specular reflection response a clear comb filtering effect can be observed. In figure 4.16 frequency responses of the impulse responses, which include the direct sound and the first specular reflection from the floor, are depicted in a case where the reflections are totally specular, in a case where diffusivity has increased so that the scattering coefficient is 0.5, and in a case of totally diffusing surfaces. From this figure the impact of increasing the diffusivity can also be perceived well. Diffuse reflections break the comb filtering effect and smooth gradually the response.

⁵Low frequency response between 0 - 500 Hz was left out here and in the following because methods based on the geometrical room acoustics are not accurate at this frequency range [68]. The low frequency response should be modelled with a wave-based method.

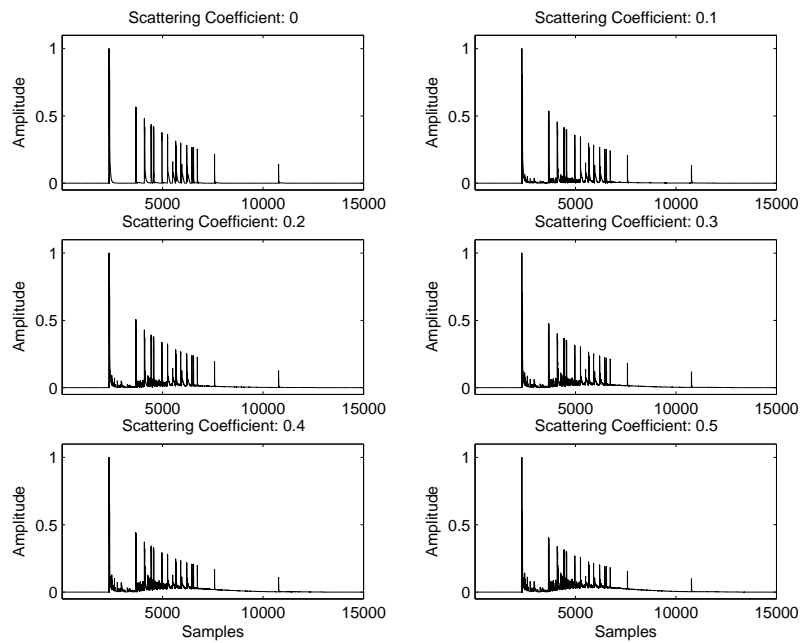


Figure 4.13: Pressure impulse responses. Scattering coefficient changes from 0.0 to 0.5. Patch size is 9 m^2 .

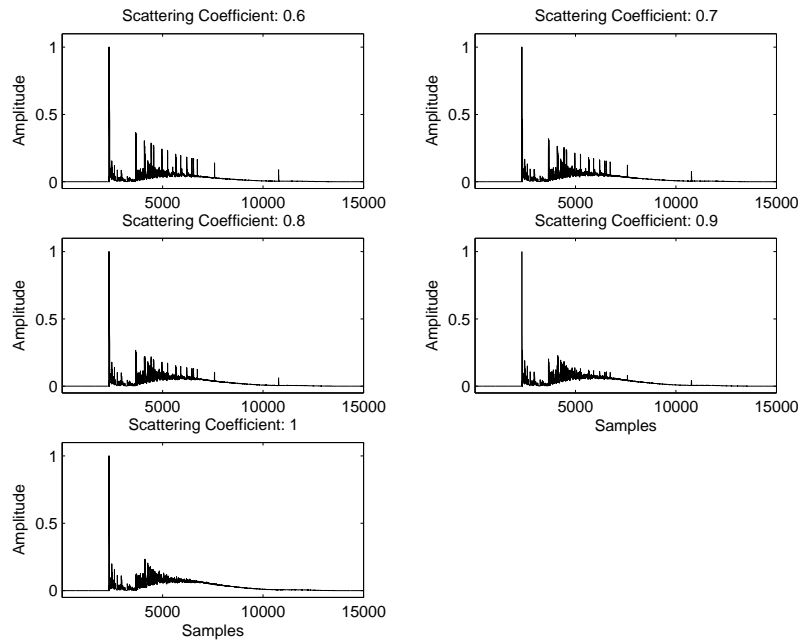


Figure 4.14: Pressure impulse responses. Scattering coefficient changes from 0.6 to 1.0. Patch size is 9 m^2 .

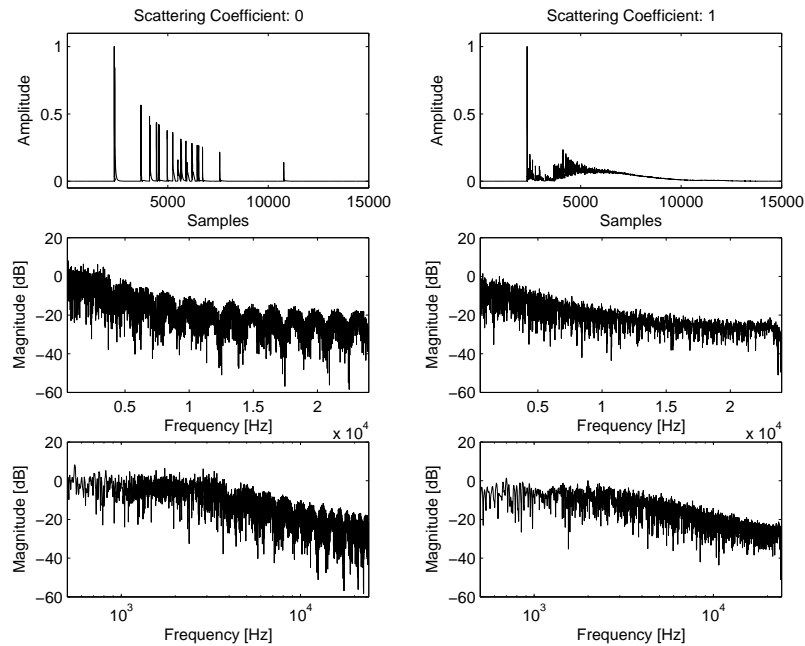


Figure 4.15: Frequency responses between 500 - 24000 Hz in cases of totally specular and totally diffuse reflections. In the middle row frequency responses are plotted with a linear frequency scale while in the bottom row logarithmic frequency scale is used.

4.2.2 Effect of the Patch Size

Also, the impact of the value of the patch size variable on the modelling result was investigated. In figure 4.17 the modelled pressure impulse responses with three different patch sizes are illustrated (36 m^2 , 9 m^2 , 2.25 m^2). In all cases the value of the scattering coefficient was kept constant (0.5). It can be perceived that changes in the modelled responses are small. When the patch size is greater, the reflections arrive more sparsely when compared to the smaller patch size responses. However, the total energy of diffuse reflections stays approximately the same in all cases. Furthermore, when frequency responses achieved with different patch size parameters are compared in figure 4.18, it is hard to find significant differences between the responses. Also in this connection anechoic recordings were convolved with the modelled responses and listened to in informal listening tests. Differences could not be perceived between the responses.

4.2.3 Discussion about Implementation

During the implementation process it was realised that physically-based diffuse reflection modelling is not trivial. Several preliminary implementations were carried out. First, lis-

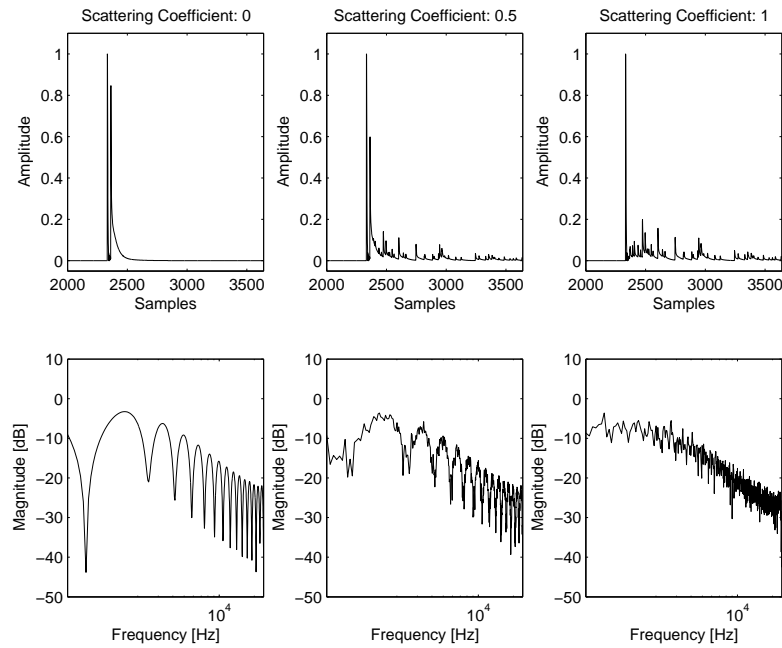


Figure 4.16: Above: Pressure impulse responses between samples 2000 - 3640 (42 ms -76 ms) in cases where the scattering coefficient is 0 (= totally specular reflections), 0.5 and 1.0. Below: Frequency responses of modelled impulse responses in the corresponding cases.

tener modelling was also meant to be integrated into the system, but in initial experiments it was noticed that filtering every diffuse reflection with corresponding head related transfer function (HRTF) results in very long execution time of the program. HRTF modelling was left out from the final system. The choice can be justified by noticing that responses modelled without HRTFs tell actually more about the acoustical characteristics of the room because inaccuracies in listener modelling do not disturb the modelling result. The fact is that HRTFs which would be used in the modelling would not correspond to individual listeners' HRTFs, except the person whom HRTFs would be used.

Advantages of the proposed kind of approach relate to the applied diffuse reflection model which is based on the radiosity. In it contribution strengths between the source, the patches, and the listener can be defined generally so that all orders of diffuse reflection responses can utilise this same information. Also, the use of the ISM guarantees that all specular reflections are found. However, if the proposed model would be used for predicting a full length response, the ISM should be replaced with some other method after a couple of reflection orders due to rapidly increasing computational requirements.

Anyway, the realised system is open to discussion in many ways. First of all, as was noticed in the previous subsection, the problem of the proposed method is that it doesn't model

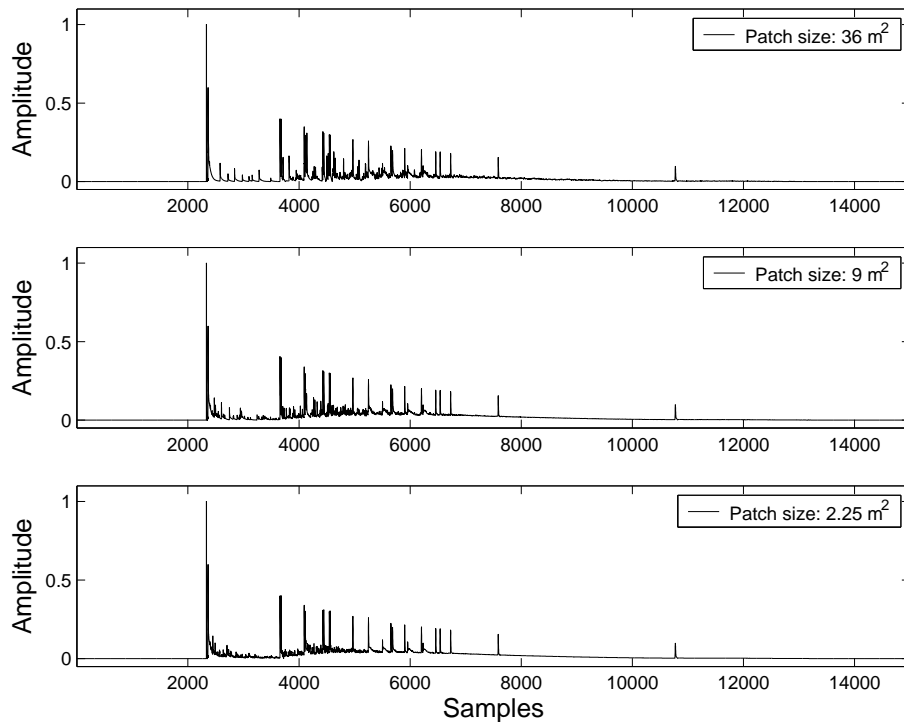


Figure 4.17: Pressure impulse responses, patch size varies, scattering coefficient: 0.5.

arrival times and magnitudes of diffuse reflections absolutely accurately. Depending on the size of a patch, arrival times, and also magnitudes of the diffuse reflections vary. When applied to room acoustics modelling, the radiosity-based approach is thus approximate, not an exact model for energy spreading out from a source to a listener.

Secondly, in many auralisation applications the processing should be done in real time. Also, dynamic changes of listener's and sound source's positions, as well as changes in the room geometry should be possible. Nowadays dynamic real-time systems are fully employed when computing the specular reflections up to order 2-3 and at the same time simulating the late reverberation with recursive filter structures [49]. In the implemented shoe-box shaped room, the number of the first and the second order diffuse reflections arise with the greatest patch size (36 m^2) to 7392 reflections, which is far more than the number of specular reflections which is 24. With a smaller patch size and in more complex geometries the number of reflections grows even further up. When these numbers are examined, it is obvious that the proposed system is not capable of real-time dynamic processing.

In the implemented system the scattering functions were supposed to follow the Lambert's law. In reality, this assumption does not apparently hold. If a real room would be modelled, more reliable scattering functions for all surfaces of the room should be found. In

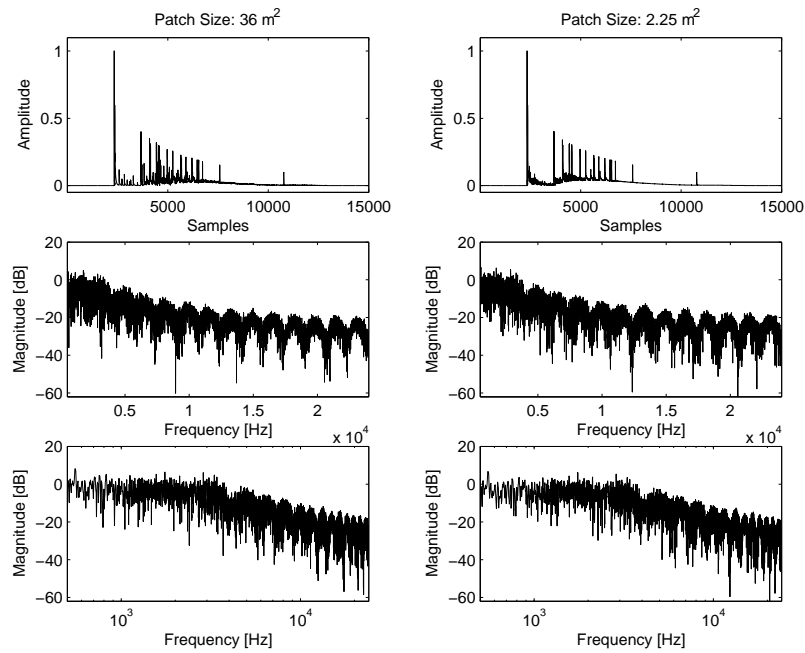


Figure 4.18: Frequency responses with patch sizes 36 m^2 and 2.25 m^2 . Middle row: linear frequency scale. Bottom row: logarithmic frequency scale.

addition, the frequency dependence of scattering would need to be taken into account. Different scattering coefficients and functions should be applied to different frequency ranges. Modelling should be done separately for individual frequency bands. The results could be combined afterwards to a single response which covers the whole frequency range.

One more disadvantage of the suggested method is that some of the initial energy originating from the sound source is lost during the modelling. This happens because, in this model, specular reflections can cause only specular reflections and diffuse reflections only diffuse reflections. All reflection combinations are thus not modelled. A better solution would be to apply a kind of method proposed by Dalenbäck [17].

Chapter 5

Discussion

In the previous chapters, the theoretical background, a few diffuse reflection modelling methods, and a simple implementation have been presented. In this chapter, on the grounds of these studies, diffuse reflection modelling techniques suitable for different purposes are discussed. First, methods most applicable for predicting acoustical quality of a real room by defining room acoustical parameters from a room impulse response are considered. Then methods most suitable for auralisation purposes are discussed. Finally, demands caused by dynamic real-time systems are covered.

5.1 Diffuse Reflection Modelling when Predicting Acoustical Quality of a Room

As was mentioned already in the beginning of section 2.4, one situation where computerised room acoustics prediction is often needed, is the designing process of a new space. Prediction is required also, when the purpose is to improve acoustics of an existing space. In these contexts, the aim of the prediction is to find out the acoustical quality of the studied space.

The characteristics of room acoustics can be estimated by defining room acoustical parameters from a modelled energy response. There exist several room acoustics prediction software¹ which aim at accurate room acoustics prediction. Diffuse reflections are modelled in these in more or less different ways. Common to the software is that they all apply physically-based modelling methods. With today's computational resources computations are forced to be executed off-line. It is not possible to get exact information about the used methods, but with the aid of publications one can familiarise him/herself with the most

¹For example Odeon (<http://www.dat.dtu.dk/~odeon/>), Catt (<http://www.catt.se/>), and Ease (<http://www.audioease.com/>)

commonly suggested methods and principles. This is what has been done in this thesis.

The emphasis in this thesis has been on the ray- and radiosity-based diffuse reflection modelling methods. Wave-based methods which predict the response of an entire room have not been considered. As a consequence, wave-based methods are left out also here, when advantages and disadvantages of the studied methods² are discussed.

Randomised Ray Tracing Methods

As was mentioned in section 3.1 the most traditional method for diffuse reflection modelling is the randomised ray tracing. The randomised ray tracing approaches are statistical. If scattering coefficients, distribution functions of diffuse reflections, and absorption properties of surfaces have been defined accurately, and in addition, if a sufficient number of rays are sent, results converge to exact results. A clear disadvantage of the method is a large number of rays required. Computations are thus usually time-consuming, especially in complex geometries.

The fact is that diffusion, as well as absorption properties of surfaces vary as a function of frequency. For this reason, when applying the randomised ray tracing, modelling is normally done separately for narrow frequency bands. Frequency dependence of scattering and absorption increases the required computation considerably. In order to reduce computation, procedures, such as suggested by Embrechts [21], can be utilised, when accuracy of the modelling result is not highly critical. However, Embrechts' method is not applicable, if the distribution functions of diffuse reflections are not similar in all frequency bands.

ISM and Hybrid Approaches

With the image source method, only specular reflections can be modelled. Therefore, it alone can not be used when modelling spaces where the surfaces are diffusely reflecting. However, if the surfaces of the room are partially diffusely reflecting, it is possible to combine the ISM with some other method which is capable for diffuse reflection modelling. Also, one possibility is to use the ISM for the early part of the response while the late part is predicted with the randomised ray tracing, as suggested by Vorländer [89]. With such a procedure all early reflections are surely found, and at the same time less rays are sufficient for the late part of the response. However, a clear disadvantage of using only the ISM for the beginning of the response is the fact that early diffuse reflections are now totally lost. Furthermore, frequency dependence of scattering and absorption must again be taken into account. This increases computational load.

²When defining room acoustical parameters from a predicted RIR

A solution, which utilises the ISM, and models also diffuse reflections for the beginning of a response, has been suggested by implementation presented in the experimental part of this thesis. With some modifications the presented model could be applied also to prediction of a full length response. The ISM should, however, be replaced with another method in this model after a couple of reflection orders due to rapidly increasing computational requirements. The model has already been analysed in section 4.2, and for this reason, its advantages and disadvantages are not repeated here. However, in summary, these mostly relate to the used radiosity model.

Beam/Cone Tracing Methods Combined with Radiosity-based Approaches

Another kind of hybrid approach is to combine the beam/cone tracing with the radiosity. An example of such an approach is Lewers' method [48] where the specular reflections were modelled with the beam tracing while the radiosity was utilised for the diffused part. As is clear on the grounds of the previous chapters, an advantage of choosing a radiosity-based diffusion model is that when contribution strengths between a listener, surfaces, and sound sources have once been determined this information can be utilised by all reflection orders. Processing of the algorithm can therefore be quite fast. A clear disadvantage of the Lewers' method is that the density of the surface grid and also the beam density influence on the spatial, temporal, and angular accuracy of the modelling result. One more problem of the method is that all reflection combinations are not included in the model.

Another presented method which grounds on the beam/cone tracing is Dalenbäck's [17] approximate cone tracing -based suggestion which combines specular and diffuse reflection modelling in the same algorithm. With this method all reflection combinations can be modelled. The algorithm is also computationally quite efficient. Despite, Dalenbäck himself has suggested that the proposed method could be utilised only for the early part of a response, so that the modelling could be done with a normal personal computer. Since Dalenbäck proposed his method, computational power has increased a lot and so, apparently more reflection orders could be modelled nowadays.

Dalenbäck has pointed out some disadvantages of his algorithm. These relate to approximations involved. A fact is that also in this method the ray and the patch density has influence on spatial, temporal, and angular accuracy. Since the centre of a patch, instead of an exact point a ray hits, is used as a secondary source, the origin of a diffuse reflection translates a little in time. In addition, a more correct method for recording reflections at patches would be to record all those covered by a cone face. However, this further complication is incompatible with approximate cone tracing. In it only a centre ray, not an actual cone face, is traced. The uncertainty is largest for grazing incidence. This could, how-

ever, be diminished for the most important surfaces by increasing the patch density. Every surface or part of the surface could have its own density.

Frequency dependence of surface diffusion (and absorption) is an issue also in context of the beam/cone tracing approaches which apply methods evolved from the radiosity for diffused part of a response. If the acoustics of a real space would be predicted, scattering coefficients of all surface materials should be available in narrow frequency bands and modelling should be done separately to each frequency band. Furthermore, in previously presented models scattering functions were expected to be Lambertian. This doesn't normally correspond to a real case. Dalenbäck has, however, suggested that also angle dependent scattering functions could be utilised with his method if angle information of hitting rays as well as the strengths would be recorded to the patches. If the purpose would be to model acoustics of a real space accurately, this should be possible with the software used for prediction.

5.2 Diffuse Reflections in Context of Auralisation

Results of the modelling process can be utilised in different ways when estimating the acoustical quality of a space. As was mentioned in the previous section, a modelled room impulse response can be used for definition of room acoustical parameters. On the other hand, room acoustical quality can be estimated by listening. In cases where the objective is to analyse acoustics of a space by listening, the accuracy of prediction result is highly critical.

If the objective would be to predict an optimal pressure impulse response for auralisation purposes, modelling would need to be done separately for each single frequency. This results from frequency dependence of diffusion and absorption. However, because diffusion and absorption properties of surfaces are not normally known accurately enough, and since there are also computational limitations, modelling with the studied ray- and radiosity-based approaches is in practice forced to be done in narrow frequency bands. As a consequence prediction results are more or less approximate. Usually they are, however, sufficiently accurate to be used for definition of room acoustical parameters from room impulse response, i.e. for a purpose where these methods have originally been developed.

In order to achieve more accurate results required in auralisation, more developed methods would be needed. Currently efficient solutions for an entire room do not exist. For this reason, in the future, the investigations should be pointed to the wave-based approaches. Already developed methods should be studied in detail. How these could be utilised and optimised for predicting an accurate pressure impulse response of the entire room should be investigated. In addition, it could be worthwhile to acquaint oneself with methods which

have been used in other fields of physics. One may find methods which have not yet been applied to room acoustics prediction and thus auralisation. One point where to start could be a study, where single reflections from diffusely reflecting surfaces would be measured in an anechoic chamber. On the grounds of measurements, suitability and accuracy of different methods for predicting a pressure impulse response could then be estimated.

Until now discussion has considered situations where an objective has been to find out an accurate room impulse response of the modelled space so that this could be used for estimation of acoustical quality of a space. However, there are also situations where the prediction result is not as critical and so more or less approximate results are adequate.

In this thesis two approaches suitable to be used in situations where highly accurate prediction result is not needed were presented. These are models proposed by Martin [52] and Pellegrini [59]. In both of these specular reflections were modelled with the ISM. Martin applied physical models of the Schroeder diffusers for predicting the diffused part of a response while Pellegrini suggested perceptually-based diffusion filter approach. A fact is that the ISM can normally be used only for an early part of a response due to computational limitations. Thus, when applying Martin's or Pellegrini's method the late part of the response needs to be modelled with some other approach. Most often late reverberation is simulated with recursive digital filter structures.

An advantage of aforementioned kind of approaches are that they allow real-time processing. However, diffuse reflection modelling in these methods does not relate actually to a modelled space. As a consequence, these methods are not suitable to be used in models which aim at prediction of acoustical quality of a space.

Is it then really possible to distinguish between responses where diffuse reflections have been modelled based on the physical reality of the space or based on some more or less perceptually-based approaches? In order to answer this question in context of early response, the following listening test is suggested.

In this test, sound samples achieved by convolving anechoic recordings with two kind of early responses are listened to. Responses of the first class are modelled in a way proposed in the experimental part in section 4.1. On the contrary, responses of the second class are modelled with the method proposed by Pellegrini [59]. The energy which is smeared between specular reflections in the Pellegrini's method, is taken from the response modelled with the method proposed in the experimental part. Comparison of sound samples achieved by convolving anechoic recordings with the modelled responses would give information about how accurately early diffuse reflections are heard. If the responses would be clearly differentiated by the listeners, it could be confirmed that the accuracy is really important, when the modelling is done for listening purposes.

5.3 Real-time Dynamic Diffuse Reflection Modelling

So far, the discussion in this chapter has restricted to a static case where the location of the listener, the location of the sound source/sound sources, and the geometry of the modelled space do not change during the modelling. However, in many cases, it would be advantageous if real-time dynamic changes in the modelled environment would be possible. Computer games and virtual reality applications are typical examples of the systems with such requirements.

Also, when the acoustical quality of the room is evaluated by listening the auralisation result, it would be advantageous, if it would be possible to move around in the modelled space during the listening. Furthermore, it would be helpful if impacts of changes in locations of the sound sources and impacts of changes in the geometry and in the surface materials could be listened to.

The fact is that dynamic real-time processing increases required computation considerably. Impulse responses need to be recomputed every time something changes in the environment. Interpolation is needed between the changing responses. The studied ray- and radiosity-based approaches can not be applied for the diffuse reflection modelling when the requirements are such. On the grounds of studied methods and realised implementation it seems that only solutions to the dynamic real-time room acoustics modelling are kind of approaches suggested by Martin [52] and Pellegrini [59] combined with the recursive digital filter structures for the late part of the response. As was already mentioned in the previous section, the clear disadvantage of these methods is that exact characteristics of the modelled space are lost.

Although physically-based approaches can not normally be applied when dynamic real-time processing is needed, with the following approach some changes in the environment could be allowed when the prediction is made with these methods. In this approach it is assumed that the sound source/sources, the geometry, and the surface properties of the modelled space do not change. However, dynamic changes in the listener position are possible.

In the proposed solution the impulse responses are computed off-line beforehand at several points in a room. These points constitute a very dense grid inside the room. When listener then moves in the modelled space, the response in the grid which is closest to the listener's location is chosen to be used in auralisation. When the listener moves to another point, the change of the response is smoothed by interpolation between the responses. This kind of procedure allows the listener to move around in the modelled space and listen to the acoustics in different locations.

Of course, modelling could be done also so that the listener would be kept at the same

position and the sound source/sources would be moved in the modelled space. One more choice could be to keep the listener and the sound sources at the fixed positions and enable certain geometrical changes or changes in surface materials, which could be controlled by the listener in real time after modelling.

The disadvantages of the proposed method relate to the huge amount of precomputing. However, the number of responses which need to be computed could be reduced if user's/-source's route/routes in the space, or choices in cases where the listener is allowed to change the geometry/surface materials of the room, would be defined before computations. This would, however, reduce flexibility of the system.

Chapter 6

Conclusions and Future Work

The objective of this thesis has been to familiarise oneself with physical principles and different methods used in diffuse reflection modelling in context of room acoustics prediction. Basic principles, several modelling methods, their suitability to different purposes, and their deficiencies have been discussed. Also, a simple implementation has been carried out. The emphasis of the work has been on the ray- and radiosity-based modelling methods. Conclusions based on the studies are summarised as follows:

- Diffuse reflection is a highly complicated phenomenon. It results from surface irregularities and/or rapidly changing surface impedance.
- How a surface reflects sound depends on frequency. Therefore, diffuse reflections should be modelled frequency dependently.
- Scattering functions for diffuse reflections have been traditionally modelled with the Lambert's law. However, there is no physical background to support it. If a reliable result is sought for, measured or theoretically computed scattering functions should be exploited.
- The ISM method is incapable for modelling diffuse reflections.
- If a sufficient number of rays is sent and if modelling is done frequency dependently, the most accurate methods¹ for predicting a room impulse response which includes also diffused reflections are approaches based on the randomised ray tracing.
- If the speed of an algorithm is essential, methods based on the beam/cone tracing combined with radiosity-based approaches are more suitable to be used for predicting a response of a room.

¹From ray- and radiosity-based methods

- Models applying the radiosity-based approaches are not absolutely accurate. For example, the patch density has influence on the spatial, temporal, and angular accuracy.
- Accurately modelled diffuse reflection response is essential especially in auralisation. Predicting response with correct magnitude and phase information is problematic due to frequency dependence of surface properties.
- Real-time dynamic auralisation is so far forced to use methods which don't model diffused part of a response physically-based.

Furthermore, in the previous chapters, some suggestions for the future studies have been given. Things to do in the future:

- Applicability of diffuse reflection modelling methods which have been utilised in other fields of physics could be studied. Do there exist methods which have not yet been fully examined from the room acoustical modelling perspective? If there exist, how these approaches could be applied and optimised for the room acoustics prediction should be studied.
- Impulse responses from a diffusely reflecting plane could be measured in an anechoic chamber. A scattering function for the plane would be defined based on the measurements. Next, different modelling methods could be used to predict computationally this response. Modelling results would be compared to the measured response and thus the accuracy and reliability of the modelling methods could be estimated.
- A listening test suggested in section 5.3 could be organised. The purpose of this test would be to investigate whether small changes in the diffused part of a response are audible or not.

Bibliography

- [1] ISO Standard 17497-1. Acoustics - Sound-scattering properties of surfaces – Part 1: Measurement of the random-incidence scattering coefficient in a reverberation room, 2004.
- [2] AES 4id 2001. AES information document for room acoustics and sound reinforcement systems - Characterization and measurement of surface scattering uniformity. *Journal of the Audio Engineering Society*, 49(3):149–165, March 2001.
- [3] ISO Standard 9613-1. Acoustics - Attenuation of sound during propagation outdoors - Part 1: Calculation of the absorption of sound by the atmosphere, 1993.
- [4] J. B. Allen and D. A. Berkley. Image method for efficiently simulating small-room acoustics. *Journal of the Acoustical Society of America*, 65(4):943–950, April 1979.
- [5] J. Baan and D. de Vries. Reflection and diffraction in room acoustic modelling. In *Proc. of Forum Acusticum*, Berlin, Germany, March 1999.
- [6] R. H. Bolt, P. E. Doak, and P. J. Westervelt. Pulse statistics analysis of room acoustics. *Journal of the Acoustical Society of America*, 22(3):328–340, May 1950.
- [7] M. M. Boone, G. Janssen, and M. van Overbeek. Modal superposition in the time domain: Theory and experimental results. *Journal of the Acoustical Society of America*, 97(1):92–97, January 1995.
- [8] J. G. Borish. Extension of the image model to arbitrary polyhedra. *Journal of the Acoustical Society of America*, 75(6):1827–1836, June 1984.
- [9] I. Bork. A comparison of room simulation software - The 2nd Round Robin on room acoustical computer simulation. *Acta Acustica - Acustica*, 86:943 – 956, 2000.
- [10] D. Botteldooren. Finite-difference time-domain simulation of low-frequency room acoustic problems. *Journal of the Acoustical Society of America*, 98(6):3302–3308, December 1995.

- [11] D. Chu and T. Stanton. Application of Twersky's boss scattering theory to laboratory measurements of sound scattered by a rough surface. *Journal of the Acoustical Society of America*, 87(4):1557–1568, April 1990.
- [12] T. J. Cox and P. D'Antonio. Fractal sound diffusers. In *Proc. 103rd Convention of the Audio Engineering Society*, New York, 1997.
- [13] T. J. Cox and P. D'Antonio. Contrasting surface diffusion and scattering coefficients. In *17th ICA Proceedings*, Rome, 2001.
- [14] T. J. Cox and P. D'Antonio. *Acoustic Absorbers and Diffusers*. Spon Press, 2004. ISBN 0-415-29649-8.
- [15] L. Cremer, H. A. Muller, and T. J. Schultz. *Principles and Applications of Room Acoustics, Volume 1*. Applied Science Publishers, 1982. ISBN 0-85334-113-3.
- [16] B.-I. L. Dalenbäck. *A New Model for Room Acoustic Prediction and Auralization*. PhD thesis, Chalmers University of Technology, Göteborg, Sweden, November 1995.
- [17] B.-I. L. Dalenbäck. Room acoustic prediction based on a unified treatment of diffuse and specular reflection. *Journal of the Acoustical Society of America*, 100(2):899–909, August 1996.
- [18] B.-I. L. Dalenbäck, M. Kleiner, and P. Svensson. A macroscopic view of diffuse reflection. *Journal of the Audio Engineering Society*, 42(10):793–807, October 1994.
- [19] I. A. Drumm and Y. W. Lam. The adaptive beam-tracing algorithm. *Journal of the Acoustical Society of America*, 107(3):1405–1412, March 2000.
- [20] J.-J. Embrechts. Sound field distribution using randomly traced sound ray techniques. *Acustica*, 51:288–295, 1982.
- [21] J.-J. Embrechts. Broad spectrum diffusion model for room acoustics ray-tracing algorithms. *Journal of the Acoustical Society of America*, 107(4):2068–2081, April 2000.
- [22] J.-J. Embrechts, D. Archambeau, and G. B. Stan. Determination of the scattering coefficient of random rough diffusing surfaces for room acoustics applications. *Acta Acustica - Acustica*, 87:482–494, 2001.
- [23] F. Fahy. *Foundations of Engineering Acoustics*. Academic Press, 2000. ISBN 0-122-47665-4.

- [24] L. P. Franzoni, D. B. Bliss, and J. W. Rouse. An acoustic boundary element method based on energy and intensity variables for prediction of high-frequency broadband sound fields. *Journal of the Acoustical Society of America*, 110:3071–3080, 2001.
- [25] T. Funkhouser, P. Min, and I. Carlbom. Real-time acoustic modeling for distributed virtual environments. In *Proc. of SIGGRAPH99, ACM Computer Graphics*, pages 365–374, 1999.
- [26] W. Gardner. *3-D Audio Using Loudspeakers*. PhD thesis, Kluwer Academic Publishers, Boston, MA, 1997.
- [27] D. Gen-hua. Estimation of the influence of diffusion on reverberation using ray-tracing simulation. *Acustica*, 54:43–45, 1983.
- [28] B. M. Gibbs and D. K. Jones. A simple image method for calculating the distribution of sound pressure levels within an enclosure. *Acustica*, 26:24–32, 1972.
- [29] D. Hammershøi and H. Møller. Methods for binaural recording and reproduction. *Acta Acustica - Acustica*, 88:303–311, 2002.
- [30] T. J. Hargreaves, T. J. Cox, Y. W. Lam, and P. D’Antonio. Surface diffusion coefficients for room acoustics: Free-field measures. *Journal of the Acoustical Society of America*, 108(4):1710–1720, October 2000.
- [31] M. Hodgson. Evidence of diffuse surface reflections in rooms. *Journal of the Acoustical Society of America*, 89(2):765–771, February 1991.
- [32] J. Huopaniemi, L. Savioja, and M. Karjalainen. Modeling of reflections and air absorption in acoustical spaces – A digital filter design approach. In *Proc. IEEE Workshop on Applications of Signal Processing to Audio and Acoustics*, Mohonk, New Paltz, NY, October 1997.
- [33] Y. Kagawa, T. Tsuchiya, B. Fujii, and K. Fujioka. Discrete Huygens’ model approach to sound wave propagation. *Journal of Sound and Vibration*, 218(3):419–444, 1998.
- [34] M. Kleiner, B.-I. L. Dalenbäck, and P. Svensson. Auralization - An overview. *Journal of the Audio Engineering Society*, 41(11):861–875, November 1993.
- [35] U. Kristiansen, A. Krokstad, and T. Follestad. Extending the image method for higher order reflections. *Applied Acoustics*, 38:195–206, 1993.
- [36] A. Krokstad, S. Strøm, and S. Sørsdal. Calculating the acoustical room impulse response by the use of a ray tracing technique. *Journal of Sound and Vibration*, 8(1):118–125, 1968.

- [37] A. Kulowski. Error investigation for the ray tracing technique. *Applied Acoustics*, 15:263–274, 1982.
- [38] A. Kulowski. Algorithmic representation of the ray tracing technique. *Applied Acoustics*, 18:449–469, 1985.
- [39] H. Kuttruff. Simulierte Nachhallkurven in Rechteckräumen mit Diffusem Schallfeld. *Acustica*, 25:333–342, 1971.
- [40] H. Kuttruff. A simple iteration scheme for the computation of decay constants in enclosures with diffusely reflecting boundaries. *Journal of the Acoustical Society of America*, 98(1):288–293, July 1995.
- [41] H. Kuttruff. *Room Acoustics*. Taylor & Francis, Fourth edition, 2000. ISBN 0-419-24580-4.
- [42] T. Lahti. *Akustinen Mittaustekniikka*. Teknillinen korkeakoulu, Sähkö- ja tietoliikennetekniikan osasto, Akustiikan ja äänenkäsittelytekniikan laboratorio, 1997.
- [43] Y. W. Lam. A comparison of three diffuse reflection modeling methods used in room acoustics computer models. *Journal of the Acoustical Society of America*, 100(4):2181–2192, October 1996.
- [44] Y. W. Lam. A boundary integral formulation for the prediction of acoustic scattering from periodic structures. *Journal of the Acoustical Society of America*, 105(2):762–769, February 1999.
- [45] A. LeBot and A. Bocquillet. Comparison of an integral equation on energy and the ray-tracing technique in room acoustics. *Journal of the Acoustical Society of America*, 108(4):1732–1740, 2000.
- [46] H. Lee and B. H. Lee. An efficient algorithm for the image model technique. *Applied Acoustics*, 24:87–115, 1988.
- [47] H. Lehnert. Systematic errors of the ray-tracing algorithm. *Applied Acoustics*, 38:207–221, 1993.
- [48] T. Lewers. A combined beam tracing and radiant exchange computer model of room acoustics. *Applied Acoustics*, 38:161–178, 1993.
- [49] T. Lokki. *Physically-Based Auralization - Design, Implementation, and Evaluation*. PhD thesis, Helsinki University of Technology, 2002.

- [50] D. Malham and A. Myatt. 3-D sound spatialization using ambisonic techniques. *Computer Music Journal*, 19(4):58–70, 1995.
- [51] G. Martin, J. Corey, W. Woszczyk, and R. Quesnel. A computer system for investigating and building synthetic auditory spaces - Part 2. In *Proc. of the 19th International Conference of the Audio Engineering Society*, Schloss Elmau, Germany, 21 - 24 June 2001.
- [52] G. Martin, P. Depalle, W. Woszczyk, J. Corey, and R. Quesnel. A hybrid model for simulating diffused first reflections in two-dimensional synthetic acoustic environments. In *Proc. of the 19th International Conference of the Audio Engineering Society*, Schloss Elmau, Germany, 21 - 24 June 2001.
- [53] R. N. Miles. Sound field in a rectangular enclosure with diffusely reflecting boundaries. *Journal of Sound and Vibration*, 92(2):203–226, 1984.
- [54] H. Møller. Fundamentals of binaural technology. *Applied Acoustics*, 36:171–218, 1992.
- [55] E. Mommertz. Determination of scattering coefficients from the reflection directivity of architectural surfaces. *Applied Acoustics*, 60:201–203, 2000.
- [56] G. R. Moore. *An Approach to the Analysis of Sound in Auditoria*. PhD thesis, Cambridge, UK, 1984.
- [57] M. Oren and S. Nayar. Seeing beyond Lambert’s law. In *Proc. of European Conference on Computer Vision (ECCV 94)*, Stockholm, May 1994.
- [58] R. S. Pellegrini. Perception-based room-rendering for auditory scenes. In *109th Convention of the Audio Engineering Society*, Los Angeles, 2000.
- [59] R. S. Pellegrini. *A Virtual Reference Listening Room as an Application of Auditory Virtual Environments*. PhD thesis, Ruhr-University Bochum, 2001.
- [60] T. Peltonen. A multichannel measurement system for room acoustics analysis. Master’s thesis, Helsinki University of Technology, 2000.
- [61] A. D. Pierce. *Acoustics – An Introduction to Its Physical Principles and Applications*. Acoustical Society of America, 1989. ISBN 0-88318-612-8.
- [62] V. Pulkki. Virtual sound source positioning using vector base amplitude panning. *Journal of the Audio Engineering Society*, 45(6):456–466, 1997.

- [63] R. Quesnel, W. Woszczyk, J. Corey, and G. Martin. A computer system for investigating and building synthetic auditory spaces - Part 1. In *107th Convention of the Audio Engineering Society*, New York, 1999.
- [64] J. Rindel. Attenuation of sound reflections due to diffraction. In *Nordic Acoustical Meeting*, pages 257–260, 1986.
- [65] J. Rindel. Scattering in room acoustics and the related activities in ISO and AES. In *17th ICA Proceedings*, Rome, 2001.
- [66] C. Roads. *The Computer Music Tutorial*. The MIT Press, Cambridge, 1996. ISBN 0-262-68082-3.
- [67] T. Rossing. *The Science of Sound*. Addison Wesley, second edition, 1990. ISBN 0-201-15727-6.
- [68] L. Savioja. Huoneakustiikan laskennallinen mallintaminen. Licentiate thesis, Helsinki University of Technology, 1995.
- [69] L. Savioja, J. Huopaniemi, T. Lokki, and R. Väänänen. Creating interactive virtual acoustic environments. *Journal of the Audio Engineering Society*, 47(9), 1999.
- [70] L. Savioja and V. Välimäki. Interpolated 3-D digital waveguide mesh with frequency warping. In *Proc. of ICASSP*, pages 3345–3348, Salt Lake City, Utah, USA, May 2001.
- [71] M. R. Schroeder. Natural sounding artificial reverberation. *Journal of the Audio Engineering Society*, 10(3):219–223, 1962.
- [72] M. R. Schroeder. Binaural dissimilarity and optimum ceilings for concert halls: More lateral sound diffusion. *Journal of the Acoustical Society of America*, 65(4):958–963, April 1979.
- [73] J. O. Smith. Physical modeling using digital waveguides. *Comput. Music Journal*, 16(4):74–91, 1992.
- [74] U. M. Stephenson. Quantized pyramidal beam tracing - A new algorithm for room acoustics and noise immission prognosis. *Acta Acustica - Acustica*, 82:517–525, 1996.
- [75] H. Strube. Scattering of a plane wave by a Schroeder diffuser: A mode matching approach. *Journal of the Acoustical Society of America*, 67(2):453–459, February 1980.

- [76] J. S. Suh and P. A. Nelson. Measurement of transient response of rooms and comparison with geometrical acoustic models. *Journal of the Acoustical Society of America*, 105(4):2304–2317, April 1999.
- [77] U. P. Svensson, R. Andersson, and J. Vanderkooy. An analytical time domain model of edge diffraction. In *Nordic Acoustical Meeting*, 1998.
- [78] U. P. Svensson, R. I. Fred, and J. Vanderkooy. An analytic secondary source model of edge diffraction impulse responses. *Journal of the Acoustical Society of America*, 106(5):2331–2344, 1999.
- [79] U. P. Svensson and U. R. Kristiansen. Computational modelling and simulation of acoustic spaces. In *The Proc. of the AES 22nd International Conference*, pages 11–30. Audio Engineering Society, Inc., June 2002.
- [80] U. P. Svensson, M. Nakano, K. Sakagami, and M. Morimoto. A study of the sound radiation from musical instruments in rooms using the equivalent source method. In *Proc. of the 16th ICA*, Seattle, WA, USA, June 1998.
- [81] U. P. Svensson, L. Savioja, T. Lokki, and U. R. Kristiansen. Low-frequency models for room acoustic prediction. In *Proc. of the 17th ICA*, Rome, Italy, 2001.
- [82] B. Szabó and I. Babuška. *Finite Element Analysis*. John Wiley & Sons, 1991. ISBN 0-471-50273-1.
- [83] M. Tanaka, Y. Furue, Y. Horinouchi, and T. Terai. Numerical calculations of transient sound response in rooms by Kirchhoff’s integral equation. In *Proc. of the 15th ICA*, Trondheim, Norway, June 1995.
- [84] T. Terai. On calculation of sound fields around three-dimensional objects by integral equation methods. *Journal of Sound and Vibration*, 69(1):71–100, 1980.
- [85] R. R. Torres, U. P. Svensson, and M. Kleiner. Computation of edge diffraction for more accurate room acoustics auralization. *Journal of the Acoustical Society of America*, 109(2):600–610, February 2001.
- [86] V. Twersky. On scattering and reflection of sound by rough surfaces. *Journal of the Acoustical Society of America*, 29(2):209–225, 1957.
- [87] D. van Maercke. Simulation of sound fields in time and frequency domain using a geometrical model. In *Proc. 12th ICA*, Toronto, Ont., Canada, July 1986.

- [88] D. van Maercke and J. Martin. The prediction of echograms and impulse responses within the Epidaure software. *Applied Acoustics*, 38:93–114, 1993.
- [89] M. Vorländer. Simulation of the transient and steady-state sound propagation in rooms using a new combined ray-tracing/image-source algorithm. *Journal of the Acoustical Society of America*, 86(1):172–178, July 1989.
- [90] M. Vorländer and E. Mommertz. Definition and measurement of random-incidence scattering coefficients. *Applied Acoustics*, 60:187–199, 2000.
- [91] O. C. Zienkiewicz and K. Morgan. *Finite Elements and Approximation*. John Wiley and Sons, New York, USA, 1983. ISBN 0-471-98240-7.